



University of
Stavanger

Faculty of Science and Technology

MASTER'S THESIS

Study program/ Specialization:

Offshore Technology/ Subsea Technology

Spring semester, 2013

Open / ~~Restricted access~~

Writer:

Se-Hoon Yoon

.....

(Writer's signature)

Faculty supervisor:

Prof. Daniel Karunakaran (Ph.D.) (University of Stavanger/ Subsea 7 Norway)

External supervisor(s):

Dr. Zhengmao Yang (Subsea 7 Norway)

Title of thesis:

Phenomenon of Pipeline Walking in High Temperature Pipeline

Credits (ECTS):

30

Key words:

**Pipeline walking, Thermal transients,
Axial friction coefficient, ANSYS**

Pages: XIII + 65

+ enclosure: 68

Stavanger, 10th June 2013

ABSTRACT

As the offshore oil and gas fields have been exploited in deeper water, subsea pipelines are increasingly required to operate at high temperatures and pressures. It causes subsea pipelines to be more susceptible to movements both in lateral and axial directions due to the loads produced by high temperatures and pressures. Some high temperature pipelines have experienced the cumulative axial displacement of an overall pipeline length over a number of start-up/shut-in cycles, which is commonly known as “Pipeline walking”. [2]

The objective of this thesis work is to describe the phenomenon of pipeline walking by specifically focusing on a short and high temperature pipeline and identify key parameters of it in terms of the pipeline design. It is because designing to control or mitigate the accumulated walking over the life of the pipeline system can lead to changing in field layouts and high installation costs related to mitigation measures. [5] It is therefore important to be able to assess if the walking is a potential issue in the early design phase.

Moreover, a literature study on contributory mechanisms to cause pipeline walking is emphasized in the thesis including general pipeline technology in terms of the pipeline expansion design: [1]

- Sustained tension at the end of the pipeline, associated with a steel catenary riser (SCR);
- Global seabed slope along the pipeline length;
- Thermal transients along the pipeline during shutdown and restart operations.

Understanding an axial movement of short pipelines due to the resultant of the thermal transient is an important consideration in the pipeline walking assessment. [1] Thus, a numerical model of pipeline walking based on the thermal transient load is established by the finite element method in the thesis. It presents the effect of the transient temperature profile on pipeline walking. In addition to that, it focuses on the effect of axial friction factors related to pipe-soil interaction as the sensitivity study.

Lastly, the thesis briefly deals with possible mitigation options to prevent pipeline walking. This global axial movement phenomenon can lead to various pipeline integrity issues although walking itself is not a limit state in design. [14] It is evident that the possible mitigation methods are to be taken into account at the design phase depending on consequential effects of accumulated axial walking. Hence, the pros and cons of possible mitigation measures are discussed in connection with the sensitivity study results.

Keywords: Pipeline walking, Thermal transients, Axial friction coefficient, ANSYS.

ACKNOWLEDGEMENTS

This thesis is made to conclude author's Master of Science education in Offshore Technology at University of Stavanger in Norway. The thesis work was mainly performed at Subsea 7 Norway, started from January 2013 and completed in June 2013. Several people have supported academically and practically for achieving this master thesis. Thus, it is glad to express my gratitude to them.

Foremost, I would like to express my deepest appreciation to my supervisor Prof. Daniel Karunakaran (Ph.D.) who gave me the opportunity to carry out the thesis work not only under his supervision but also with Subsea 7. His valuable comments and discussions are gratefully acknowledged.

My sincere gratitude is also given to Dr. Zhengmao Yang who provided me with detailed instructions on my thesis as well as useful practical tips on analytical calculations in ANSYS. His excellent guidance helped me in all the time of performing the thesis work.

I would like to thank Mr. Bjørn Lindberg Bjerke who is a Department Engineering Manager at Subsea 7 in Oslo. His permission for me to stay and carry out the thesis work in Subsea 7 Oslo office provided me with an excellent atmosphere for doing the thesis work.

Furthermore, I would also like to acknowledge with much appreciation to Mr. Helge Dykesteen and Ms. Giovanna Fong who welcomed me every visit to Stavanger. I could not have successfully completed the thesis without their sincere hospitality.

Last but definitely not least, I wish to give special thanks to my wife Jang Mee Hong who was always cheering me up and gave me big encouragement to complete not only the thesis but also the entire master degree program. In addition, a special gratitude is also given to my family in Korea: my parents as well as parent in law. Their sincere supports were directly delivered to me even long distance and it really encouraged me.

Stavanger, 10th June 2013

Se-Hoon Yoon

NOMENCLATURE

1. SYMBOLS

① Roman Symbols

| | |
|---------------------|---|
| a_T | Thermal expansion coefficient |
| A_e | Cross sectional area of pipe (OD: m^2) |
| A_i | Cross sectional area of pipe (ID: m^2) |
| A_s | Cross sectional area of pipe wall (ID: m^2) |
| A_{ext} | Cross sectional area of pipe insulation coating (m^2) |
| A_{conc} | Cross sectional area of pipe concrete coating (m^2) |
| B_{pipe} | Mass of pipe buoyancy per unit length (kg/m) |
| $D(= D_i)$ | Pipeline internal diameter (mm) |
| D_o | Pipeline outer diameter (mm) |
| E | Young's modulus (N/m^2) |
| EA | Axial stiffness (N) |
| $f(= F_{friction})$ | Axial friction force (N/m) |
| f^* | Constraint friction force = $\frac{ \Delta P }{L}$ |
| f_θ | Thermal gradients force per unit length (N/m) |
| g | Acceleration of gravity (= $9.81m/s^2$) |
| KP | Kilometer point |
| L | Length of pipeline (m) |
| m_{conc} | Mass of pipe concrete coating per unit length (kg/m) |
| m_{ext} | Mass of pipe insulation coating per unit length (kg/m) |
| m_{oil} | Mass of fluid content in pipe per unit length (kg/m) |
| m_{pipe} | Mass of pipe steel per unit length (kg/m) |
| m_{sub} | Mass of submerged pipeline (in water) per unit length (kg/m) |
| m_{total} | Total mass of pipeline (in air) per unit length (kg/m) |
| P_e | External pressure (Pa) |
| P_{hyd} | Hydrostatic pressure (Pa) |
| P_i | Internal pressure (Pa) |
| ΔP | Differential internal pressure across the pipe wall |
| P_{OP} | Operating pressure (Pa) |
| q_θ | Thermal gradient in degrees per unit length ($^{\circ}C/m$) |
| S | Effective axial force (N) |
| S_L | Residual lay tension (N) |
| S_R | SCR tension (N) |
| S_w | True axial tension (N) |
| t_{eff} | Effective pipe diameter (mm) |
| t | Pipeline wall thickness |
| t_e | Pipeline external (insulation) coating thickness (mm) |

| | |
|-----------|---|
| t_c | Pipeline concrete coating thickness (mm) |
| T_{OP} | Operating temperature (°C) |
| T_{SD} | Shutdown temperature (°C) |
| V_{ab} | Distance between two virtual anchors |
| W_{air} | Weight of pipeline (dry weight) per unit length (N/m) |
| W_{sub} | Weight of submerged pipeline per unit length (N/m) |

② Greek Symbols

| | |
|--------------------------|--|
| β | Parameter in walking due to thermal transients |
| Δ_R | Walk per cycle due to SCR Tension (m) |
| Δ_\emptyset | Walk per cycle due to Seabed slope (m) |
| Δ_θ | Walk per cycle due to Thermal Transients (m) |
| ΔS | Change in fully constrained force (N) |
| ΔS_f | Change in effective axial force over V_{ab} for SCR (N) |
| ΔS_S | Change in effective axial force over V_{ab} for slope (N) |
| ΔT | Temperature difference (°C) |
| $\Delta\theta_{in}$ | Inlet temperature difference |
| ε_T | Thermal strain |
| $\varepsilon_{end\ cap}$ | Strain due to end cap effect |
| $\varepsilon_{poisson}$ | Strain due to Poisson's effect |
| ε_{total} | Total strain due to combined thermal and pressure Poisson's effect (For the unrestrained condition) |
| θ_i | Temperature |
| $\mu_a (= \mu)$ | Friction coefficient |
| ν | Poisson's ratio |
| ρ_{pipe} | Density of pipe steel (kg/m ³) |
| ρ_{ext} | Density of pipe insulation coating (kg/m ³) |
| ρ_{conc} | Density of pipe concrete coating (kg/m ³) |
| ρ_{oil} | Density of fluid content in oil (kg/m ³) |
| ρ_{sw} | Density of seawater (= 1027kg/m ³) |
| σ_{SMYS} | SMYS of pipe steel (MPa) |
| \emptyset | Seabed slope (°) |

2. ABBREVIATIONS

| | |
|-------|----------------------------------|
| BE | Best Estimate |
| DISP | Displacement |
| DNV | Det Norske Veritas |
| EAF | Effective Axial Force |
| FE | Finite Element |
| FEA | Finite Element Analysis |
| HP/HT | High Pressure / High Temperature |
| ID | Inner Diameter |
| JIP | Joint Industry Project |
| LB | Lower Bound |
| OD | Outer Diameter |
| OTC | Offshore Technology Conference |
| PLET | Pipeline End Terminations |
| SCR | Steel Catenary Riser |
| SMYS | Specified Minimum Yield Stress |
| THK | Thickness |
| TDP | Touchdown Point |
| UB | Upper Bound |
| VAP | Virtual Anchor Point |
| WD | Water Depth |

TABLE OF CONTENTS

| | |
|---|------|
| ABSTRACT ----- | I |
| ACKNOWLEDGEMENTS ----- | II |
| NOMENCLATURE ----- | III |
| TABLE OF CONTENTS ----- | VI |
| TABLE OF FIGURES ----- | X |
| TABLE OF TABLES ----- | XIII |
| | |
| 1. Introduction ----- | 1 |
| 1.1 Background----- | 1 |
| 1.2 Problem Identification----- | 1 |
| 1.3 Purpose and Scope----- | 2 |
| 1.4 Organization of Thesis----- | 3 |
| 2. Literature Review ----- | 4 |
| 2.1 General----- | 4 |
| 2.2 Pipeline Expansion----- | 4 |
| 2.2.1 Causes of Expansion [6]----- | 4 |
| 2.2.1.1 Thermal Strain ($\epsilon_{thermal}$)----- | 4 |
| 2.2.1.2 Pressure Effects----- | 5 |
| 2.2.1.3 Combined Thermal and Pressure----- | 5 |
| 2.2.2 Effective Axial Force----- | 6 |
| 2.2.2.1 Fully-Constrained Effective Force----- | 7 |
| 2.2.2.2 Build-up of Effective Axial Force----- | 8 |
| 2.2.3 Virtual Anchor Point (VAP)----- | 9 |
| 2.3 Governing Parameters in Pipeline Walking [1]----- | 10 |
| 2.3.1 Fully Mobilized----- | 10 |

| | |
|---|-----------|
| 2.3.2 Full Cyclic Constraint----- | 11 |
| 2.3.3 Cyclic Constraint----- | 11 |
| 2.4 Pipeline Walking Mechanisms----- | 13 |
| 2.4.1 Steel Catenary Riser (SCR) Tension----- | 13 |
| 2.4.1.1 Derivation of Walk per cycle due to SCR Tension [1]----- | 15 |
| 2.4.2 Seabed Slope----- | 17 |
| 2.4.2.1 Derivation of Walk per cycle due to Seabed Slope [1]----- | 17 |
| 2.4.3 Thermal Transients along the Pipeline----- | 18 |
| 2.4.3.1 Thermal loading and transients----- | 19 |
| 2.4.3.2 Derivation of Walk per cycle due to Thermal Transients [1]----- | 21 |
| 2.5 Pipe-Soil Interaction----- | 23 |
| 2.5.1 Pipeline Embedment----- | 23 |
| 2.5.2 Axial Pipe-Soil Resistance [30]----- | 24 |
| 2.6 Summary----- | 25 |
| 3. Research Design----- | 27 |
| 3.1 General----- | 27 |
| 3.2 Preparation for Research Model [20]----- | 27 |
| 3.2.1 Modeling a Pipeline----- | 27 |
| 3.2.2 Temperature Profile Preparation----- | 27 |
| 3.2.3 Thermal Load Application----- | 28 |
| 3.2.4 Pipe-Soil Interaction Application----- | 28 |
| 3.3 Element Types Used in Finite Element Analysis Model----- | 29 |
| 3.3.1 Pipeline Model----- | 29 |
| 3.3.2 Seabed Model----- | 30 |
| 3.4 Process of Finite Element Analysis (FEA)----- | 33 |
| 4. Case Study Description----- | 35 |

| | |
|--|-----------|
| 4.1 General----- | 35 |
| 4.2 Pipeline Model ----- | 35 |
| 4.2.1 Pipeline Parameter----- | 35 |
| 4.2.2 Pipe Material Property----- | 36 |
| 4.3 Input Data ----- | 37 |
| 4.3.1 Operating Data ----- | 37 |
| 4.3.2 Environmental and Soil Data ----- | 38 |
| 5. Results and Discussion ----- | 39 |
| 5.1 General----- | 39 |
| 5.2 Pipeline Response Analysis Results ----- | 39 |
| 5.2.1 Effective Axial Force Profile----- | 40 |
| 5.2.2 Pipeline Cumulative Displacement----- | 43 |
| 5.2.3 Axial Displacement: Walking----- | 47 |
| 5.2.3.1 Walking at Mid-Point ----- | 47 |
| 5.2.3.2 Walking at Two Ends (Hot/Cold)----- | 48 |
| 5.3 Pipeline Response upon Axial Friction Factor----- | 50 |
| 5.3.1 Effective Axial Force Profile----- | 50 |
| 5.3.2 Axial Displacement----- | 54 |
| 5.3.2.1 Mid-Point Axial Displacement----- | 54 |
| 5.3.2.2 Axial Displacement with Friction Factor 2.0----- | 56 |
| 5.4 Mitigation Measures for Pipeline Walking----- | 57 |
| 5.4.1 Anchoring [11] ----- | 57 |
| 5.4.2 Increase Axial Friction [1] ----- | 58 |
| 5.4.2.1 Pipe-Soil Interaction----- | 58 |
| 5.4.2.2 Pipeline Weight Coating----- | 58 |
| 5.4.2.3 Trench and Bury----- | 58 |

| | |
|---|---------------|
| 5.4.2.4 Rock Dumping and Mattress----- | 59 |
| 5.4.3 Increase Subsea Connection Line Capacity----- | 60 |
| 5.5 Summary ----- | 60 |
| 6. Conclusion and Further Study ----- | 61 |
| 6.1 General----- | 61 |
| 6.2 Conclusions ----- | 61 |
| 6.3 Further Study ----- | 62 |
| REFERENCE ----- | 63 |
| Appendix I----- | AI-1 |
| Appendix II ----- | AII-1 |
| Appendix III ----- | AIII-1 |
| Appendix IV-1----- | AIV-1 |
| Appendix IV-2----- | AIV-26 |
| Appendix V----- | AV-1 |

TABLE OF FIGURES

| | |
|--|----|
| Figure 1.1: Offshore Pipeline System (Yong Bai, 2005) [24] | 2 |
| Figure 2.1: Conventional S-lay Installation (Olav Fyrileiv et al., 2005) [9]..... | 6 |
| Figure 2.2: Effective Axial Force for a Range of Friction in a Straight Pipeline (David A.S. Bruton et al., 2008) [10] | 7 |
| Figure 2.3: Typical Virtual Anchor Point for Pipeline (Class note by Qiang Chen) [6] | 9 |
| Figure 2.4: Effective Axial Force in a Short Straight Pipeline (David Bruton et al., 2005) [12] | 9 |
| Figure 2.5: A Typical Force Profile for a Fully Mobilized Pipeline (D. Bruton et al., 2006) [1]..... | 10 |
| Figure 2.6: A Typical Force Profile for a Fully Constrained Pipeline (D. Bruton et al., 2006) [1]..... | 11 |
| Figure 2.7: A Typical Force Profile for a Cyclically Constrained Pipeline (D. Bruton et al., 2006) [1].... | 12 |
| Figure 2.8: A Typical Subsea Tieback with SCR, Pipeline and PLET (M. Brunner et al., 2006) [17] | 13 |
| Figure 2.9: A Force Profile – SCR at Cold End (D. Bruton et al., 2006) [1]..... | 14 |
| Figure 2.10: An Axial Force Profile by Asymmetrical Loading (Gautam Chaudhury, 2010) [11]..... | 15 |
| Figure 2.11: Seabed Slope including its sign convention (D. Bruton et al., 2006) [1] | 17 |
| Figure 2.12: A Force Profile - Seabed Slope (D. Bruton et al., 2006) [1] | 17 |
| Figure 2.13: A Typical Thermal Transients (D. Bruton et al., 2006) [1]..... | 19 |
| Figure 2.14: An Example of Force Profile – First Heat-up (D. Bruton et al., 2006) [1]..... | 20 |
| Figure 2.15: An Example of Force Profile – Second Heat-up (D. Bruton et al., 2006) [1] | 20 |
| Figure 2.16: Analytical Model (D. Bruton et al., 2006) [1] | 22 |
| Figure 2.17: Initial Pipeline Embedment (D. Bruton et al., 2008) [10] | 23 |
| Figure 2.18: Axial Pipe-Soil Resistance Behavior (D. Bruton et al., 2008) [10]..... | 24 |
| | |
| Figure 3.1: Temperature Transients used in Pipeline Walking Analysis..... | 28 |
| Figure 3.2: PIPE288 Geometry (ANSYS Inc. 2009) [21] | 29 |
| Figure 3.3: Pipeline Model of PIPE288 Element..... | 30 |
| Figure 3.4: Node-to-Surface Contact Elements (ANSYS Inc. 2009) [23]..... | 31 |
| Figure 3.5: Geometry of TARGE170 (ANSYS Inc. 2009) [21] | 32 |
| Figure 3.6: Segment Types of TARGE170 (ANSYS Inc. 2009) [21] | 32 |
| Figure 3.7: Pipeline and Seabed Modeling in ANSYS | 33 |
| | |
| Figure 4.1: Proposed de-rating values for yield stress of C-Mn steel (DNV-OS-F101, 2012)..... | 37 |

| | |
|---|-------|
| Figure 4.2: Ramberg-Osgood Stress-Strain Curve for API 5L X65 (at 20°C & 88°C) | 37 |
| Figure 5.1: Interpolated Temperature Load Profile for 88°C | 39 |
| Figure 5.2: Effective Axial Force for 1st Cycle | 40 |
| Figure 5.3: Effective Axial Force for 2nd Cycle | 40 |
| Figure 5.4: Effective Axial Force for 3rd Cycle | 41 |
| Figure 5.5: Effective Axial Force for 4th Cycle | 41 |
| Figure 5.6: Effective Axial Force for 5th Cycle | 42 |
| Figure 5.7: Pipeline Displacement for 1st Cycle | 43 |
| Figure 5.8: Pipeline Displacement for 2nd Cycle | 43 |
| Figure 5.9: Pipeline Displacement for 3rd Cycle | 44 |
| Figure 5.10: Pipeline Displacement for 4th Cycle | 44 |
| Figure 5.11: Pipeline Displacement for 5th Cycle | 45 |
| Figure 5.12: Axial Walking at Mid-Point | 47 |
| Figure 5.13: Axial Walking at Hot End | 48 |
| Figure 5.14: Axial Walking at Cold End | 48 |
| Figure 5.15: Axial Walking Displacement | 49 |
| Figure 5.16: Effective Axial Force for 1st Cycle with Friction factor 0.3 | 50 |
| Figure 5.17: Effective Axial Force for 1st Cycle with Friction factor 0.5 | 50 |
| Figure 5.18: Effective Axial Force for 1st Cycle with Friction factor 0.7 | 51 |
| Figure 5.19: Effective Axial Force for 1st Cycle with Friction factor 2.0 | 51 |
| Figure 5.20: Effective Axial Force for 4th Cycle with Friction Factor 0.5 | 52 |
| Figure 5.21: Effective Axial Force for 5th Cycle with Friction Factor 0.5 | 52 |
| Figure 5.22: Effective Axial Force for 4th Cycle with Friction Factor 0.7 | 53 |
| Figure 5.23: Effective Axial Force for 5th Cycle with Friction Factor 0.7 | 53 |
| Figure 5.24: Axial Walking Displacement at Mid-Point with Friction Factor 0.3, 0.5 & 0.7 | 55 |
| Figure 5.25: A Typical Pipeline Restraining Anchor (Ryan Watson et al., 2010) [16] | 57 |
| Figure 5.26: A Trenching Operation (from www.theareofdreiging.com) | 59 |
| Figure 5.27: A Rock Dumping Operation (from www.nordnes.nl) | 59 |
| Figure A-II.1 Temperature Transients used in Pipeline Walking Analysis | AII-2 |
| Figure A-V.1: Effective Axial Force for 2nd Cycle with Friction factor 0.5 | AV-2 |

| | |
|--|------|
| Figure A-V.2: Effective Axial Force for 3rd Cycle with Friction factor 0.5 | AV-2 |
| Figure A-V.3: Effective Axial Force for 2nd Cycle with Friction factor 0.7 | AV-3 |
| Figure A-V.4: Effective Axial Force for 3rd Cycle with Friction factor 0.7 | AV-3 |
| Figure A-V.5: Effective Axial Force for 2nd Cycle with Friction factor 2.0 | AV-4 |
| Figure A-V.6: Effective Axial Force for 3rd Cycle with Friction factor 2.0 | AV-4 |
| Figure A-V.7: Effective Axial Force for 4th Cycle with Friction factor 2.0 | AV-5 |
| Figure A-V.8: Effective Axial Force for 5th Cycle with Friction factor 2.0 | AV-5 |
| Figure A-V.9: Axial Walking Displacement at Mid-Point | AV-6 |

TABLE OF TABLES

| | |
|--|----|
| Table 4.1: Pipeline Design Data and Material Properties | 35 |
| Table 4.2: Coating Parameters | 36 |
| Table 4.3: Operating parameters | 37 |
| Table 4.4: Environmental Data | 38 |
| Table 4.5: Environmental Data (Soil Conditions)..... | 38 |
| | |
| Table 5.1: Hot-End Pipe Displacement..... | 45 |
| Table 5.2: Cold-End Pipe Displacement..... | 46 |
| Table 5.3: Mid-Point Pipe Displacement..... | 46 |
| Table 5.4: Mid-Point Axial Displacement with Friction Factor 0.5 | 54 |
| Table 5.5: Mid-Point Axial Displacement with Friction Factor 0.7 | 55 |
| Table 5.6: Results of Walking Rate | 56 |
| Table 5.7: Mid-Point Axial Displacement with Friction Factor 2.0 | 56 |

1. Introduction

1.1 Background

The instability phenomenon of subsea pipelines associated to high pressures and temperatures has become a critical aspect for the design of pipelines. As design conditions become more challenging, primarily due to increasing operating temperatures, much attention has been focused on controlling thermal expansion. The pipelines particularly are laid down on the seabed and the capacity of PLETs (pipeline end terminations) and/or in-line structure to absorb expansion may be limited. [3]

Conventionally, it interprets the design criteria of such structures by calculating the expansion under maximum operating conditions, and the pipeline is assumed to expand and contract within the stable limit. However, the real situation shows much more complicated than that under cyclic loadings. As the operating conditions are cycled the basic expansion and contraction can be accompanied by axial ratcheting behavior. This behavior is known as “pipeline walking”. [2]

Pipeline walking is another major design challenge, which has been observed in operating pipeline systems. This phenomenon occurring in start-up/shut-down cycles cause a cumulative axial displacement of a high temperature and short pipeline¹. It expands and contracts when it is subjected to different operational conditions: starting from hydro-test to operational pressure, operational temperature heating, and shut-down cooling to ambient temperature.

The pipeline failure will not happen due to the axial walking itself unless the pipeline is susceptible to buckling. However, as a result of the accumulated global displacement over a number of cycles, the axial walking may make an impact on the failure of tie-in jumpers/spools. It may also lead to localized failure because of the increased loading within a lateral buckle. [3] Therefore, this issue is worth taking into account at the design stage since its occurrence may have a major influence on the field layout and development, which can have a huge impact on the project cost and development.

1.2 Problem Identification

When it comes to the short HT/HP pipeline, i.e. a partially restrained system, a large transient cumulative expansion is to be considered during the design phase. [5] It is because when the pipeline undergoes multiple operational cycles (start-up/shutdown) with thermal gradients, the entire system experiences a global axial displacement (walking) phenomenon.

¹ The term ‘short’ related to pipelines that do not reach full constraint, but expand about a virtual anchor point located at the middle of the pipeline. [1]

Besides, the presence of a tension due to a steel catenary riser (SCR) connected to the pipeline or a significant seabed slope also causes the walking.

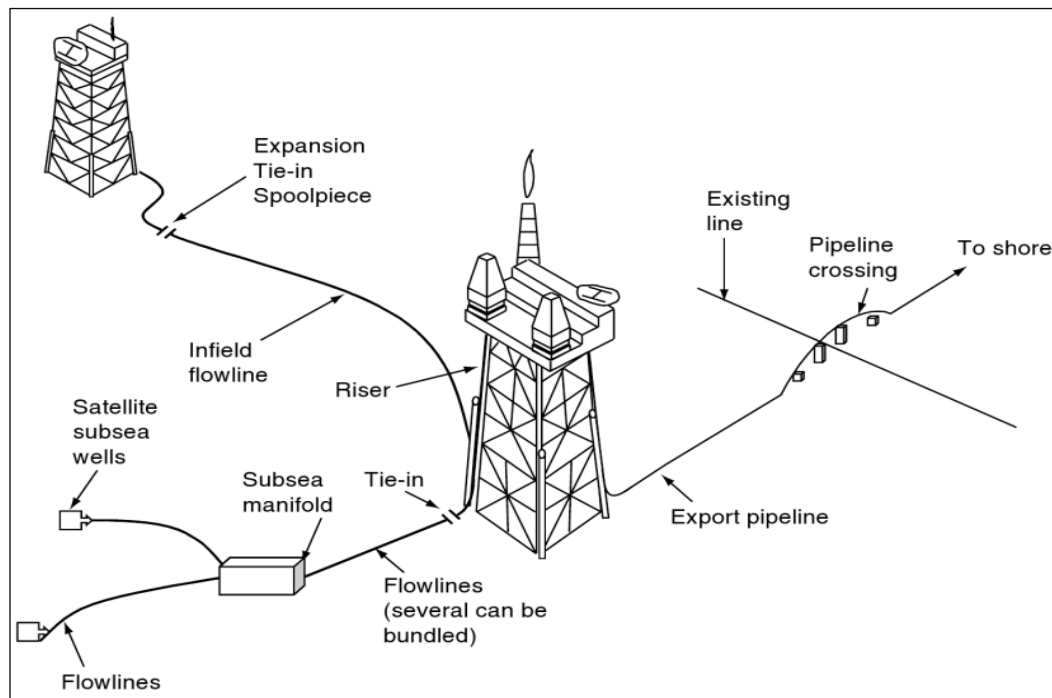


Figure 1.1: Offshore Pipeline System (Yong Bai, 2005) [24]

Consequently, the walking phenomenon may lead to irreparable damage to the subsea structures which are shown in Figure 1.1, Moreover, six failures were reported by the end of 2000 in North Sea due to excessive expansion of the pipeline, and at least one loss of containment failure due to pipeline walking has been observed. [19]

1.3 Purpose and Scope

The aim of the thesis work is to understand the pipeline walking phenomenon, key factors that influence on walking and study how to assess the severity of the walking problem particularly focusing on the pipeline under the high temperature condition.

The scope is to be based on the pipeline walking mechanisms that have been investigated by SAFEBUCK JIP: [1]

- Sustained tension at the end of the pipeline, associated with a steel catenary riser (SCR);
- Global seabed slope along the pipeline length;
- Thermal transients along the pipeline during shutdown and restart operations.

The finite element analysis modeling is used to identify and analyze the pipeline walking phenomenon. The short and high temperature pipeline is demonstrated with asymmetric loads originated from the thermal transients. In addition to that, it defines a relevant walking scenario to look into parameters such as axial friction factors that influence on occurring the walking as a sensitivity study. Based on it, the possible mitigation methods are discussed.

1.4 Organization of Thesis

- Chapter 2: Presents the theoretical background of important parameters related to the temperature and pressure loadings causing pipeline axial displacements including the pipe-soil interaction. Furthermore, main mechanisms for the pipeline to walk are dealt with.
- Chapter 3: Provides the methodology that is used in the thesis work. It presents preparation of research models such as pipeline/seabed models, and temperature load profiles in the FEA by using ANSYS 13.0 (Mechanical APDL) software.
- Chapter 4: Describes data in the case study in order to perform the FEA. It gives detailed values of pipeline modeling information and the environmental conditions for the pipeline walking analysis.
- Chapter 5: Explains the results of the FEA based on Ch.3 and Ch.4. The sensitivity study results are also presented considering the interaction between the walking rate and axial friction factors. Lastly, mitigation measures for pipeline walking are briefly introduced in connection with the results in the chapter.
- Chapter 6: Presents the conclusions of the thesis work based on Ch.5 and the further works.

2. Literature Review

2.1 General

It is to be easy to manage the axial stability of the subsea pipelines if they are under comparatively low pressures and temperatures because their responses to the loading, by high axial force distribution along the length of the pipelines, are not the serious problem. In contrast, a HP/HT pipeline system impacts on the pipeline design since the instability phenomenon such as end-expansion and potential for high stresses can be severe, which deteriorates the pipeline integrity.

This chapter presents the theoretical explanation of important subjects and parameters related to the HP/HT loadings leading to pipeline axial movements, and mechanisms of pipeline walking. Furthermore, it deals with the pipe-soil interaction to look into the effect of the soil resistance (parameters) for preparation of the sensitivity study.

2.2 Pipeline Expansion

The pipeline expansion may takes place due to operating pressures and temperatures at its two ends. As being developed in higher pressure and temperature fields, the pipeline expansion instability phenomenon such as axial creeping (walking), buckling (upheaval and lateral movements), or a combination of both is taken into account in the pipeline design. The substantial movement by expansion, particularly at platforms, is important because it can overstress risers and elbows, and bring the pipe into contraction with the platform itself. [4]

2.2.1 Causes of Expansion [8]

Three main reasons are contributing to the end force and expansion which are inducing pipeline walking and lateral/upheaval buckling as follows:

- Temperature (Thermal);
- Pressure (End-cap force);
- Poisson contraction (associated with pressure effects).

2.2.1.1 Thermal Strain ($\epsilon_{thermal}$)

The thermal strain occurs due to temperature difference between installation and operation. When it is under unrestrained condition, the temperature rise causes an expansion given by equation 2.1:

$$\epsilon_T = a_T \Delta T \quad (2.1)$$

Where,

a_T : Thermal expansion coefficient ;

ΔT : Temperature difference ($^{\circ}\text{C}$).

2.2.1.2 Pressure Effects

a) End-Cap effect

It occurs at any curvatures along the pipeline, and the axial loadings take place due to the differential pressure loading across the pipe, i.e. compression. The strain at the pipeline due to end cap effect becomes equation 2.2:

$$\varepsilon_{end\ cap} = \frac{\Delta P \cdot D}{4t \cdot E} \quad (2.2)$$

Where,

ΔP : Differential internal pressure across the pipe wall ($=P_i - P_{hyd}$);

D : Internal diameter;

E : Young's modulus.

b) Poisson Effect

The hoop stress and the corresponding circumferential strain are induced by the internal pressure. The former causes a longitudinal contraction, and the latter gives axial contraction on pipeline, i.e. the pipe expands in the hoop direction, and the Poisson's effect results in an axial contraction (opposite to end cap pressure effect). Under the unrestrained condition, the expansion/strain due to Poisson's effect becomes equation 2.3:

$$\varepsilon_{poisson} = -\frac{\nu\sigma_H}{E} \quad (2.3)$$

Where,

ν : Poisson's ratio;

σ_H : Hoop stress.

2.2.1.3 Combined Thermal and Pressure

Consequently, the total strain for the unrestrained condition is given by equation 2.4:

$$\varepsilon_{total} = \frac{\sigma_H (1 - 2\nu)}{2E} + a_T \Delta T \quad (2.4)$$

2.2.2 Effective Axial Force

The concept of the effective axial force can be used to understand the pipeline expansion phenomenon. It is composed of the true axial force in the pipe wall and the pressure induced axial force, so it is defined as equation 2.5: [1]

$$S = S_w + P_e A_e - P_i A_i \quad (2.5)$$

Where,

- S: Effective axial force (N);
- S_w : True axial force (N);
- P_e : External pressure (Pa);
- P_i : Internal pressure (Pa);
- A_e : Cross sectional area of pipe (OD: m^2);
- A_i : Cross sectional area of pipe (ID: m^2).

By considering a conventional S-lay installation illustrated in Figure 2.1, the effective axial force in the pipeline after installation can be estimated, and the concept of residual lay tension (S_L) can be used to define the effective axial force after installation as given by equation 2.6: [9]

$$S_w = S_L - P_e A_e \quad (2.6)$$

Where,

- S_L : Residual lay tension (N).

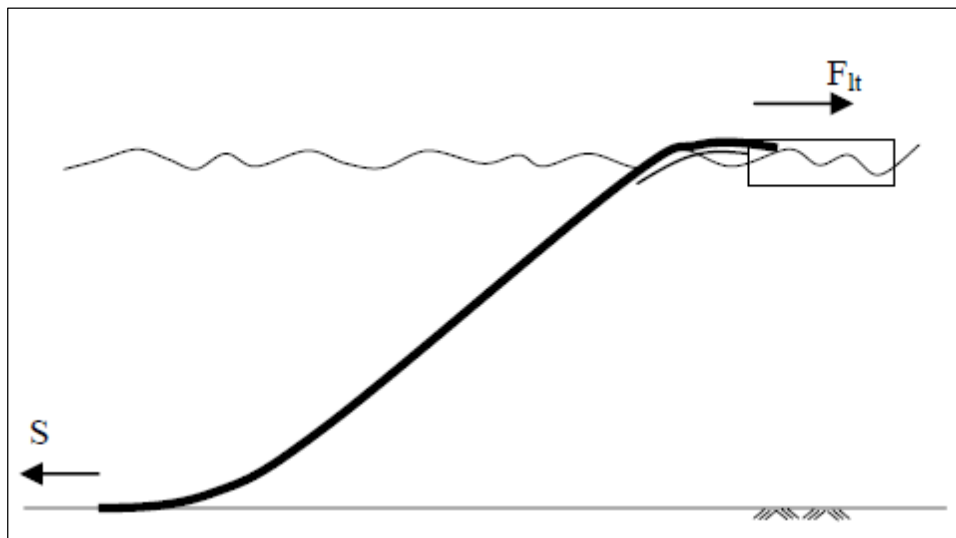


Figure 2.1: Conventional S-lay Installation (Olav Fyrileiv et al., 2005) [9]

As the pipeline operated, the thermal expansion ($-A_s a_T E \Delta T$) takes place and it makes the true axial force get into compression. At the same time, the hoop stress and Poisson's effect

($v\sigma_H A_s$) lead to tension in the true axial force. [9] Thus, based on the equation 2.5, the effective axial force can be shown as equation 2.7 if fully restrained²:

$$S = S_L - P_i A_i + v A_s \sigma_H - A_s a_T E \Delta T$$

$$\approx S_L - P_i A_i [1 - 2v] - A_s a_T E \Delta T \quad (2.7)$$

Where,
 $\sigma_H: \frac{P_i \cdot D_i}{2t}$;
 A_s : Cross sectional area of pipe wall (m^2).

Moreover, the change in fully constrained force associated with an unload case is given as equation 2.8 since it considers cyclic loadings of the pipeline: [1]

$$\Delta S = -(P_2 - P_1) A_i [1 - 2v] - A_s a_T E (\theta_2 - \theta_1) \quad (2.8)$$

Where,
 Subscript figures (1 & 2) indicate conditions before and after the operating changes.

2.2.2.1 Fully-Constrained Effective Force

The fully-constrained effective force represents the maximum effective axial force that occurs in the pipeline. Since the ends of the pipeline are usually free to expand, the force at the ends is zero. However, as the cumulative axial resistance increases with distance from the pipeline ends, the force can reach to a fully-constrained condition, as presented in Figure 2.2. [10]

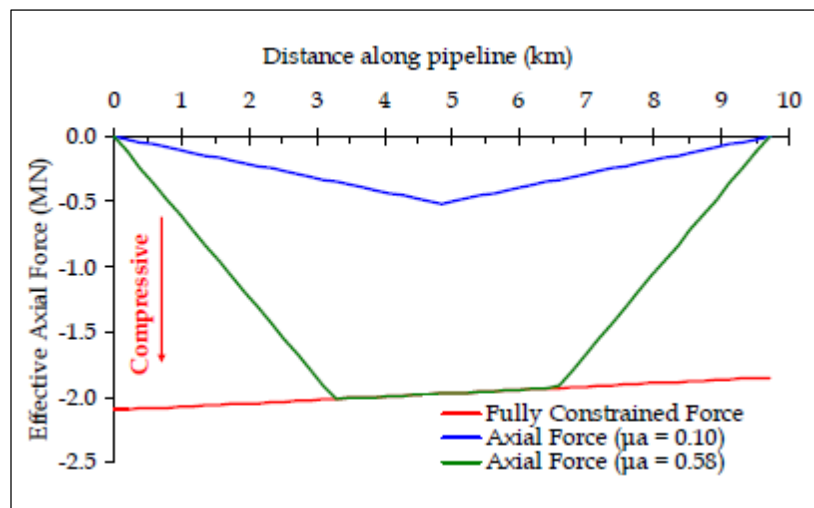


Figure 2.2: Effective Axial Force for a Range of Friction in a Straight Pipeline (David A.S. Bruton et al., 2008) [10]

² The axial strain in the pipeline is zero is known as the fully constrained – not allows to slide axially. [1]

The Figure 2.2 also shows that the fully-constrained force is to change (slightly fall) with the variation of pressure and temperature along the pipeline length.

2.2.2.2 Build-up of Effective Axial Force

The level of the cumulative axial restraint due to the seabed resistance influences on increments of the effective axial force. As it moves toward the pipeline end, furthermore, the effective axial force is reduced from the virtual anchor zone due to end expansion as shown in Figure 2.2. The axial force decrease along the pipeline from anchor point is governed by the axial friction between the pipeline and soil. Hence, the selection of the pipe-soil axial resistance factor is important for the load force calculations. [31]

It is defined as “full cyclic constraint” when no axial displacement occurs over a certain length of pipe, and “fully mobilized” where axial displacement occurs over the full length of the pipeline. In addition, the slope of the force profile shown in the Figure 2.2 is defined by the axial resistance (force) per unit length: [11]

$$f = \mu_a \cdot W_{\text{sub}} \quad (2.9)$$

Where,

f : Axial friction force (N/m);

μ_a : Friction coefficient;

W_{sub} : Submerged pipeline weight (N/m).

Regarding a free-ended short pipeline (curved in blue in Figure 2.2, it does not reach the full constraint, and the maximum axial force can be significantly below the fully constraint force. In this case the effective axial force is solely produced by friction force. Hence, the effective axial force can be defined by the axial friction force.

The level of axial friction on the effective force profile in Figure 2.2 is an important parameter. Depending on either the lower bound friction or the upper bound friction (here $\mu_a = 0.1$ and 0.58 respectively), which are based on lower and upper bound soil responses that correspond to drained and undrained axial movements, variations in the EAF can be expected. Thus, the pipe-soil interaction has been importantly taken into account in a real design case. [10]

The operating condition and the axial friction influence on compressive effective axial forces in the pipeline. Particularly, when the compressive force is large enough, the pipeline may be susceptible to lateral buckling. However, a deeper investigation and demonstration on the issue of lateral buckling is not performed in this thesis. Instead, the theoretical research on the pipe-soil interaction is briefly dealt with at the end of this chapter.

2.2.3 Virtual Anchor Point (VAP)

The term of VAP is defined that the point where the expansion force (restraining force) is equivalent to the soil frictional force, so the pipeline becomes fully restrained at this point. [7]

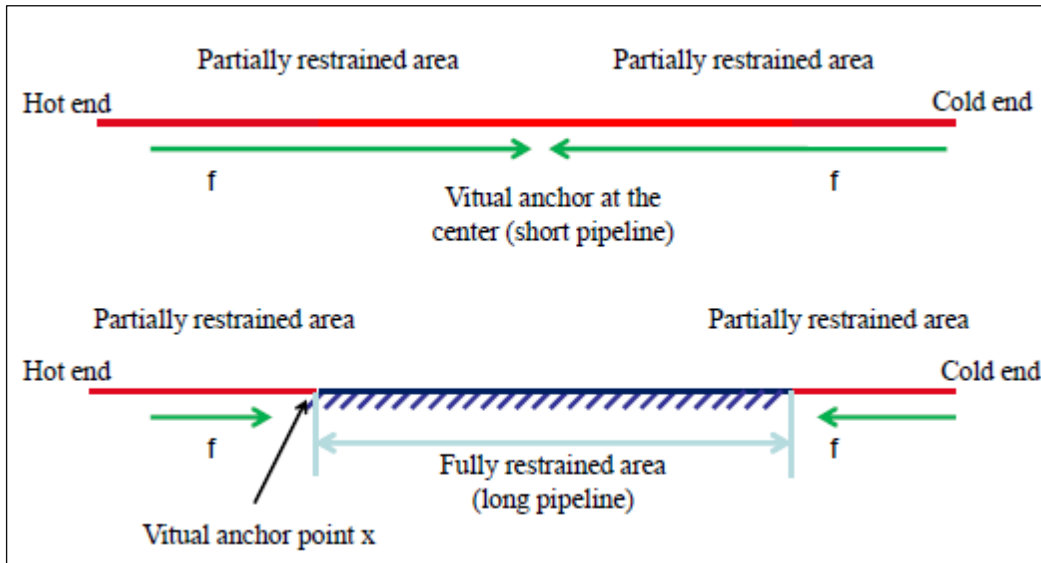


Figure 2.3: Typical Virtual Anchor Point for Pipeline (Class note by Qiang Chen) [6]

For a short pipeline, the overall length may be insufficient to reach full restraint and the VAP is generally situated at the middle of it where the effective axial force gets the maximum value. [13]

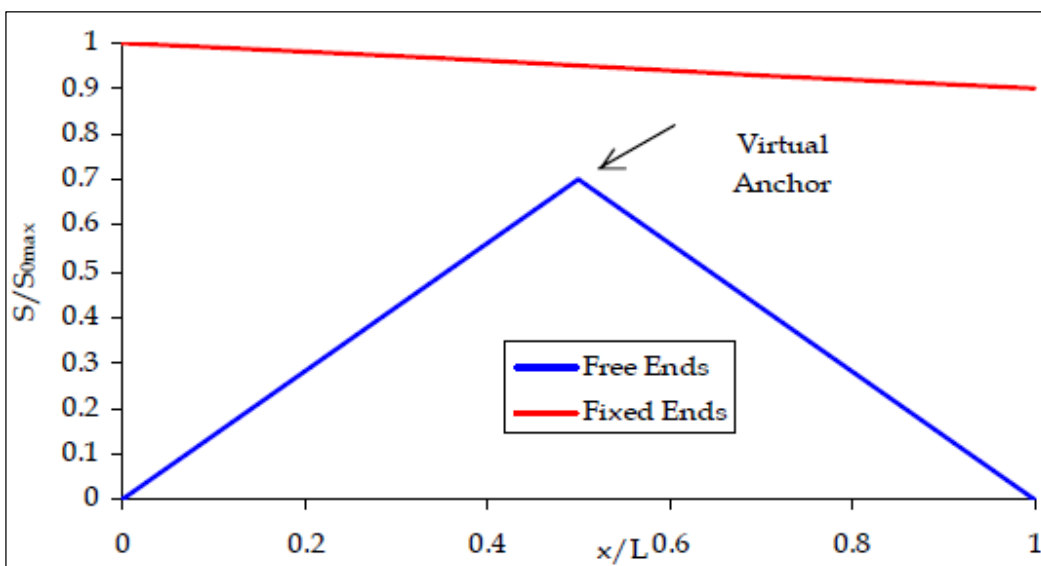


Figure 2.4: Effective Axial Force in a Short Straight Pipeline (David Bruton et al., 2005) [12]

2.3 Governing Parameters in Pipeline Walking [1]

As the level of axial friction (constraint) is the important parameter on the effective axial force, it is also one of the essential parameters to assess pipeline walking since its value varies during start-up and shutdown cycles. This section deals with parameters and their conditions for occurring the walking in terms of the constraint friction force and the axial friction force.

2.3.1 Fully Mobilized

Generally, a pipeline is considered as a short pipeline under the fully mobilized condition which is leading to pipeline walking. The mathematical definition of the fully mobilized condition in the pipeline is given in terms of the relationship between the constraint friction force (f^*) and the axial friction force (f):

$$\frac{f}{f^*} < 1 \quad (2.10)$$

Where,

f^* : Constraint friction force = $\frac{|\Delta P|}{L}$;

L: Length of pipeline.

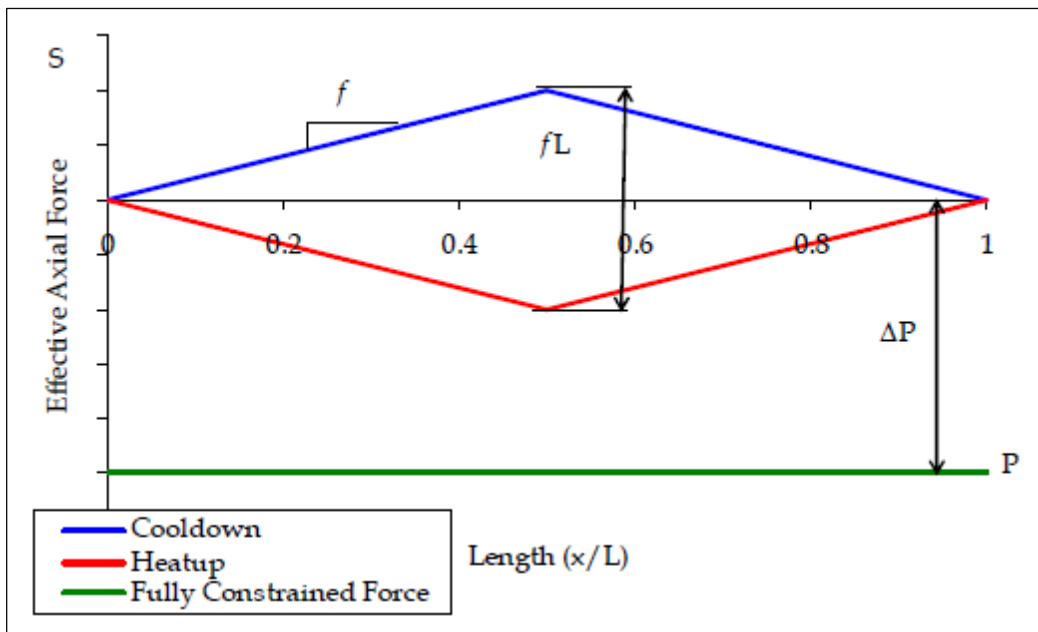


Figure 2.5: A Typical Force Profile for a Fully Mobilized Pipeline (D. Bruton et al., 2006) [1]

2.3.2 Full Cyclic Constraint

Being fully constrained means no occurrence of axial displacement over a portion of the pipeline, and it is applied to the long pipeline whose force profiles change considerably, as illustrated in Figure 2.6:

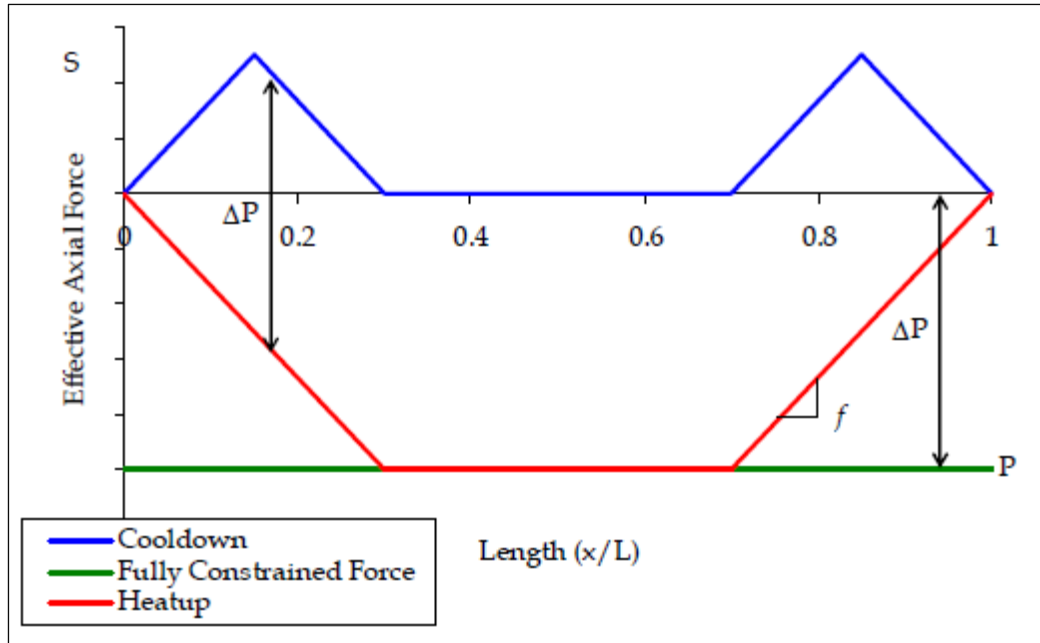


Figure 2.6: A Typical Force Profile for a Fully Constrained Pipeline (D. Bruton et al., 2006) [1]

According to the Figure 2.6, it shows the relationship between the constraint friction force (f^*) and the axial friction force (f) for the pipeline to reach full constraint, and the relationship is given as equation 2.11:

$$\frac{f}{f^*} > 2 \quad (2.11)$$

In addition to that, it indicates the walking phenomenon is to be prevented especially in the fully constrained section unless the gradient of the thermal transient is tremendously high.

2.3.3 Cyclic Constraint

In some cases, the pipeline becomes cyclically constrained after a certain number of cycles when the partial restraint is achieved along the pipeline and walking curtailed. [3] The cyclically constrained case is shown in Figure 2.7. The walking phenomenon is depending on whether the system is reaching full constraint or not. If the system only just reaches cyclic constraint then the walking will be similar to that of the short pipeline. However, it will become constrained as the friction increases, i.e. reducing the walking. It appears when the constraint friction force (f^*) and the axial friction force (f) are in the relationship as equation 2.12:

$$1 < \frac{f}{f^*} < 2 \quad (2.12)$$

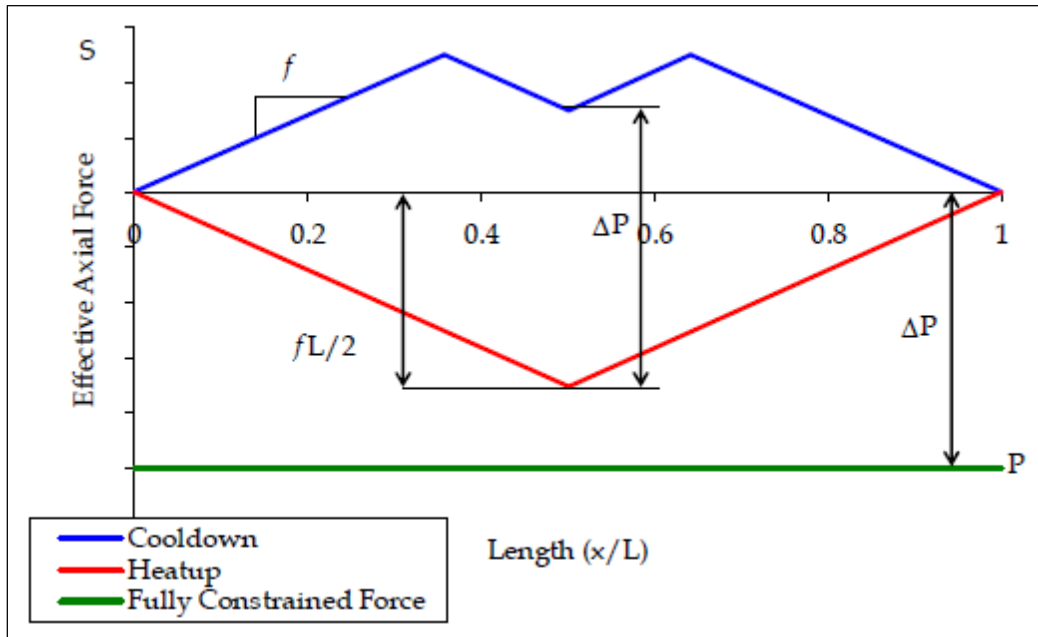


Figure 2.7: A Typical Force Profile for a Cyclically Constrained Pipeline (D. Bruton et al., 2006) [1]

2.4 Pipeline Walking Mechanisms

This section presents three main mechanisms in the pipeline walking phenomenon, which are related to a stepwise ratcheting that occurs during operations (shutdown and restart): [15]

- Steel catenary riser (SCR) tension;
- Seabed slope;
- Thermal transients along the pipeline (during heat-up/cooling cycles).

The recent researches and monitoring have identified a multiphase flow behavior during shutdown/restart operation as a new mechanism associated with pipeline walking. [16] However, the impact of multiphase flow on pipeline walking is not dealt with in this study.

2.4.1 Steel Catenary Riser (SCR) Tension

A SCR system is commonly used to tie the subsea pipeline into a floating facility in deepwater field development shown as Figure 2.8:

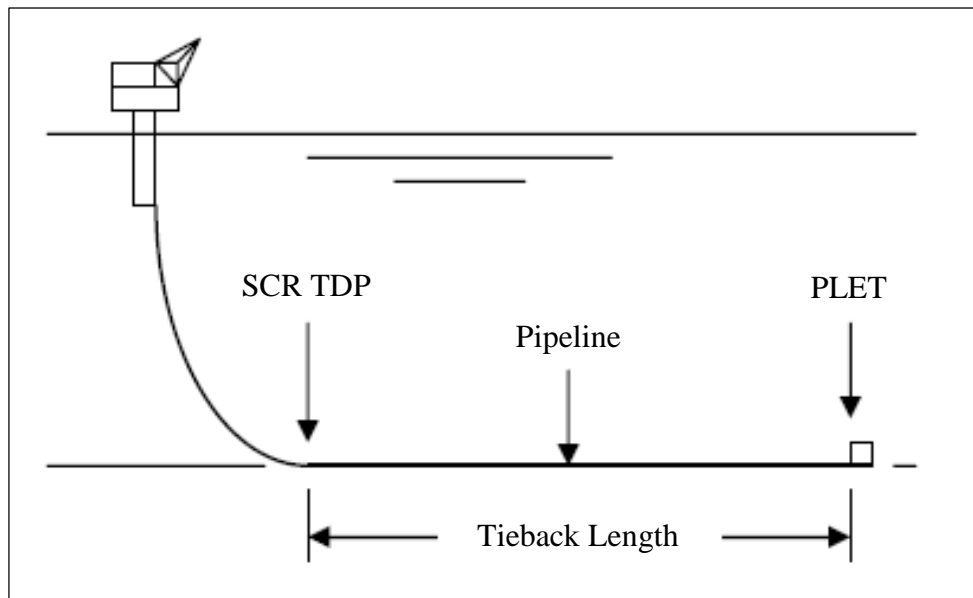


Figure 2.8: A Typical Subsea Tieback with SCR, Pipeline and PLET (M. Brunner et al., 2006) [17]

Pipeline walking is to take place in this system. It is not only because the pipeline is short enough to be considered under the fully mobilized condition but also a tension (S_R) applied by the SCR at the touch downpoint (TDP) can cause the short pipeline to walk during the heating and cooling cycles. This tension is specifically considered as constant since it assumes that a sufficient axial friction is axially stable in spite of the highest axial riser tension. [1]

An asymmetric load can occur from the applied tension either at one end or seabed slope or a combination of both (the seabed slope case is presented in section 2.4.2). It separates virtual anchors (between the heating and cooling) which are equivalent to net transferred force acting on the soil [11]. The Figure 2.9 shows the force profile for the fully mobilized pipeline attached to the SCR at the cold end. It indicates that the pipeline between point A and B expands towards the SCR during heat-up while contracts when cooling down.

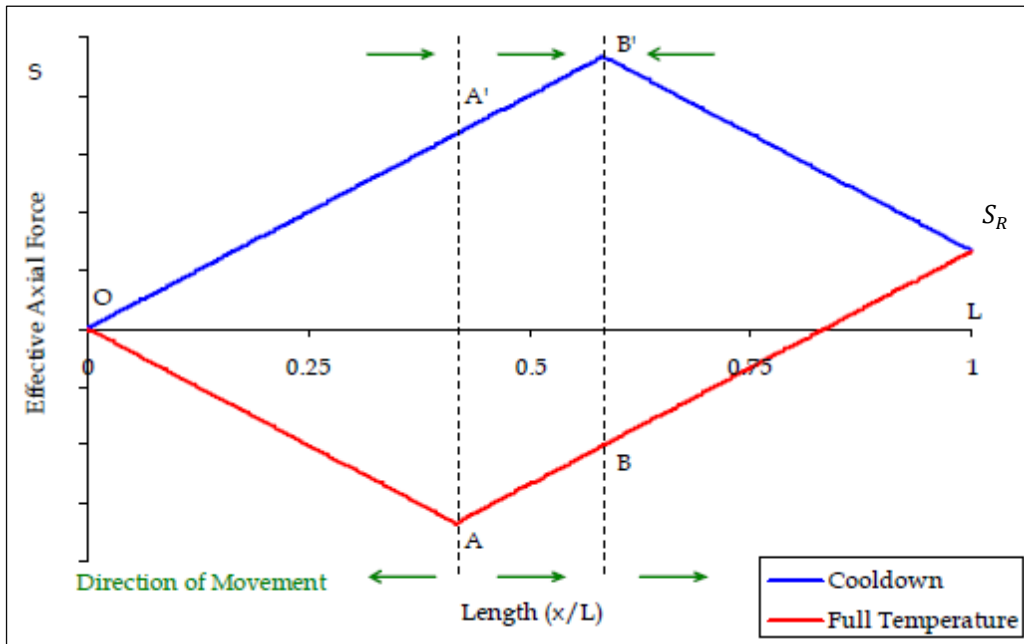


Figure 2.9: A Force Profile – SCR at Cold End (D. Bruton et al., 2006) [1]

2.4.1.1 Derivation of Walk per cycle due to SCR Tension [1]

The development of the analytical calculation for the pipeline walking rate can be derived by a typical axial force profile of the pipeline. If it is assumed that the pipeline system is under uniform heating and cooling cycle conditions during operation, it can be shown as Figure 2.10:

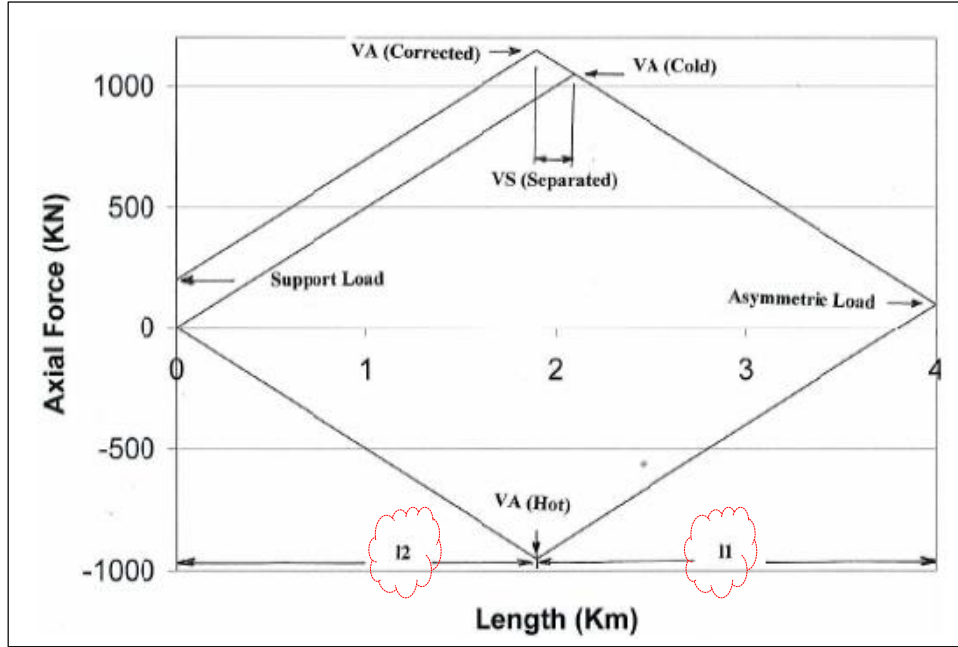


Figure 2.10: An Axial Force Profile by Asymmetrical Loading (Gautam Chaudhury, 2010) [11]

The separation distance between two virtual anchors (V_{ab}) can be given by equation 2.13:

$$V_{ab} = \frac{S_R}{f} \quad (2.13)$$

Where,

S_R : SCR Tension (N);

f : Axial friction force (N/m).

The lengths l_1 and l_2 given in Figure 2.10 (marked with circle), which is a distance between the virtual anchor point to pipe end (hot and cold end respectively), can be determined by equation 2.14: [11]

$$l_1 = \frac{L \cdot f + S_R}{2f}; \quad l_2 = \frac{L \cdot f - S_R}{2f} \quad (2.14)$$

Where,

L : Length of pipeline ($= l_1 + l_2$) (m).

The pipeline walking is the result of irregular strains during heating and cooling operations, so the analytical solutions of it is to be developed based on such strains. To derive the change in axial strain, the change in force over the length (V_{ab}) of the pipeline is firstly to be considered as equation 2.15:

$$\Delta S_f = S_R - L \cdot f \quad (2.15)$$

Where,

ΔS_f : Change in effective axial force over V_{ab} (N).

Hence, the change in axial strain that is related to the force change can be given by equation 2.16:

$$\Delta \varepsilon = \frac{(\Delta S_f - \Delta P)}{EA} \quad (2.16)$$

Where,

ΔP : Change in fully constrained force (N);

EA: Axial stiffness (N).

The walk per cycle (Δ_R) of the pipeline is the strain difference between two lengths: l_1 and l_2 . It is obtained by equation 2.17 which is based on equation 2.13 and 2.14:

$$\begin{aligned} \Delta_R &= l_1 \left(\Delta \varepsilon - \frac{l_1 \cdot f}{EA} \right) - l_2 \left(\Delta \varepsilon - \frac{l_2 \cdot f}{EA} \right) \\ &= \Delta \varepsilon (l_1 - l_2) - \frac{L \cdot f}{EA} (l_1 - l_2) = \Delta \varepsilon \cdot V_{ab} - \frac{L \cdot f}{EA} \cdot V_{ab} \\ &= V_{ab} \left(\Delta \varepsilon - \frac{L \cdot f}{EA} \right) \end{aligned} \quad (2.17)$$

Where,

Δ_R : Walk per cycle due to SCR Tension (m).

Finally, the walk per cycle due to the SCR tension is simply derived as equation 2.18 by combining equations 2.13 to 2.16:

$$\Delta_R = \frac{(|\Delta P| + S_R - L \cdot f) \cdot S_R}{EA} \quad (2.18)$$

Where,

$|\Delta P|$ implies conditions as follows: $\Delta P + S_R > L \cdot f$;

$\Delta P + S_R \leq L \cdot f$.

2.4.2 Seabed Slope

The fundamental analysis of a seabed slope condition case is essentially the same as the SCR tension case. [11] The difference between two cases is the resistance requires correction of the sine component load since a pipeline is laid on a seabed with a certain angle of slope (ϕ), as illustrated in Figure 2.11:

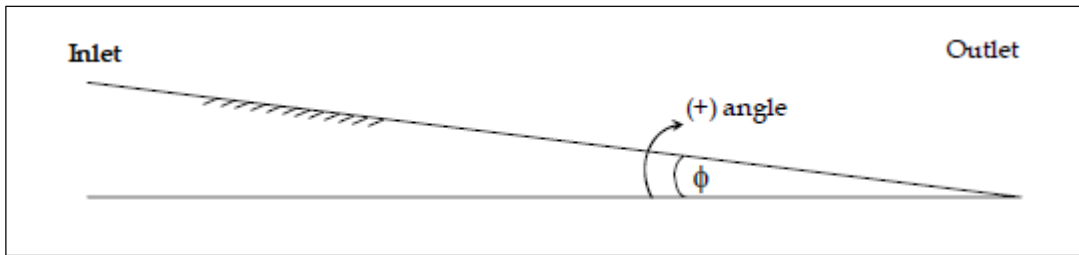


Figure 2.11: Seabed Slope including its sign convention (D. Bruton et al., 2006) [1]

However, the deriving equation of the walking rate in this section is based on a constant slope(ϕ). According to SAFEBUCK JIP design guideline, the average slope over the pipeline can be employed if the slope varies slowly, and a more complex assessment is to be required if the variation of slope is significant along the length. [15]

2.4.2.1 Derivation of Walk per cycle due to Seabed Slope [1]

The occurrence of the external unbalanced force in the seabed slope case is interpreted with a component of the pipeline weight which acts in the direction of expansion. Thus, depending on the position of slope (sloping down from inlet or sloping up from inlet), an asymmetry force profile can be presented as Figure 2.12, which is similar to the SCR case:

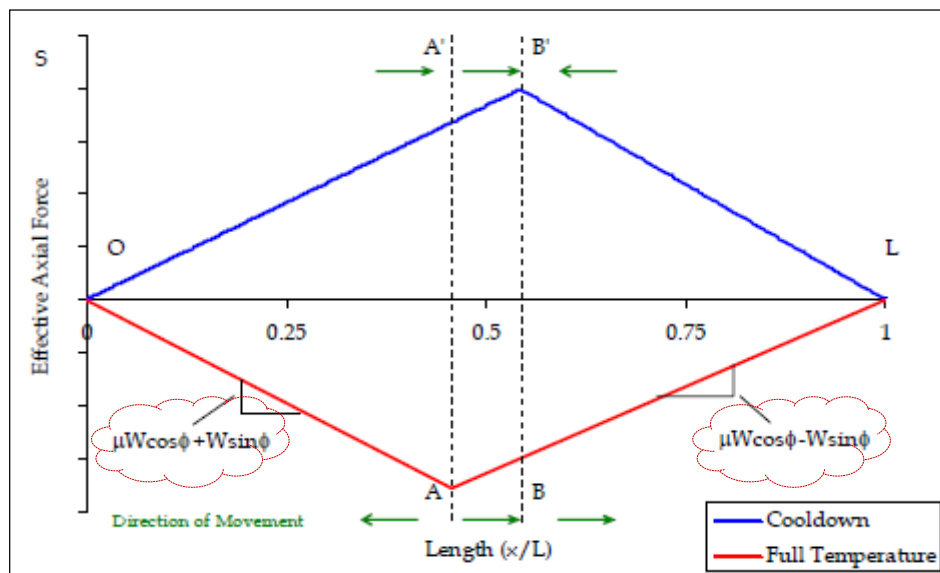


Figure 2.12: A Force Profile - Seabed Slope (D. Bruton et al., 2006) [1]

Therefore, the position of the two virtual anchors can be decided depending on a situation of pipeline sloping. For instance, if a pipeline slopes downwards from the inlet, the hot anchor (A) is located closer to the hot end and the cold anchor (B') closer to the cold end. The slope of the force profile (between A and B) remains the same on heat-up and cool-down. It indicates that the pipeline expands downhill towards B on heat-up and contracts downhill towards B on cool-down. As for the SCR case, the overall global displacement of the pipeline is governed by the central section (AB), which causes the whole pipeline to displace downhill, towards the cold end.

The distance between two virtual anchors (V_{ab}) in the seabed slope case can be given by equation 2.19:

$$V_{ab} = \frac{WL \cdot \sin \phi}{W\mu_a \cos \phi} = \frac{L \cdot \tan \phi}{\mu_a} \quad (2.19)$$

Where,
W (=W_{sub}): Submerged pipeline weight (N/m).

The change in force over the length of V_{ab} is given by equation 2.20, which is similar to equation 2.15:

$$\Delta S_s = -WL(\mu_a \cos \phi - |\sin \phi|) \quad (2.20)$$

Where,
|sin ϕ | implies the pipeline weight direction in Figure 2.12.

Finally, the derivation of walking rate (per cycle) due to seabed slope can be obtained as equation 2.21 based on the definitions, which is similar to SCR tension case, and equations both in section 2.4.1 and 2.4.2:

$$\Delta_{\phi} = \frac{[|\Delta P| + WL|\sin \phi| - WL \cdot \mu_a \cos \phi] \cdot L \tan \phi}{EA \cdot \mu_a} \quad (2.21)$$

Where,
 Δ_{ϕ} : Walk per cycle due to Seabed slope (m).

2.4.3 Thermal Transients along the Pipeline

Earlier two cases of the pipeline walking mechanism (SCR tension and seabed slope) are basically assumed with no thermal gradient. [11] As heating the pipeline, however, it is always associated with a temperature gradient. The asymmetric heating process due to the thermal gradient leads to shifting the virtual anchor points (VAP) during heat-up and cool-down cycles, and eventually pipeline walking occurs.

This section presents one of important mechanisms for pipeline walking: thermal transients. To assess pipeline walking when dominated by the thermal loading and transients, it is

vital to understand and examine the relationship between the transient thermal force profile and pipeline displacement in each cycle during heating and cooling. [1] Thus, it derives equations with respect to magnitude of walk from thermal gradient heating and presents relevant force profiles in the section.

Furthermore, the thesis work is to more focus on the thermal transient case since the main aim of it is to research the short and high temperature pipeline. It demonstrates the relevant numerical model to analyze and understand the pipeline walking phenomenon.

2.4.3.1 Thermal Loading and Transients

The thermal transient is defined by changes in fluid temperature and thermal loading during shutdown and restart operations. The pipe is to walk under this condition, and its direction generally towards the cold end of the pipeline. Hence, a steep temperature gradient results in a higher rate of walking. [2]

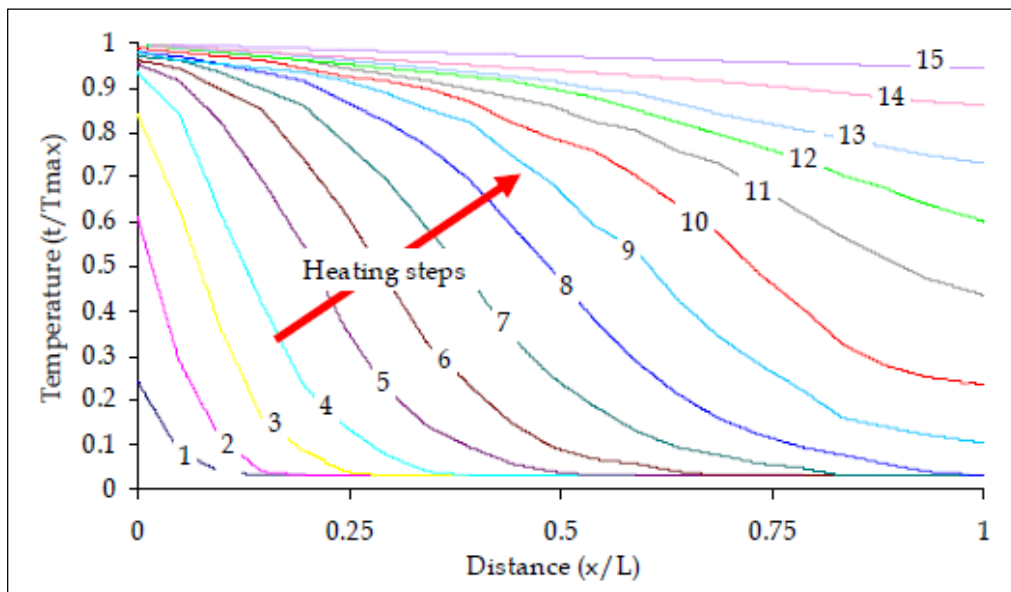


Figure 2.13: A Typical Thermal Transients (D. Bruton et al., 2006) [1]

When it comes to the heating and cooling cycles in the pipeline, both cycle conditions are to be different. The cooling, normally occurring after shutting down, gradually moves to ambient conditions without thermal transient loading. In contrast, the heating takes place non-uniformly from one side to the other with some gradients with temperature rising. [1] For this reason, walking generally occurs on heating (start-up) but no reversal of walking on cool down (shutdown). Consequently, the shape of thermal profile established over time during heating up in the pipeline is essential for the phenomenon, and its typical profile is presented in Figure 2.13.

Besides, the pipeline behavior in this case is different between the first start up heating process and the subsequence heating (from 2nd heating). This is because of a near zero axial

condition along the pipeline length during the first heat operation. [11] The example force profiles of first heat-up and second heat-up are illustrated in Figure 2.14 and 15 respectively:

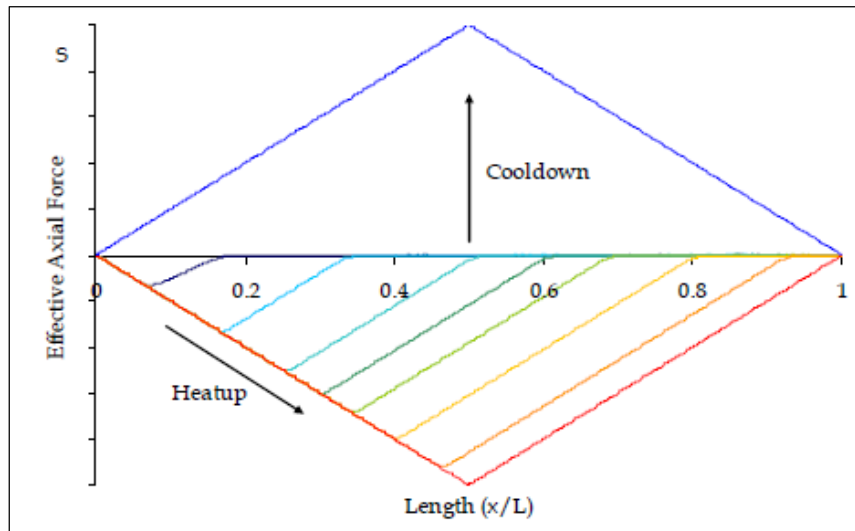


Figure 2.14: An Example of Force Profile – First Heat-up (D. Bruton et al., 2006) [1]

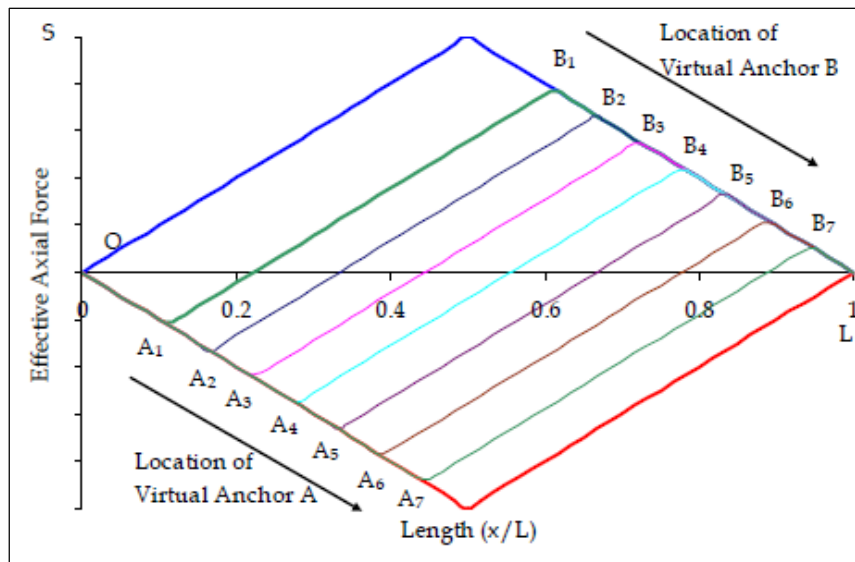


Figure 2.15: An Example of Force Profile – Second Heat-up (D. Bruton et al., 2006) [1]

The Figure 2.14 presents that the virtual anchor begins to move from the heat source towards the mid-line of a pipe because the heat increases the compressive axial force and the pipeline finally becomes fully mobilized. On the other hand, the pipeline contracts about the virtual anchor point at the center when cooled overall pipeline.

Due to the occurrence of residual axial tension on cool-down, the force profile in the pipeline on the second and subsequent heating cycles forms differently from the first cycle.

These cycles dominate the walking process, so the second loading response is considered to understand the pipeline walking mechanism. [1]

The process of thermal transients resumes when the pipeline is reheated. It results in the asymmetric expansion along the pipeline, the mid-point movements towards the cold end, the occurrence of full mobilization, and the position of virtual anchor in the center of the line. Afterwards the pipe contracts equally about the midline anchor on cool-down.

2.4.3.2 Derivation of Walk per cycle due to Thermal Transients [1]

The thermal gradients force (f_θ) per unit length is given by equation 2.22:

$$f_\theta = a_T \cdot q_\theta \cdot EA \quad (2.22)$$

Where,

f_θ : Thermal gradients force per unit length (N/m);

q_θ : Thermal gradient in degrees per unit length ($^\circ\text{C}/\text{m}$).

Besides, the walk per cycle can be expressed by equation 2.23 by following the same principle of driving strain and resistance as before. It is because the thermal gradient heating causes the pipe to walk towards the cold end: [11]

$$\Delta_T = \frac{1}{EA} \int_0^{\frac{L}{2}} [f_\theta \cdot l - \frac{L-l}{2} f] \cdot dl \quad (2.23)$$

Where,

Δ_T : Walk per cycle due to Thermal transients (m);

dl : Small segments of the complete pipeline (m).

Consequently, integrating the equation 2.23 is to become equation 2.24:

$$\Delta_T = \frac{L^2}{8EA} (f_\theta - 1.5 f) \quad (2.24)$$

Based on the equation 2.24, the thermal gradient force is to be 1.5 times more than the frictional resistance force for pipeline walking to take place:

$$f_\theta > 1.5f \quad (2.25)$$

According to SAFEBUCK JIP design guideline, it presents that a pipeline is not prone to walking if the axial friction force (f) exceeds the following value as given by equation 2.26: [15]

$$f > \beta \cdot (a_T \cdot \Delta\theta_{in} \cdot EA) / L \quad (2.26)$$

Where,

β : Parameter in walking due to thermal transients, which is obtained from

$$2\beta^3 - 8\beta^2 + 6\beta + \frac{q\theta \cdot L}{\Delta\theta_{in}} = 0 \quad [\Delta\theta_{in} : \text{Inlet temperature difference}]$$

Additionally, the guideline shows the estimation of walking per cycle due to thermal transient as equation 2.27: [15]

$$\Delta_T = \frac{L^2}{16EA} (\sqrt{24 \cdot f_\theta \cdot f} - f_\theta - 4f) \quad \text{if } f > \frac{f_\theta}{6}$$

$$\Delta_T = \frac{fL^2}{8EA} \quad \text{if } f \leq \frac{f_\theta}{6} \quad (2.27)$$

The analytical model demonstrated by SAFEBUCK JIP presents the valid range: the walk as a function of the axial friction force (f), shown as Figure 2.16. The result specifically shows that the walking rate has its highest value when the pipeline becomes fully mobilized. The maximum rate of walking occurs when: [15]

$$f_{\max} > \frac{3}{8} \cdot f_\theta \quad (2.28)$$

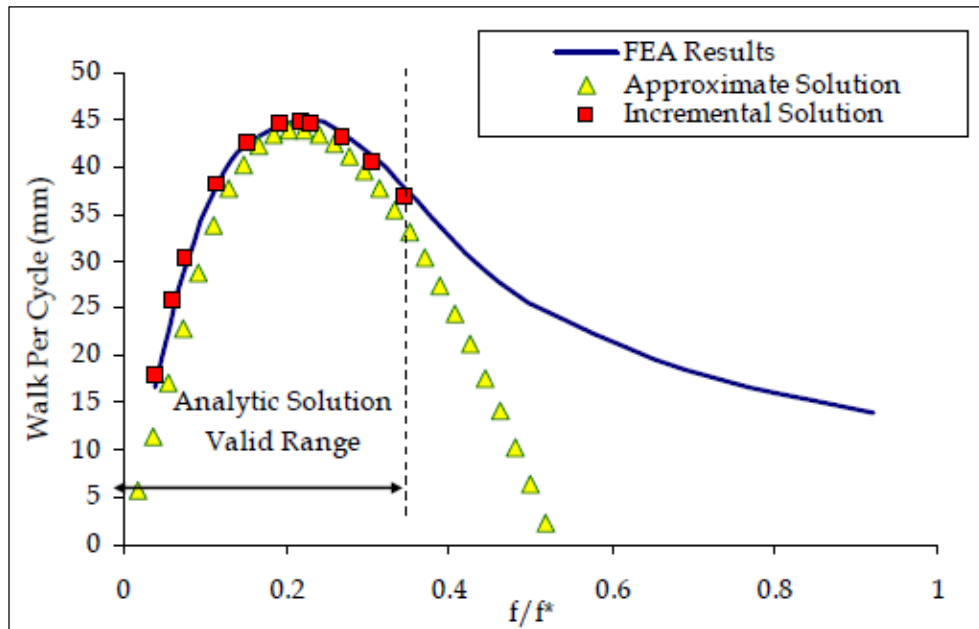


Figure 2.16: Analytical Model (D. Bruton et al., 2006) [1]

2.5 Pipe-Soil Interaction

When it comes to pipeline walking, the soil friction is one of important factors for its occurrence. It is because that the walking phenomenon can happen when the axial restraint, which is supported by the soil, is insufficient to overcome the loading due to pipeline loading. [10] Besides, the pipeline walking analyses are tremendously sensitive to pipe-soil interaction since their response possesses the biggest uncertainty, which is not only applicable to walking but also to lateral buckling assessment in the design. This section briefly looks into the theoretical background of pipe-soil interaction and deals with the parameters to predict their pipe-soil interaction.

Its prediction heavily relies on estimations of uncertain parameters such as soil properties, and pipeline installation effects. [26] With respect to pipe-soil interaction in the design methodology, the concepts: Pipeline embedment, Lateral resistance and Axial resistance are introduced and considered. In the thesis, however, the specific numerical researches are not presented regarding aforementioned subjects since it is beyond the objective of the thesis work. Instead, only the pipeline embedment and axial resistance are briefly presented in the following subsections for the background of the sensitivity study.

2.5.1 Pipeline Embedment

The pipeline embedment is defined as the depth of penetration of the pipe into the seabed as shown in Figure 2.17. [10] It affects the axial resistance since it is related to the pipe-soil contact area.

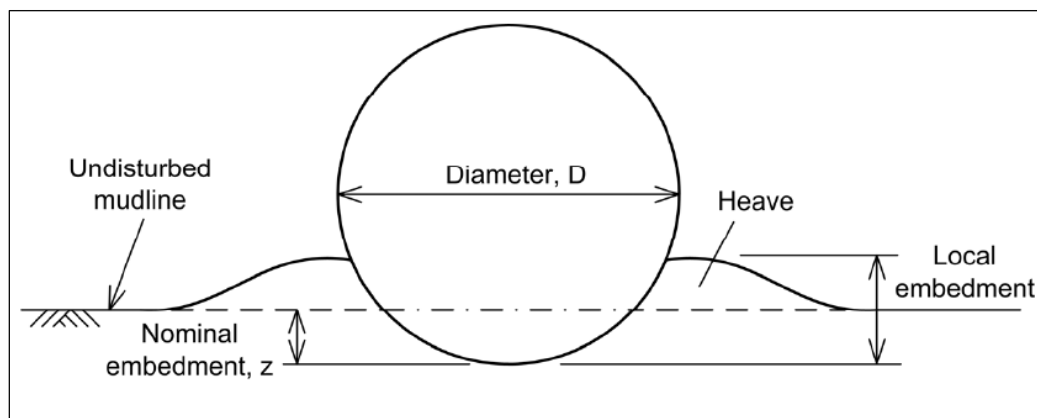


Figure 2.17: Initial Pipeline Embedment (D. Bruton et al., 2008) [10]

Its calculation has been performed by using the SAFEBUCK JIP guideline and the equation presented by Verley & Lund, which are based on the pipe penetration due to the pipe self-weight during installation. Additionally, its prediction is made with the upper bound, best bound and lower bound soil shear strength conditions. [27]

2.5.2 Axial Pipe-Soil Resistance [30]

The axial resistance is affected by the interface friction factor and the duration of pipeline loading. [29] Particularly, the former is related to adhesion factor, soil shear strength, and pipeline embedded surface area, which are based on the pipe-soil interface. Besides, those are uncertainties and used in the prediction of not only the axial but also the lateral resistance of a pipe. The adhesion factor is affected by the magnitude of soil shear strength and both are in inverse proportion relationship. The soil shear strength is relevant to the soil response that can be bounded by drained and undrained conditions. The definitions of them are directly cited from ref [28] as follows:

- Drained: the condition under which water is able to flow into or out of a mass of soil in the length of time that the soil is subjected to some change in load.
- Undrained: the condition under which there is no flow of water into or out of a mass of soil in the length of time that the soil is subjected to some change in load.

Furthermore, two concepts of axial friction are introduced to define the axial response (Breakout and Residual), as illustrated in Figure 2.18:

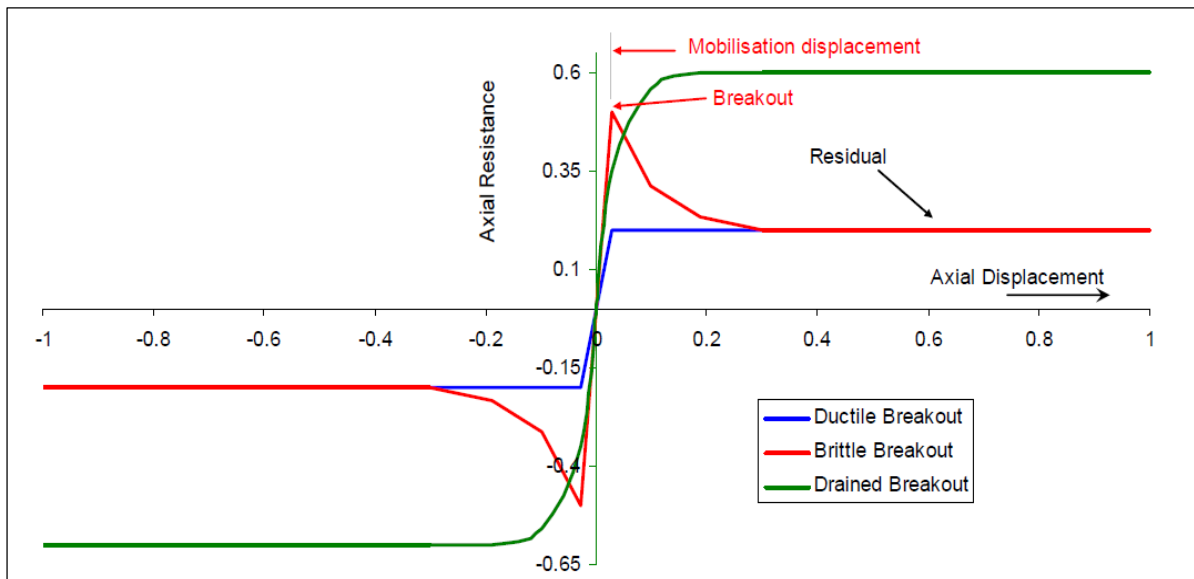


Figure 2.18: Axial Pipe-Soil Resistance Behavior (D. Bruton et al., 2008) [10]

It shows that the frictional resistance is reached at a relatively very small displacement and then gradually reduced to a residual value at a relatively large displacement.

Depending upon a type of soils, the axial resistance can vary. For instance, a drained response defines the axial friction in non-cohesive soils (clay). In cohesive soils, in contrast, undrained (fast) and drained (slow) responses commonly hold different values of axial resistance, as given by the Brittle and Drained response curves in Figure 2.18. It is because of the pore

pressure occurred by the vertical load and the pipe velocity. [18] In addition to that, the thermal expansion is not likely to be affected during the Breakout, so the residual axial resistance should be used for the pipeline walking analysis.

2.6 Summary

This chapter deals with the theoretical background of the pipeline expansion that takes place due to operational pressures and temperatures. Plus, the concept of the effective axial force is discussed. After that, most sections present the concept of pipeline walking.

The pipeline expansion occurs when it is heated (startup), which is opposed by axial resistance, and it contracts when cooling down (shutdown). The axial resistance prevents the pipeline from contracting to its original position. Subsequent restart and shutdown cycles in the pipeline are normally accompanied by steady-state expansion and contraction between established pipe-end positions. In some cases, however, this cycling can lead to a global axial movement of the pipeline, which is defined as “pipeline walking”. [10]

Pipeline walking is the phenomenon when the pipeline become fully mobilized during shutdown and restart operations and normally associated with the short and high temperature pipeline. It can, of course, take place on long pipelines especially coming along with lateral buckling by dividing the long line into a series of short lines [12], but it is not to be dealt with in the thesis.

The SAFEBUCK JIP has researched on pipeline walking and defined the key factors that affect this phenomenon. The design guidance and analytical expressions for the pipeline walking assessment have been provided by them as well. Accordingly, the main causes of pipeline walking (mechanisms) are presented as follows:

- Tension at the end of the pipeline, associated with an SCR;
- A global seabed slope along the pipeline length;
- Thermal gradients along the pipeline during changes in operating conditions.

Particularly, walking can lead to significant global displacement of the pipeline over a number of thermal cycles. Although walking is not a limit state for the pipeline itself, without careful consideration can lead to failures as follows: [2]

- Overstressing of connections;
- Loss of tension in a SCR (steel catenary riser);
- Increased loading within a lateral buckle;
- The need for anchors to restrain walking;
- Route curve pullout of restrained systems.

Thus, it is important to be aware of contributions from each driving mechanism and proper analytical performance is to be considered.

Lastly, understanding the pipe-soil interaction is important to analyze the walking phenomenon. The axial resistance, particularly related to the walking, depends on several factors that have a wide range of uncertainties due to unpredictable parameters such as soil shear strength, pipeline embedment, and adhesion factor. Moreover, the selection of axial friction coefficients is important with respect to pipeline walking in the design. In the thesis work, hence, the sensitivity study on axial friction factors is considered when creating the simulation model to analyze pipeline walking in the finite element analysis (FEA).

3. Research Design

3.1 General

This chapter presents the methodology used in the thesis work to analyze the pipeline walking phenomenon particularly due to the thermal transients. The methodology is prepared based on Design guidelines for pipeline walking analysis [20] and OTC technical paper [1]. The finite element analysis (FEA) is carried out by using ANSYS 13.0 (Mechanical APDL) software.

It consists of several sections that give detail descriptions regarding creating a suitable model for the analysis such as selections of a pipeline and a seabed model in the FEA, and a preparation for the temperature profile which is used in the case study. Furthermore, the modeling for the sensitivity analysis is presented to look into the effects of axial friction factors on pipeline walking. Its detail discussion is to be given in Ch. 5 (Results and discussion) as well.

3.2 Preparation for Research Model [20]

The objective of this section is to make a brief guidance for generating the research model. It basically focuses on analyzing the susceptibility of pipeline walking under the effects of thermal transients during start-ups and shutdowns.

3.2.1 Modeling a Pipeline

Modeling a pipeline for the walking analysis is based on:

- a) A 3-D and two-node pipe element from ANSYS;
- b) A pipe-seabed contact is created based on the Coulomb friction law;
- c) The linear material stress-strain properties of the pipe are used in the model.

3.2.2 Temperature Profile Preparation

- a) Temperature profile is developed over time as the pipeline heats up;
- b) No pressure variation is applied. [1]

The thermal transient is created by using a typical temperature profile which is shown in Figure 2.13 in Ch. 2. The temperature values are read upon the each temperature load step with a maximum operating temperature 88°C. Consequently, the profile is given as Figure 3.1:

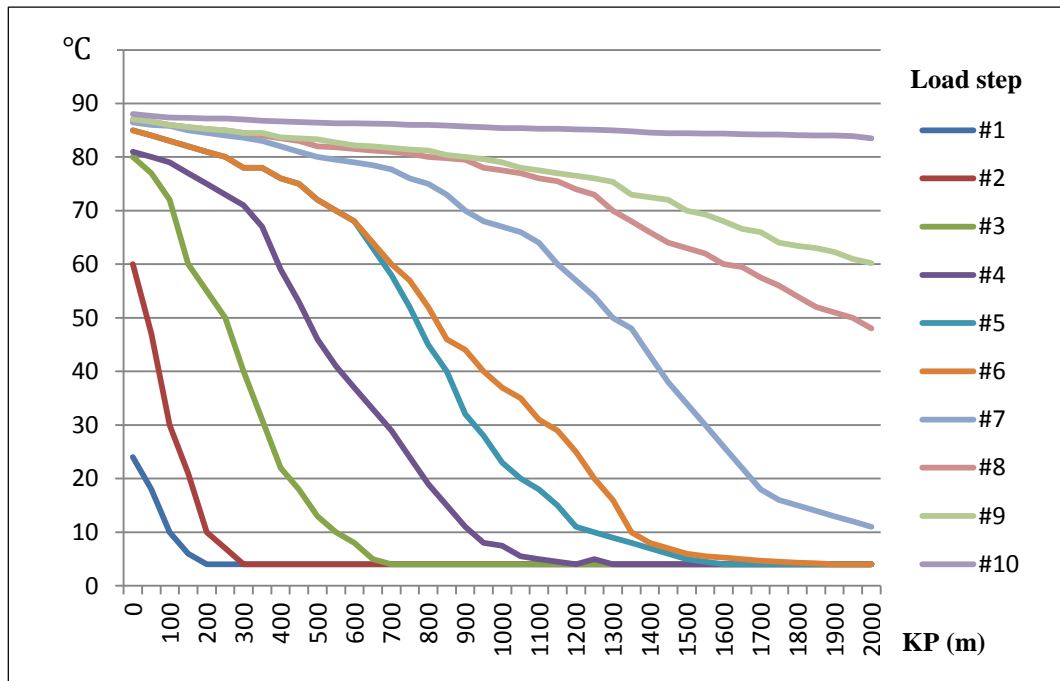


Figure 3.1: Temperature Transients used in Pipeline Walking Analysis

The Mathcad v15 is used to interpolate the temperatures. It generates the temperature load profiles that are applied to the pipeline model in the FEA, which is composed of 1999 elements. The separate sheets regarding preparation of the temperature load profile are presented in Appendix II.

3.2.3 Thermal Load Application

In the FEA, it is arranged as the following sequence:

- The ambient temperature (3.5°C) is applied as an initial condition;
- The first temperature load step profile is applied;
- The temperature loads are continuously applied in series order until the 10th load step;
- For the shutdown condition, the ambient temperature is re-applied, which implies one cycle is completed.

3.2.4 Pipe-Soil Interaction Application

The pipe-soil interaction possesses the biggest uncertainties in the design of pipeline walking. [29] It indicates that the pipeline walking analysis is very sensitive to it. Hence, the measurement uncertainty of soil properties and conditions are one of important factors in this kind of analysis.

However, due to the limited research and literature regarding that topic, different values of friction coefficients (axial and lateral) are assumed on the basis of factors that are commonly considered in the pipeline design. Moreover, the pipe-soil frictional model is created based on the orthotropic friction model for making the stick-slip condition in different directions. [21] The selected values of the axial friction factor used in the analysis and sensitivity study are presented in Ch. 4.

3.3 Element Types Used in Finite Element Analysis Model

This section deals with detailed descriptions of the finite element model for the analysis. All relevant models are based on the software of ANSYS 13.0 (Mechanical APDL) that is used to perform the FEA.

3.3.1 Pipeline Model

It considers the straight rigid pipeline with a length of 2km and being laid on the flat seabed. The feature of the pipeline model is selected from the ANSYS (Mechanical APDL) element of PIPE288 as shown in Figure 3.2. The PIPE288 element is suitable for analyzing a hollow thin-wall slender pipe structures with external and internal pressure. [22]

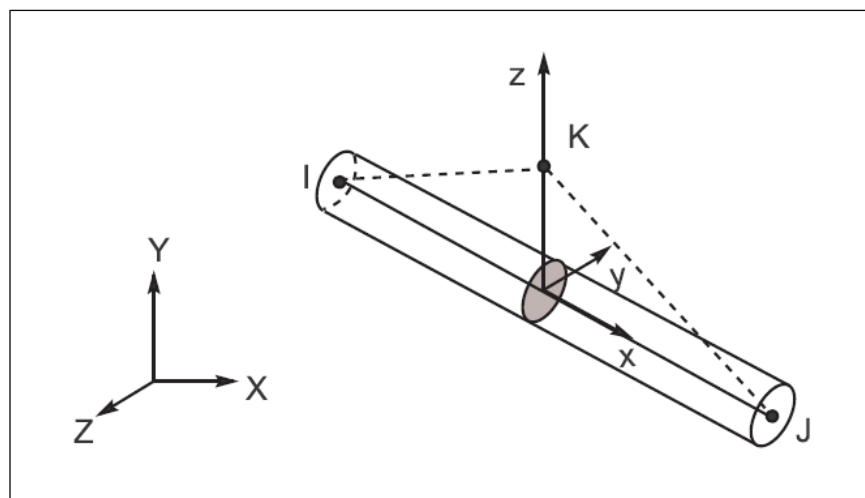


Figure 3.2: PIPE288 Geometry (ANSYS Inc. 2009) [21]

Settings of the element condition are accomplished by giving values of “KEYOPT”, and the followings are vital conditions in the model:

- KEYOPT (0) into 1 for Temperature input (Through wall gradient);
- KEYOPT (4) into 4 for Hoop strain treatment (Thin pipe theory);
- KEYOPT (6) into 0 for End cap loads (Internal and external pressure cause load on end caps).

When it comes to the value of the temperature input (KEYOP (0)), the temperature load profile is defined as element body loads. It implies that the operating temperature varies linearly through wall gradient.

The pipeline model generated in ANSYS is shown in Figure 3.3. The Cartesian coordinates in three dimensions indicates the position of the pipeline. It is laid on the XZ-plane and Y-axis is used to measure the water depth.

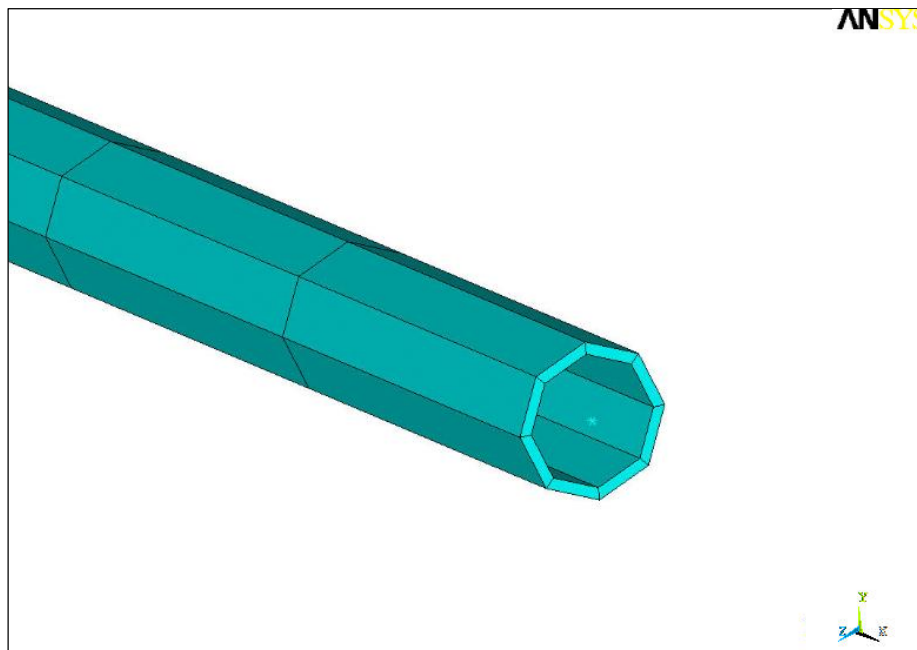


Figure 3.3: Pipeline Model of PIPE288 Element

The section of the PIPE288 element is created based on the command “SECDATA” in ANSYS. The default value of 8 is given for the number of cells along the circumference in the model. Hence, the section of the pipe is shown as Figure 3.3.

The further specific ANSYS Script (commands) for running ANSYS is separately presented in Appendix IV-1.

3.3.2 Seabed Model

The data from measurements (survey) of the seabed topography plays a critical role for constructing the 3-D seabed model. It is to make sure that the FE model is to ensure a realistic environment during carrying out the analysis of the pipeline behavior. [24]

However, the seabed is assumed as a flat non-deformable area in this study. Based on it, the Node-to-surface contact is selected for the seabed model. In this contact selection, the elements of CONTA175 and TARGE170 are used for a contact pair and a 3-D associated target surface respectively from the ANSYS model. It is because the concept of Contact-Target pair is

widely used in the finite element modeling of the contact between two bodies [21], and it is shown as Figure 3.4:

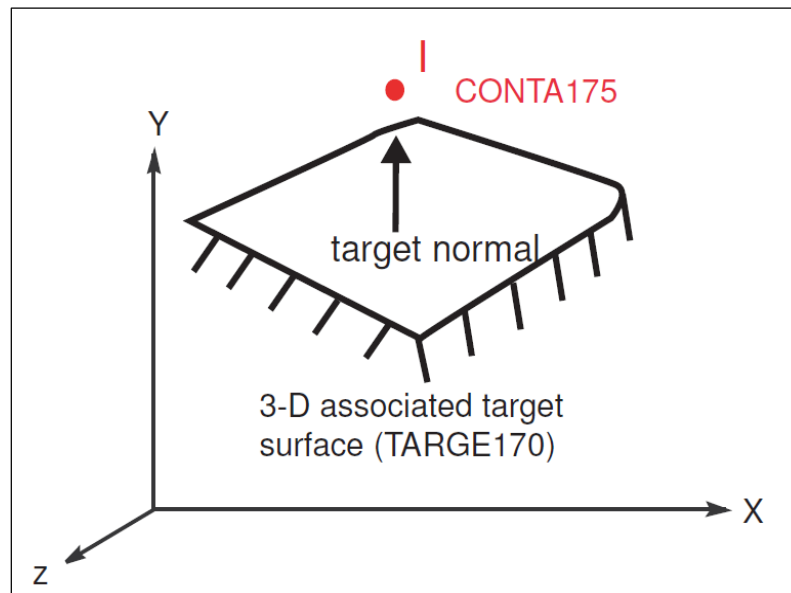


Figure 3.4: Node-to-Surface Contact Elements (ANSYS Inc. 2009) [23]

The followings are the main features of those elements:

- TARGE170 is selected to represent rigid target surface and Figure 3.5 shows its geometry;
- The selection of the TARGE170 segment type is also applicable. In this thesis “4-Node Quadrilateral” is used to define the target surface, which is set with commands of “TSHAP, QUAD”. The Figure 3.6 shows the segment type of TARGE170;
- In the contact pair condition, i.e. Node-to-surface contact, CONTA175 is selected and established between the seabed (TARGE170) and the pipeline element (PIPE288);
- CONTA175 deals with orthotropic Coulomb friction as the friction model [21]. Axial and lateral directions are introduced in the pipe-soil (seabed) interaction model by applying two friction factors (axial and lateral). The command of “TB, FRIC” is used to set the orthotropic friction command by setting the value of “TBOPT” into “ORTHO”. The axial and lateral friction factors are defined using “TBDATA” command.

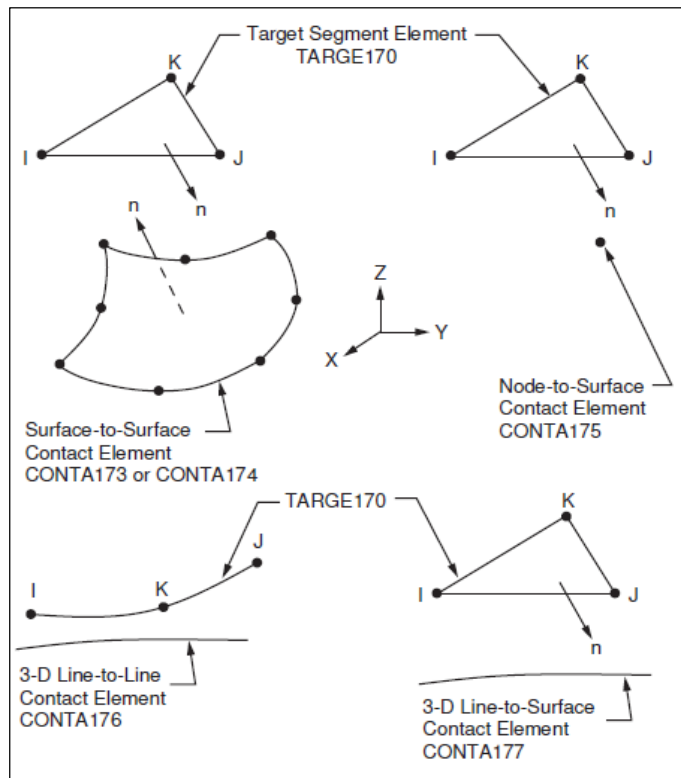


Figure 3.5: Geometry of TARGE170 (ANSYS Inc. 2009) [21]

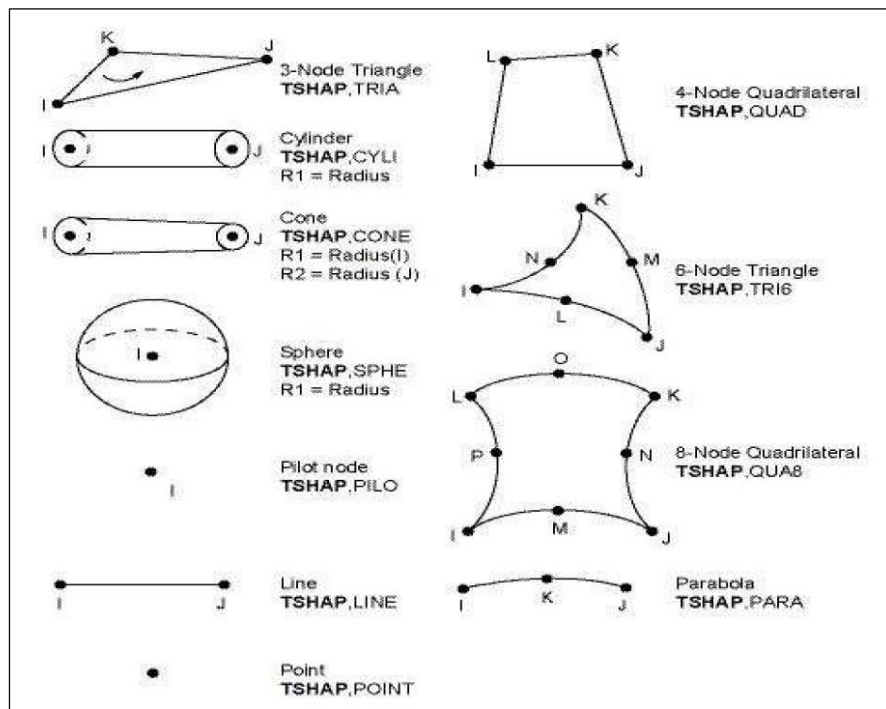


Figure 3.6: Segment Types of TARGE170 (ANSYS Inc. 2009) [21]

3.4 Process of Finite Element Analysis (FEA)

This section presents the description of an initial condition and the process of the FEA performance. The pipeline is generated as a 2km length straight pipeline laid on the flat/even seabed illustrated as Figure 3.7, which is under thermal cyclic loadings. However, the behavior of the pipeline during installation such as lay-tension and lay angle is not considered, and no bending moment in the pipeline is assumed in this analysis.

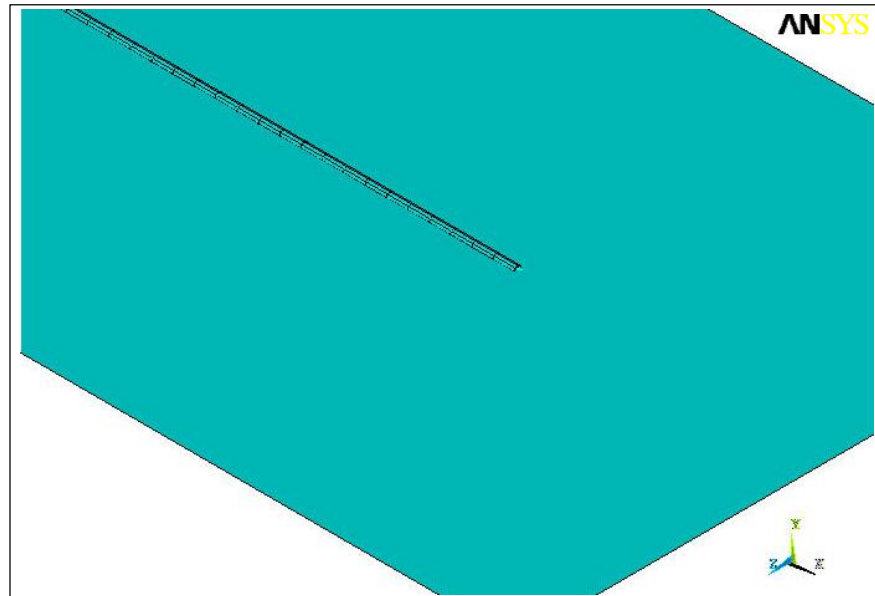


Figure 3.7: Pipeline and Seabed Modeling in ANSYS

The temperature profile created according to section 3.2.2 is applied to the pipeline model. The following procedures are conducted in the FEA based on the thermal load application presented in section 3.2.3:

- Initial condition:

It is assumed that the pipeline is initially laid on the seabed under an ambient temperature (3.5°C) condition.

- Subsequent events to initial condition:

The temperatures are gradually stepped up according to the temperature profiles until 10th temperature load step. The interpolated temperatures are particularly applied to each node of the pipeline model.

To make a shutdown (cool down) condition, it lets the temperature be the ambient temperature. After that, it sets a restart condition by re-applying the first temperature load step and repeats 5 times as operational cycles.

- Temperature load step application:

It uses the command of “TIME” that is a word to set the time for a load step in ANSYS. The each interpolated temperature load step is saved as the filename extension of “Tx.inp”³, and the command of “INPUT” is used for applying the saved temperature loads.

- Results extraction:

The results of the FEA are extracted by the ANSYS macro function, so the effective axial force and the axial displacement (x-direction in the case) are consequently presented and saved as “.txt” files. The ANSYS Script for the extraction is given in Appendix IV-2.

³ ‘x’ implies the numerical digit: 1 through 10 for the saved each load step.

4. Case Study Description

4.1 General

This chapter presents the basic data to create the finite element (FE) model in order to check the walking phenomenon. The analytical model considered is a typical production pipeline with 2km in length under the thermal transient loadings. Given data and parameters are based on reasonable assumptions.

4.2 Pipeline Model

4.2.1 Pipeline Parameter

The selected pipeline is based on the API 5L X65, and its properties are presented in Table 4.1:

Table 4.1: Pipeline Design Data and Material Properties

| Parameter | Value | Unit |
|---|-------------------------|----------------------------|
| Pipe material | API 5L X65 | - |
| Production method | Seamless | - |
| Outer diameter | 323.9 | mm |
| Wall thickness | 25.4 | mm |
| Corrosion allowance | 6 | mm |
| Density | 7850 | kg/m ³ |
| SMYS | 450 | MPa (= N/mm ²) |
| SMTS | 535 | MPa (= N/mm ²) |
| Young's modulus | 207 x 10 ³ | MPa (= N/mm ²) |
| Thermal expansion coefficient | 1.17 x 10 ⁻⁵ | / °C |
| Poisson's ratio | 0.3 | - |
| De-rating value for yield stress (Max. operating Temp. 88°C) | 22.8 | MPa (= N/mm ²) |

Regarding the de-rating value for yield stress is calculated according to DNV-OS-F101 Sec.5 C300 and its relevant graph is shown in Figure 4.1:

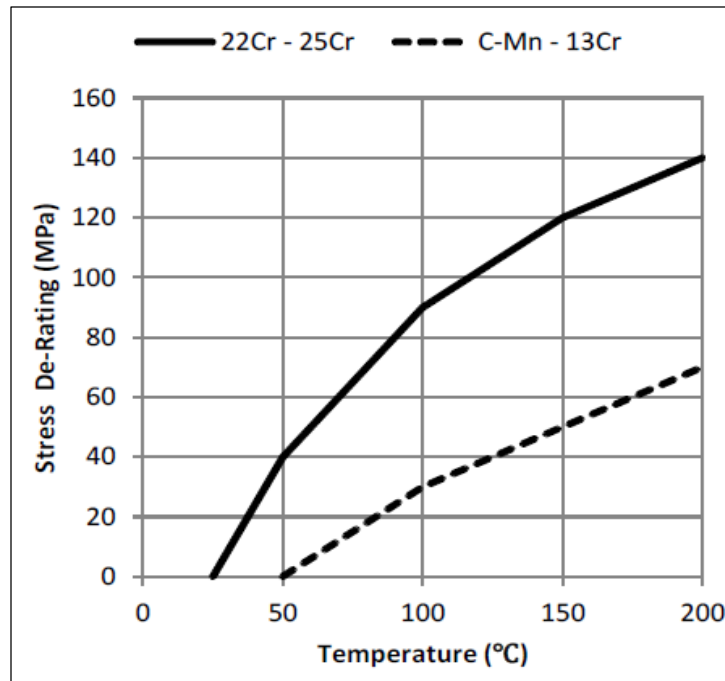


Figure 4.1: Proposed de-rating values for yield stress of C-Mn steel (DNV-OS-F101, 2012)

The properties of insulation coating and concrete coating on the pipeline, which give a realistic model in the analysis, are shown in Table 4.2:

Table 4.2: Coating Parameters

| Parameter | Value | Unit |
|----------------------------|-------|-------------------|
| Insulation thickness | 5 | mm |
| Insulation density | 910 | kg/m ³ |
| Concrete coating thickness | 30 | mm |
| Concrete coating density | 2400 | kg/m ³ |

4.2.2 Pipe Material Property

The material property of the pipeline model is defined by a Ramberg-Osgood stress-strain curve to take account of exceedance of the pipeline linear elastic limits during operations. [18] The FE model, therefore, is analyzed based on its stress-strain curve of the pipe material (API 5L X65). The Figure 4.2 is generated based on calculations of the Ramsberg-Osgood stress-strain relation. In Figure 4.2, 88°C implies the max. operational temperature and 20°C refers to room temperature. Its numerical analysis is separately presented in Appendix III.

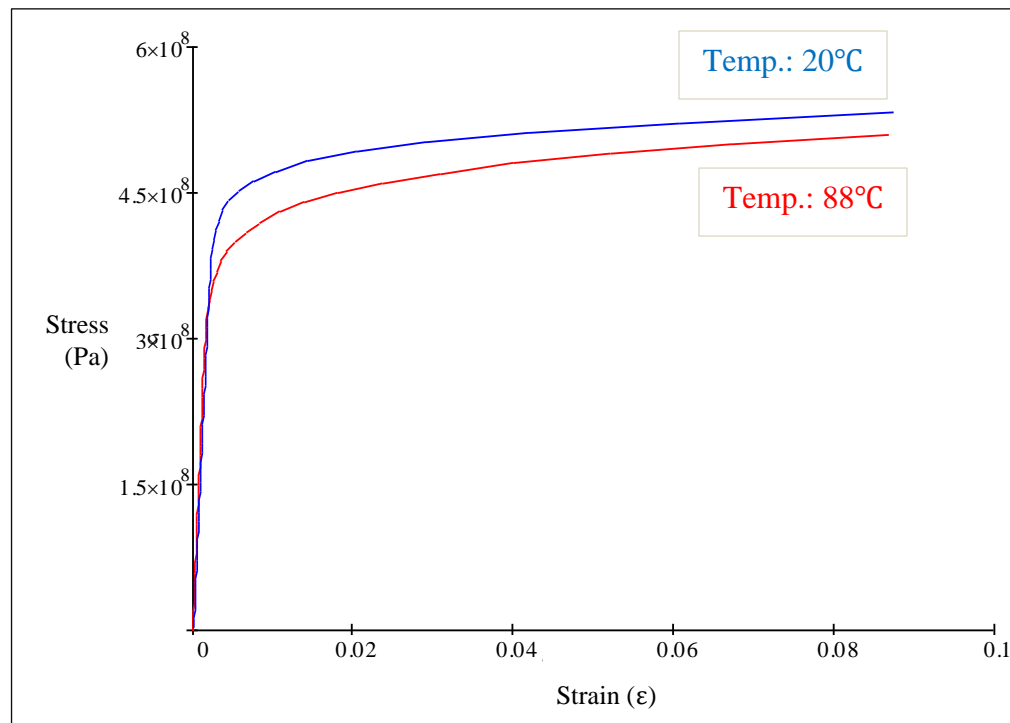


Figure 4.2: Ramberg-Osgood Stress-Strain Curve for API 5L X65 (at 20°C & 88°C)

4.3 Input Data

This section shows conditions of the subject pipeline used for the walking analysis.

4.3.1 Operating Data

The Table 4.3 gives the summary of the operational conditions and the density of content in the pipe. It is assumed that the pipe is filled with oil in the analysis.

Table 4.3: Operating parameters

| Parameter | Value | Unit |
|--------------------------------|-------|-------------------|
| Content density (Oil) | 900 | kg/m ³ |
| Operating internal pressure | 15 | MPa |
| Operating temperature | 88 | °C |
| Shutdown (ambient) temperature | 3.5 | °C |

4.3.2 Environmental and Soil Data

The Table 4.4 and 4.5 gives the data regarding environmental and soil conditions respectively:

Table 4.4: Environmental Data

| Parameter | Value | Unit |
|------------------|-------|-------------------|
| Seawater density | 1027 | kg/m ³ |
| Water depth | 100 | m |

Table 4.5: Environmental Data (Soil Conditions)

| Parameter | | Value |
|-------------------|----|-----------|
| Axial friction | LB | 0.3 |
| | BE | 0.5 |
| | UB | 0.7 |
| Lateral friction | | 0.8 |
| Soil mobilization | | 2mm ~ 4mm |

With regards to the pipe-soil interaction, it contains a hardly predictable uncertainty in the design of pipeline walking. [18] Hence, the performance of the sensitivity analysis is required to determine the effect of friction on pipeline walking. In the thesis work, the axial friction factor of 0.3 is initially used for the analysis and then other values of factors are applied. Furthermore, the value of 2.0 as the friction factor is additionally used for a wider analysis in the effect of friction factor on the walking phenomenon.

5. Results and Discussion

5.1 General

The objective of this chapter is to explicate the results of the thesis work. The methodology described in Ch. 3 is conducted to analyze the pipeline walking phenomenon under the transient thermal cycling. Basically, it presents the responses of the pipeline resting on the seabed described in the analytical FE modeling. The sensitivity study is also discussed in the chapter to understand the critical parameter for the walking phenomenon. Hence, the results of different axial friction factor applications are presented. Lastly, the chapter deals with the necessity of mitigation measures in order to eliminate or prevent pipeline walking in connection with the sensitivity study results. Moreover, the numerical calculation of the walking rate according to SAFEBUCK JIP pipeline design guidelines [15] is separately presented in Appendix I to confirm the validation of the FEA results in the chapter.

5.2 Pipeline Response Analysis Results

This section preferentially deals with the results based on the model conditions as follows:

- Pipe wall thickness: 25.4mm;
- Operating temperature: max. 88°C;
- Axial friction factor: 0.3 (LB).

The interpolated temperature load profile is shown as Figure 5.1:

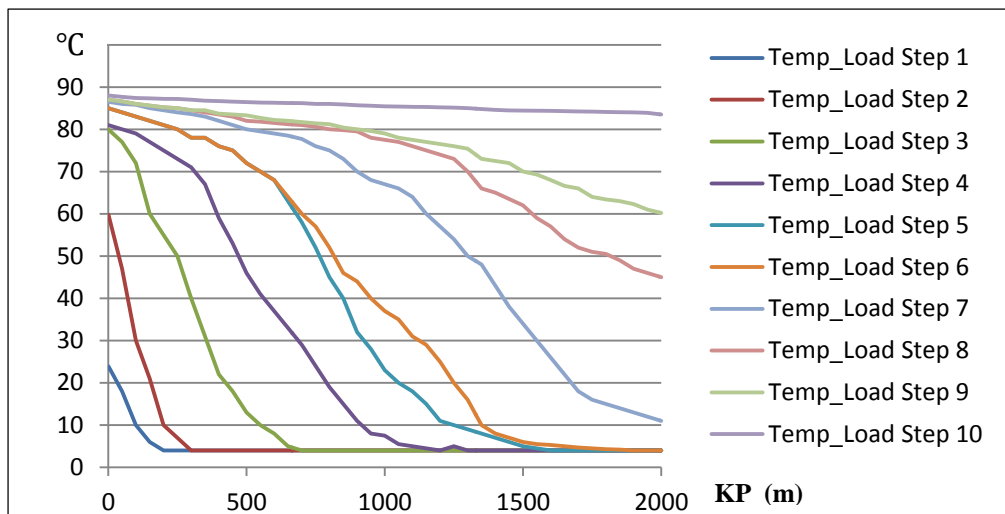


Figure 5.1: Interpolated Temperature Load Profile for 88°C

5.2.1 Effective Axial Force Profile

The Figures 5.2 through 5.6 show the profiles of the effective axial force developed from the first to the fifth cycle respectively. The “load1” in the Figure 5.2 indicates the initial condition in the pipeline (referring to staying in an ambient temperature). While, it implies restarting the operation in Figures 5.3 through 5.6, which means the first temperature load step is applied to the pipeline in the FEA. The consecutive load numbers stand for the temperature load step application in the FEA. The “load12” displays the shut-down condition in the first cycle, whereas the “load11” refers to that condition in the rest of cycles. Both load numbers are referring to the pipeline turned to the ambient temperature as shutting-down.

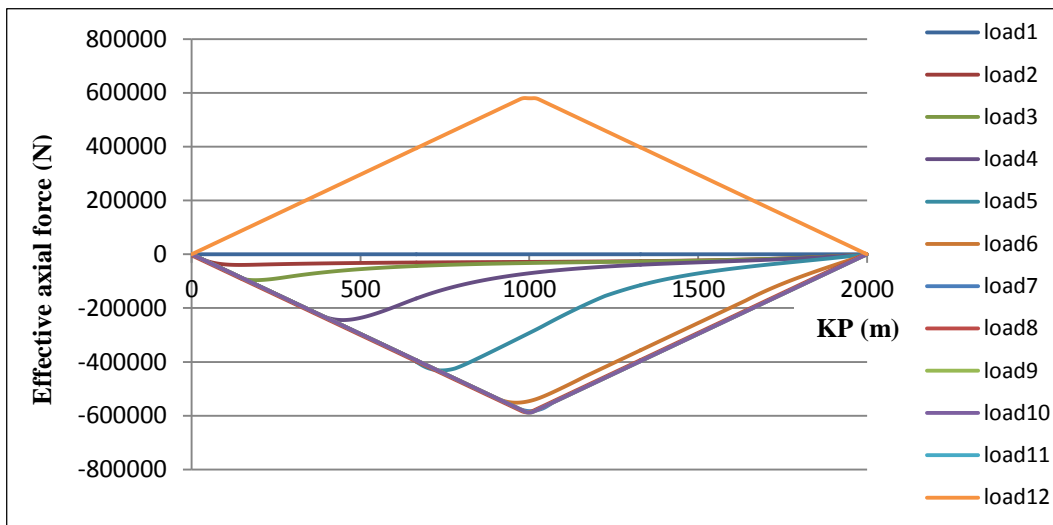


Figure 5.2: Effective Axial Force for 1st Cycle

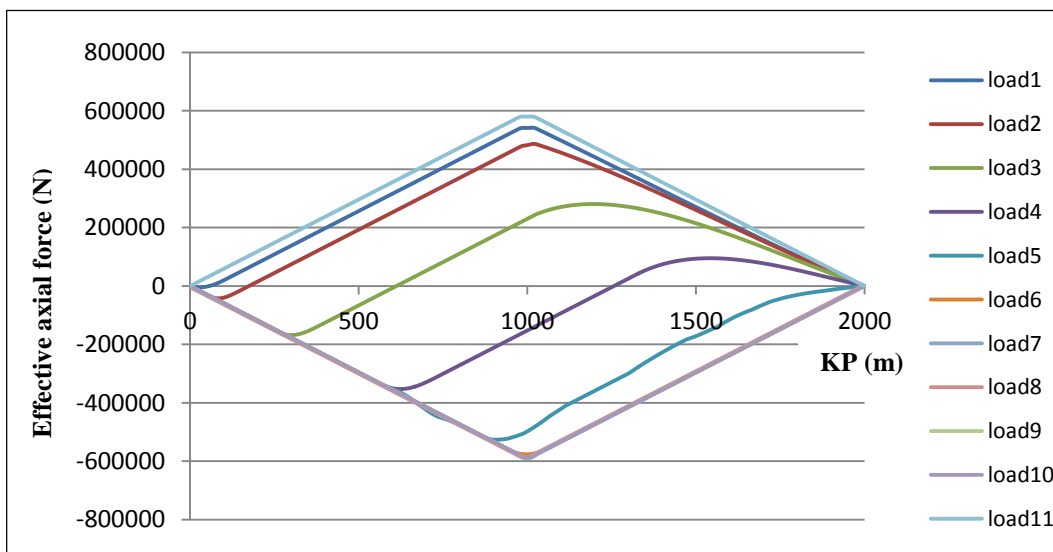


Figure 5.3: Effective Axial Force for 2nd Cycle

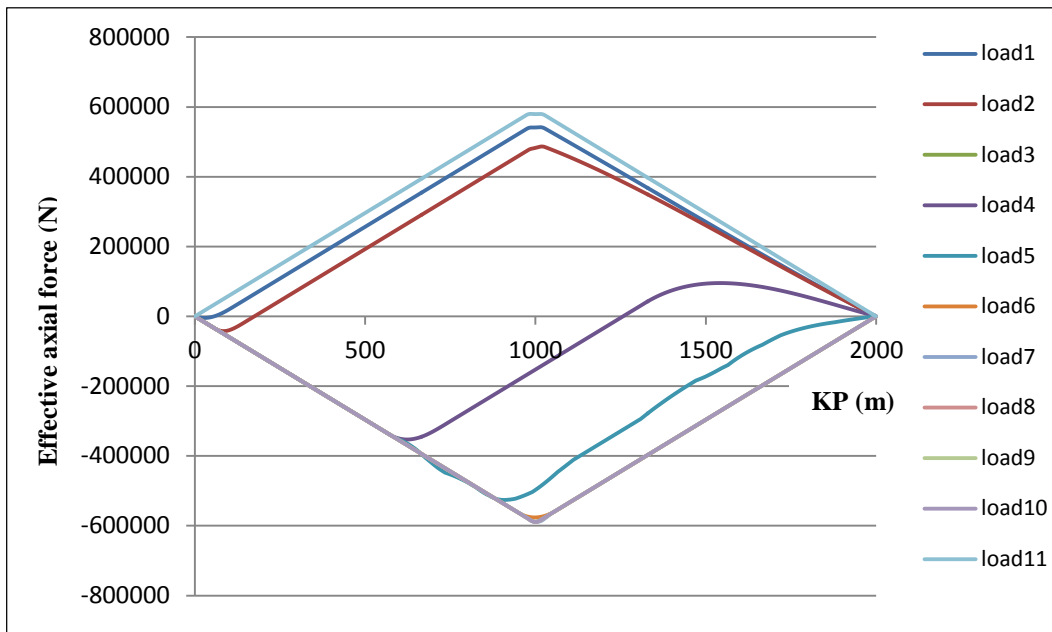


Figure 5.4: Effective Axial Force for 3rd Cycle

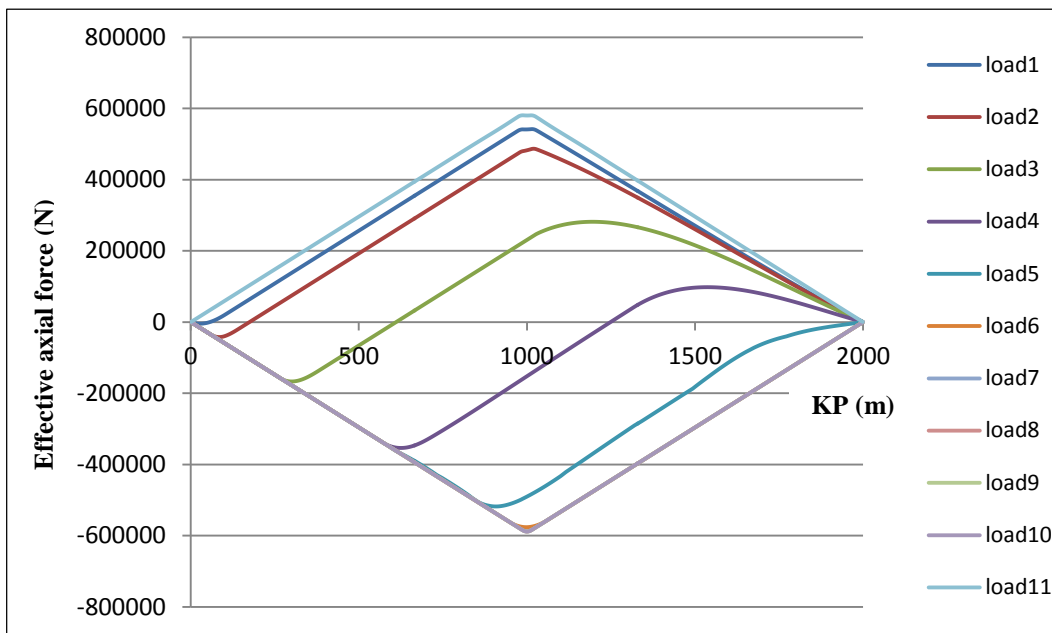


Figure 5.5: Effective Axial Force for 4th Cycle

The Figures 5.2 through 5.6 also indicate that as the pipeline is gradually heated, the effective axial force (compressive force) builds up until the pipeline is entirely mobilized (it happens after the 7th load step in this case). Once the pipeline turns to fully mobilized, the profiles show that there are less variations in force over the length of the pipeline. Moreover, The VAP (virtual anchor point) is situated in the middle of the pipeline when fully mobilized. On

shut-down condition, which is cooled down at a uniform rate, the contraction takes place about the VAP.

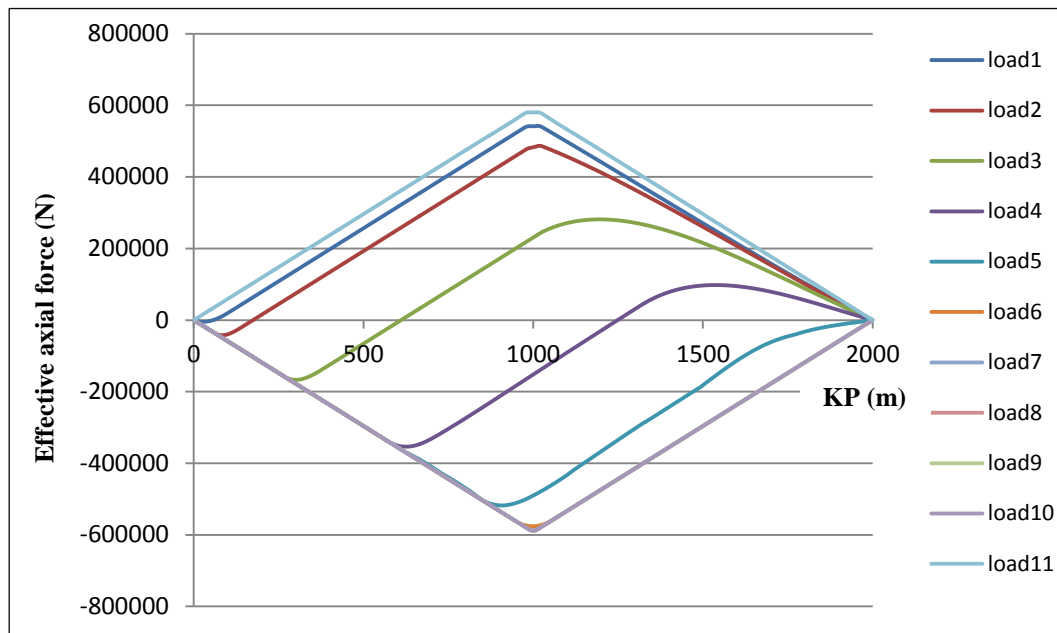


Figure 5.6: Effective Axial Force for 5th Cycle

The case in the study has the similar aspect of the pipeline behavior that has been presented in Ch.2.4.3.1. The EAF profile is developed in a different form from the second cycle compared with the first cycle profile. It is because that the occurrence of residual tension (caused by friction) when cooling-down. Hence, the pipeline does not return to its original position/size.

According to the Figure 5.3 (2nd cycle), two VAPs are observed when the “load1” is applied in the pipeline, and both are located at KP 28 and KP 1015 respectively. As the pipeline gets heated up, the positions of the VAPs move towards the mid-point and the cold-end (here, at KP 1000 and KP 2000 respectively), specifically it gets the maximum effective axial force at the mid-point ($-5.898 \times 10^5 \text{ N}$ in the case). Other profiles also show the similar aspects, as illustrated in Figures 5.4 through 5.6. Due to that phenomenon, i.e. the shift of the VAP, the asymmetrical expansion from the second heat-up takes place, and the pipeline system in the case study can be expected to “walk”.

5.2.2 Pipeline Cumulative Displacement

The FEA of the case study presents the occurrence of expansion along the full length of the pipeline. The following Figures 5.7 through 5.11 show the profiles of the pipeline expansion developed from the first cycle to the fifth cycle respectively. Similar to the EAF case, the load numbers in the Figures also imply the temperature load steps and operating conditions in the FEA.

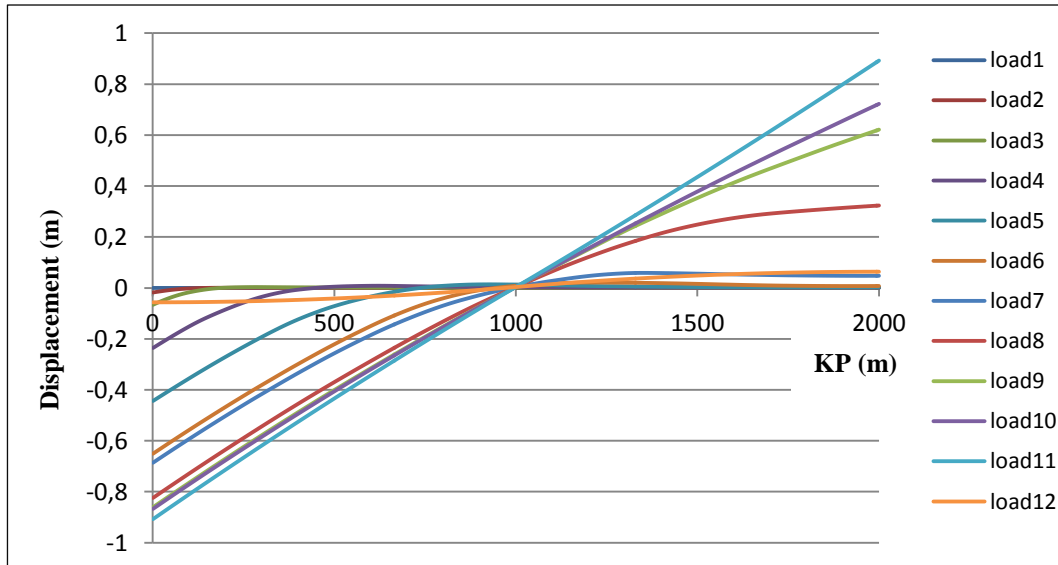


Figure 5.7: Pipeline Displacement for 1st Cycle

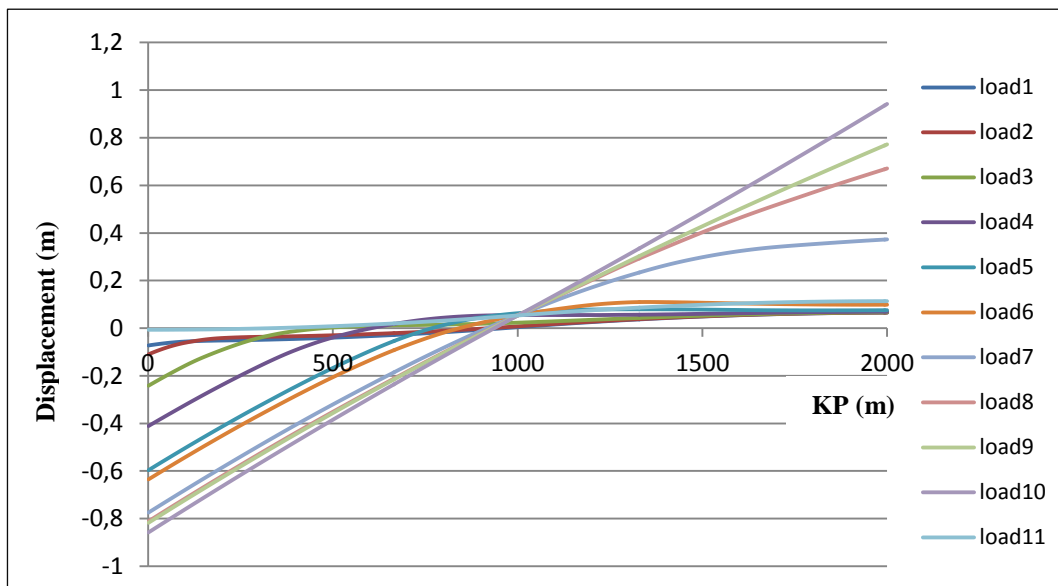


Figure 5.8: Pipeline Displacement for 2nd Cycle

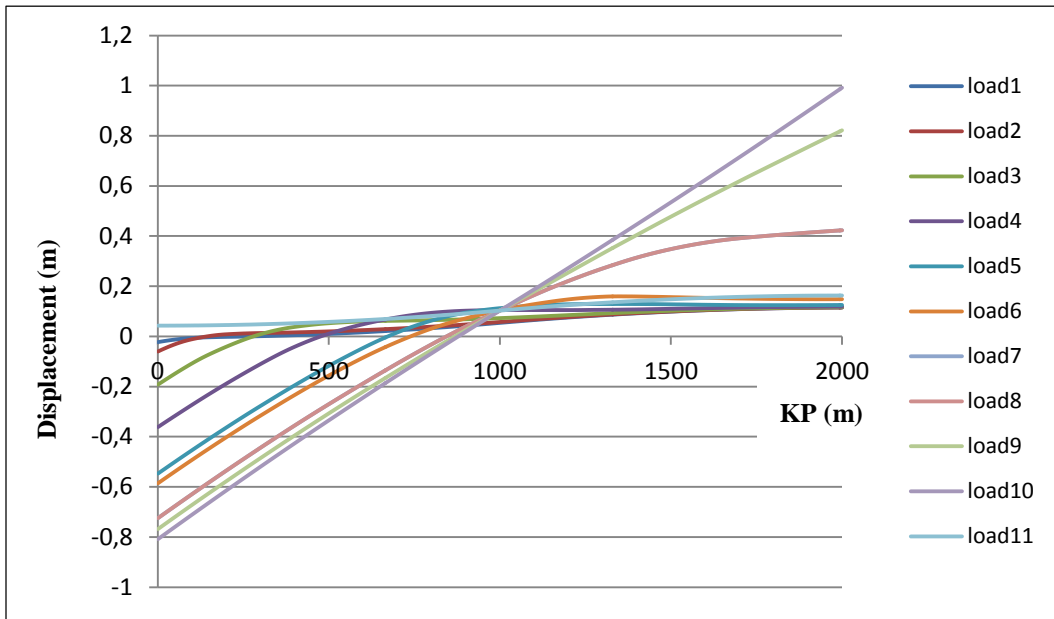


Figure 5.9: Pipeline Displacement for 3rd Cycle

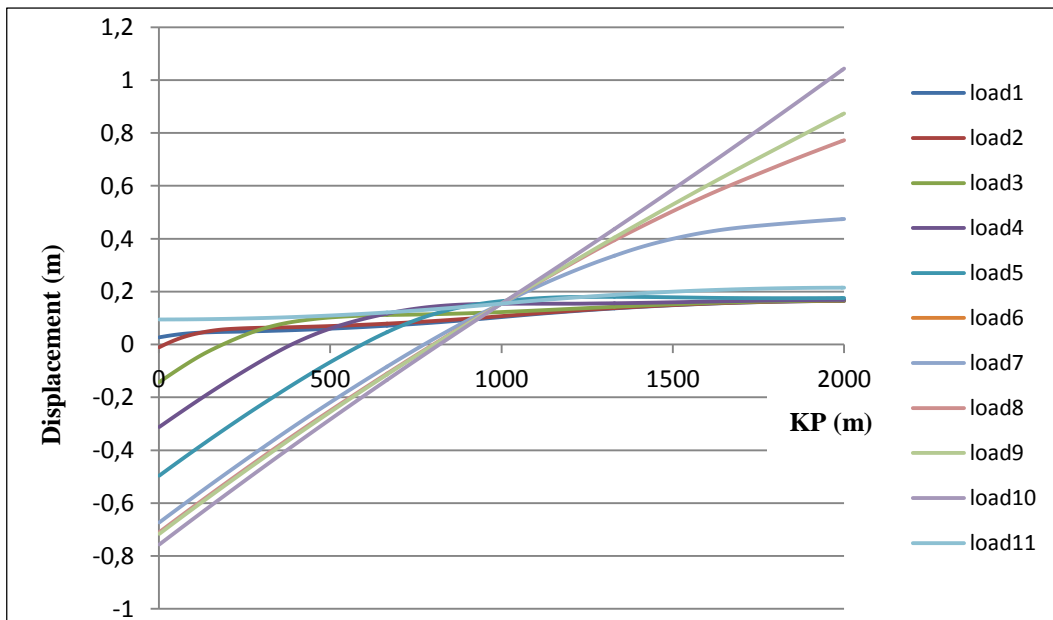


Figure 5.10: Pipeline Displacement for 4th Cycle

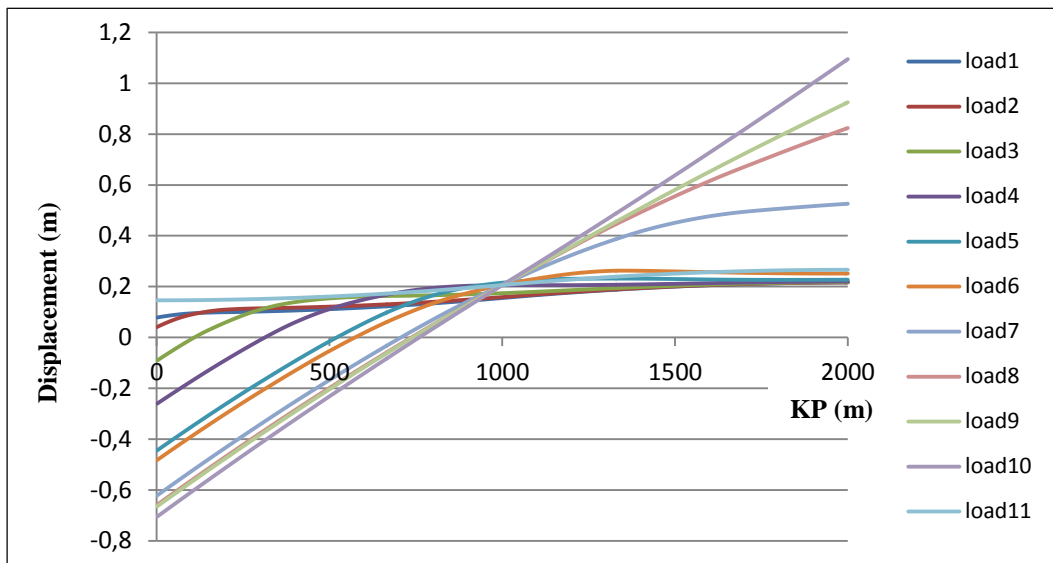


Figure 5.11: Pipeline Displacement for 5th Cycle

As the pipeline is progressively hotter, the figures indicate that the non-uniform expansions take place. When KP is adjacent to zero, i.e. close to the hot end, the pipeline is prone to expand towards to its end. Other parts of the line, on the other hand, the shift is made towards the cold end, i.e. KP close to 2000. The figures in Table 5.1 and 5.2 also show displacement in meter at hot/cold ends of the pipeline in each load step.

Table 5.1: Hot-End Pipe Displacement

| 1st Cycle | | 2nd Cycle | | 3rd Cycle | | 4th Cycle | | 5th Cycle | |
|-----------|----------|-----------|----------|-----------|----------|-----------|----------|-----------|----------|
| Load No. | DISP (m) | Load No. | DISP (m) | Load No. | DISP (m) | Load No. | DISP (m) | Load No. | DISP (m) |
| 1 | 0 | 1 | -0.0725 | 1 | -0.0226 | 1 | 0.027 | 1 | 0.0785 |
| 2 | -0.0179 | 2 | -0.1099 | 2 | -0.06 | 2 | -0.0104 | 2 | 0.0412 |
| 3 | -0.0661 | 3 | -0.2416 | 3 | -0.1919 | 3 | -0.1424 | 3 | -0.0908 |
| 4 | -0.2356 | 4 | -0.411 | 4 | -0.3612 | 4 | -0.3119 | 4 | -0.2604 |
| 5 | -0.4435 | 5 | -0.5965 | 5 | -0.5467 | 5 | -0.496 | 5 | -0.4445 |
| 6 | -0.6506 | 6 | -0.6351 | 6 | -0.5854 | 6 | -0.5338 | 6 | -0.4823 |
| 7 | -0.686 | 7 | -0.7746 | 7 | -0.7244 | 7 | -0.6731 | 7 | -0.6216 |
| 8 | -0.8241 | 8 | -0.8111 | 8 | -0.7614 | 8 | -0.7098 | 8 | -0.6582 |
| 9 | -0.8607 | 9 | -0.8175 | 9 | -0.7679 | 9 | -0.7162 | 9 | -0.6647 |
| 10 | -0.8672 | 10 | -0.8579 | 10 | -0.8082 | 10 | -0.7565 | 10 | -0.705 |
| 11 | -0.9075 | 11 | -0.0066 | 11 | 0.043 | 11 | 0.0945 | 11 | 0.146 |
| 12 | -0.0565 | | | | | | | | |

Table 5.2: Cold-End Pipe Displacement

| 1st Cycle | | 2nd Cycle | | 3rd Cycle | | 4th Cycle | | 5th Cycle | |
|-----------|----------|-----------|----------|-----------|----------|-----------|----------|-----------|----------|
| Load No. | DISP (m) | Load No. | DISP (m) | Load No. | DISP (m) | Load No. | DISP (m) | Load No. | DISP (m) |
| 1 | 0 | 1 | 0.0654 | 1 | 0.1152 | 1 | 0.1649 | 1 | 0.2164 |
| 2 | 0.0019 | 2 | 0.0656 | 2 | 0.1154 | 2 | 0.1651 | 2 | 0.2166 |
| 3 | 0.0033 | 3 | 0.0666 | 3 | 0.1164 | 3 | 0.1661 | 3 | 0.2176 |
| 4 | 0.0085 | 4 | 0.0693 | 4 | 0.1192 | 4 | 0.1687 | 4 | 0.2202 |
| 5 | 0.0141 | 5 | 0.0794 | 5 | 0.1293 | 5 | 0.1801 | 5 | 0.2316 |
| 6 | 0.0211 | 6 | 0.11 | 6 | 0.1598 | 6 | 0.2113 | 6 | 0.2628 |
| 7 | 0.059 | 7 | 0.373 | 7 | 0.4231 | 7 | 0.4745 | 7 | 0.526 |
| 8 | 0.3235 | 8 | 0.671 | 8 | 0.7206 | 8 | 0.7723 | 8 | 0.8238 |
| 9 | 0.6214 | 9 | 0.7721 | 9 | 0.8217 | 9 | 0.8735 | 9 | 0.925 |
| 10 | 0.7225 | 10 | 0.9419 | 10 | 0.9917 | 10 | 1.0433 | 10 | 1.0949 |
| 11 | 0.8924 | 11 | 0.1135 | 11 | 0.1632 | 11 | 0.2147 | 11 | 0.2662 |
| 12 | 0.0637 | | | | | | | | |

According to Figures 5.7 through 5.11, the expansion at the cold end (i.e. KP 2000) starts to sharply increase with the continuous increase in temperature once the pipeline becomes fully mobilized (in this case, it occurs after “load7”). With regards to the fully mobilized status, it can also be recognized by the values of the pipeline mid-point (i.e. KP 1000) displacement as given in Table 5.3. It shows that less variations of the expansion after the 7th load step in each cycle.

Table 5.3: Mid-Point Pipe Displacement

| 1st Cycle | | 2nd Cycle | | 3rd Cycle | | 4th Cycle | | 5th Cycle | |
|-----------|----------|-----------|----------|-----------|----------|-----------|----------|-----------|----------|
| Load No. | DISP (m) | Load No. | DISP (m) | Load No. | DISP (m) | Load No. | DISP (m) | Load No. | DISP (m) |
| 1 | 0 | 1 | 0.0042 | 1 | 0.0541 | 1 | 0.1037 | 1 | 0.1552 |
| 2 | 0.0001 | 2 | 0.0077 | 2 | 0.0575 | 2 | 0.1071 | 2 | 0.1587 |
| 3 | 0.0004 | 3 | 0.0232 | 3 | 0.073 | 3 | 0.1226 | 3 | 0.1741 |
| 4 | 0.0026 | 4 | 0.0551 | 4 | 0.1048 | 4 | 0.1539 | 4 | 0.2054 |
| 5 | 0.0133 | 5 | 0.0628 | 5 | 0.1126 | 5 | 0.1639 | 5 | 0.2154 |
| 6 | 0.0083 | 6 | 0.0538 | 6 | 0.1036 | 6 | 0.1551 | 6 | 0.2066 |
| 7 | 0.0029 | 7 | 0.0531 | 7 | 0.1033 | 7 | 0.1546 | 7 | 0.2061 |
| 8 | 0.0036 | 8 | 0.0532 | 8 | 0.1029 | 8 | 0.1546 | 8 | 0.2061 |
| 9 | 0.0036 | 9 | 0.0533 | 9 | 0.1028 | 9 | 0.1546 | 9 | 0.2061 |
| 10 | 0.0036 | 10 | 0.0531 | 10 | 0.1029 | 10 | 0.1546 | 10 | 0.2061 |
| 11 | 0.0036 | 11 | 0.0534 | 11 | 0.103 | 11 | 0.1545 | 11 | 0.206 |
| 12 | 0.0035 | | | | | | | | |

5.2.3 Axial Displacement: Walking

The cumulative axial displacement is to be considered to perceive the effect of the thermal cyclic loading on the movement of the pipeline. [1] This section handles axial walking results at the mid-point and two ends due to the expansion and contraction with the subject temperature profiles.

5.2.3.1 Walking at Mid-Point

The Table 5.3 in Ch. 5.2.2 shows the axial displacement at the mid-point of the pipeline through entire cycles (5-cycle). It also presents that each cycle consists of 11 load steps except for the first cycle which has 12 load steps due to the initial condition. Hence, totally 56 temperature load steps are applied to the pipeline model in the FEA. Eventually, the graph of the mid-point displacement under the 5-cycle operation is illustrated as Figure 5.12:

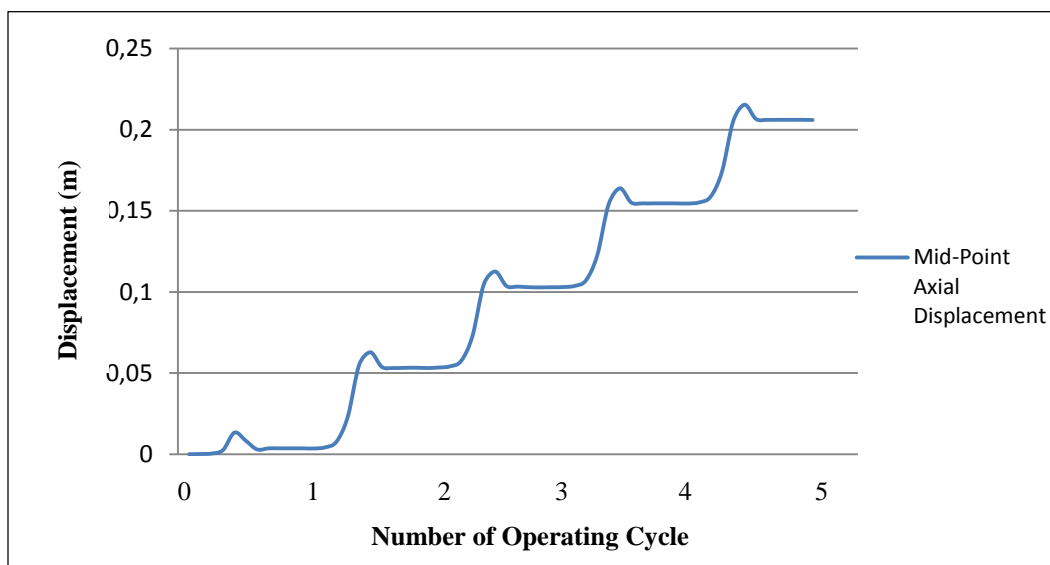


Figure 5.12: Axial Walking at Mid-Point

The Figure 5.12 indicates the walking begins to occur during the second heat-up and becomes stabilized as the operating cycles continue. It is because the constant growth of the displacement under the FE model condition. It shows approximate 0.05m walk in every cycle in the case. The walking rate screening calculation based on ref. [15] also shows about 0.05m per cycle. Its numerical calculation sheet is presented in Appendix I.

Therefore, it can be assumed that it will have the same displacement increase (i.e. same walking rate) in subsequent cycles after the fifth. If the allowable walking distance is 1.0 meter, it can say that the subject pipeline system will be able to operate 20 startup/shutdown cycles based on the results of it.

5.2.3.2 Walking at Two Ends (Hot/Cold)

The data based on the Table 5.1 and 5.2 in Ch. 5.2.2 is used to present the graph of the axial displacement at the two ends (Hot/Cold) of the pipeline over 5 cycles. The temperature load conditions are the same as the mid-point (totally 56 temperature load steps). Accordingly, both ends displacement are illustrated as Figure 5.13 and 5.14 respectively:

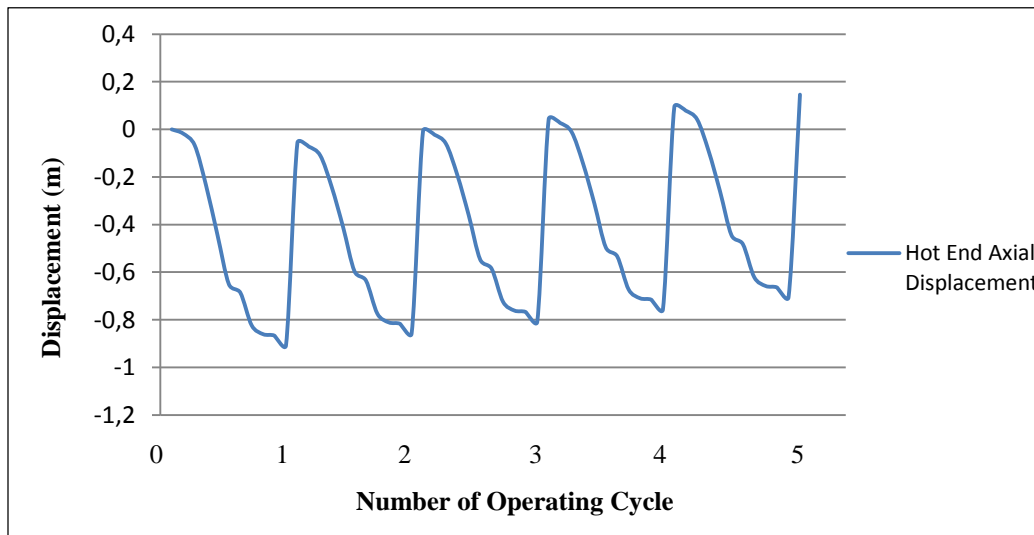


Figure 5.13: Axial Walking at Hot End

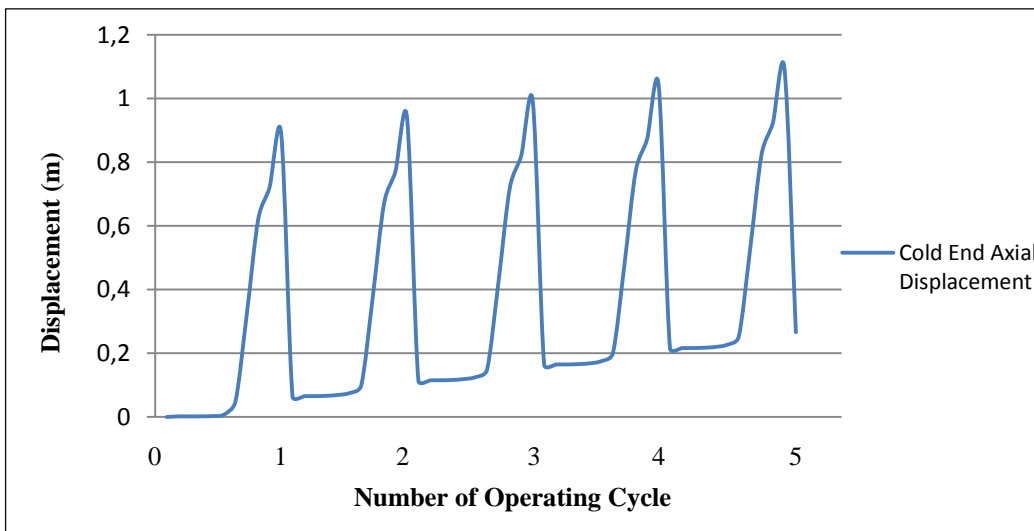


Figure 5.14: Axial Walking at Cold End

Finally, graphs of axial walking results can be plotted together and it is shown as Figure 5.15:

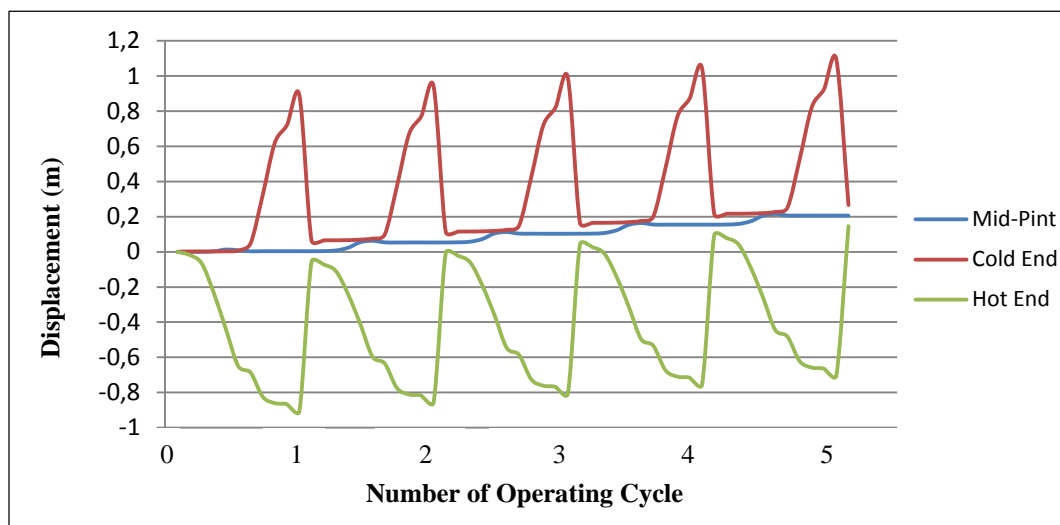


Figure 5.15: Axial Walking Displacement

The Figure 5.15 shows that over the shut-in and restart cycles, i.e. operations after completing the first cycle, the pipeline has a tendency not to return to the same position/condition. It means that a relative axial movement is made with those repeated cycles and consequently, the pipeline in the case study experiences an accumulated walking.

5.3 Pipeline Response upon Axial Friction Factor

This section discusses the analysis results regarding the impact of axial friction factors on the walking phenomenon. Basically, three models are generated with different friction coefficients described in Ch.4.3.2, and the additional coefficient value of 2.0 is modeled for the extensive analysis on the walking.

5.3.1 Effective Axial Force Profile

The graphs of the first cycle effective axial force for each model (LB: 0.3, BE: 0.5, UB: 0.7) are illustrated as Figures 5.16 through 5.18 respectively:

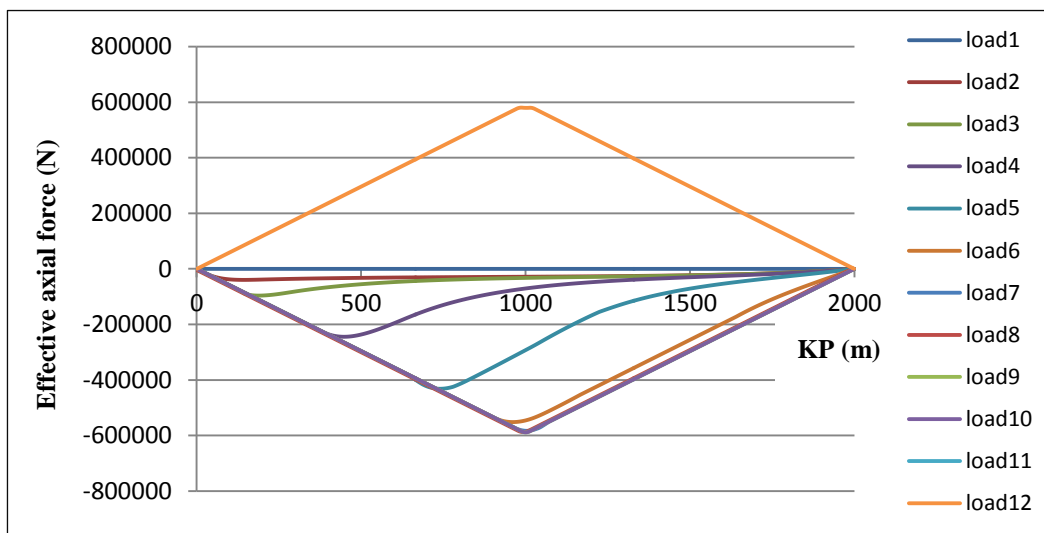


Figure 5.16: Effective Axial Force for 1st Cycle with Friction factor 0.3

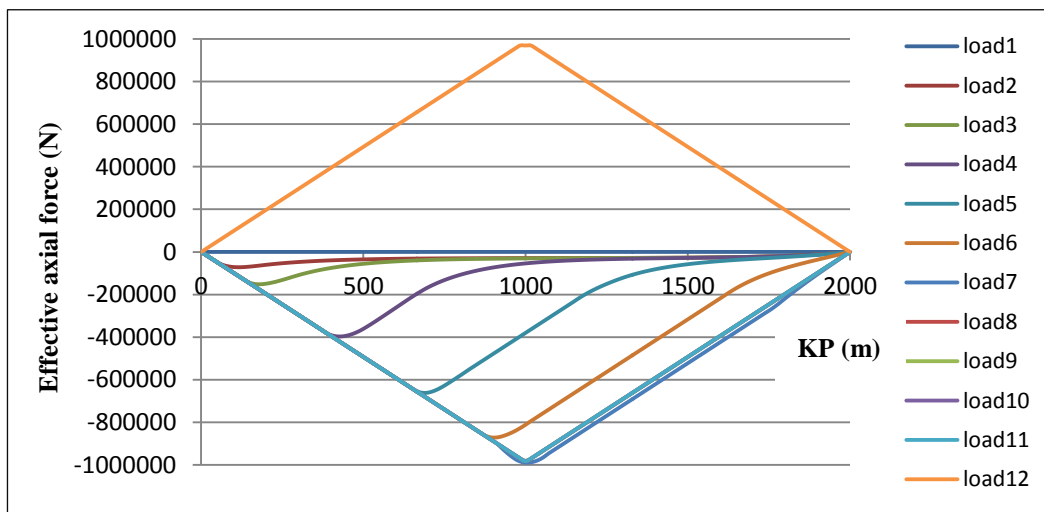


Figure 5.17: Effective Axial Force for 1st Cycle with Friction factor 0.5

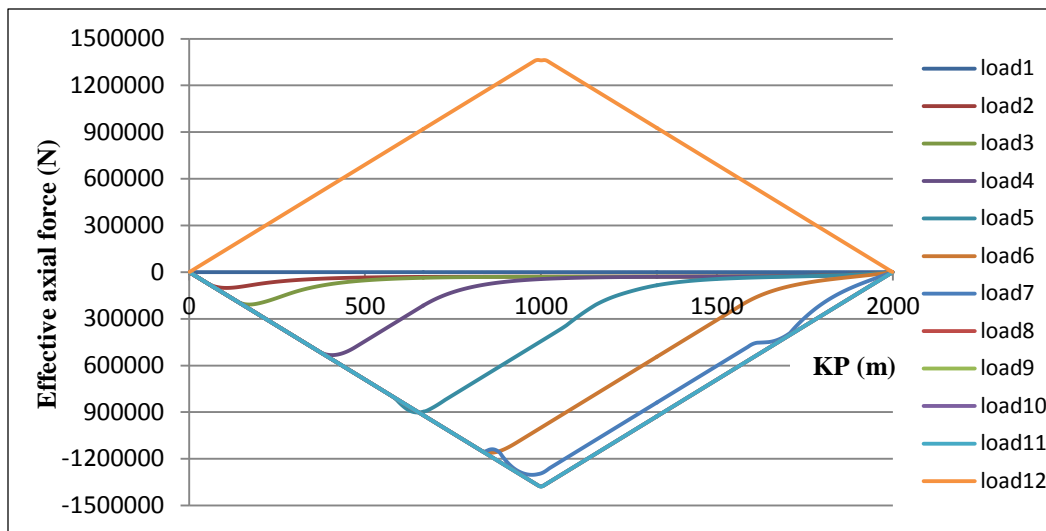


Figure 5.18: Effective Axial Force for 1st Cycle with Friction factor 0.7

It shows that the EAF increases as the friction factor rises. The VAPs are located in the middle of the pipeline when the pipeline becomes fully mobilized (after “load7” in all cases), and the EAFs at the positions are $-5.8 \times 10^5 \text{N}$, $-9.7 \times 10^5 \text{N}$ and $-1.3 \times 10^6 \text{N}$ respectively. It is because that the axial resistance (force) per unit length is directly related with the submerged pipeline weight and the friction factor, which is also presented in Ch.2.2.2.2.

However, it gives the different results when the axial friction coefficient becomes bigger than aforementioned factors and reaches a certain value (2.0 in the study). The EAF decreases with that value shown as Figure 5.19. Besides, the force profile is similar to the case of the cyclically constrained pipeline that is presented in Ch.2.3.3.

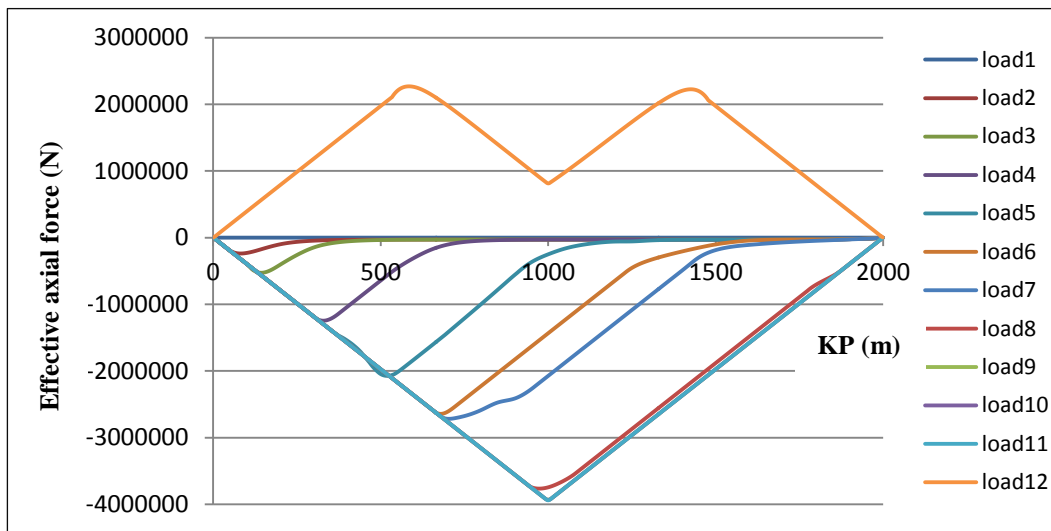


Figure 5.19: Effective Axial Force for 1st Cycle with Friction factor 2.0

Another observation considering variations in axial friction factor is given from the developed EAF profiles during subsequent operating cycles. The force profiles particularly for 4th and 5th cycles under the friction factor 0.5 and 0.7 are shown as Figures 5.20 through 5.23 respectively:

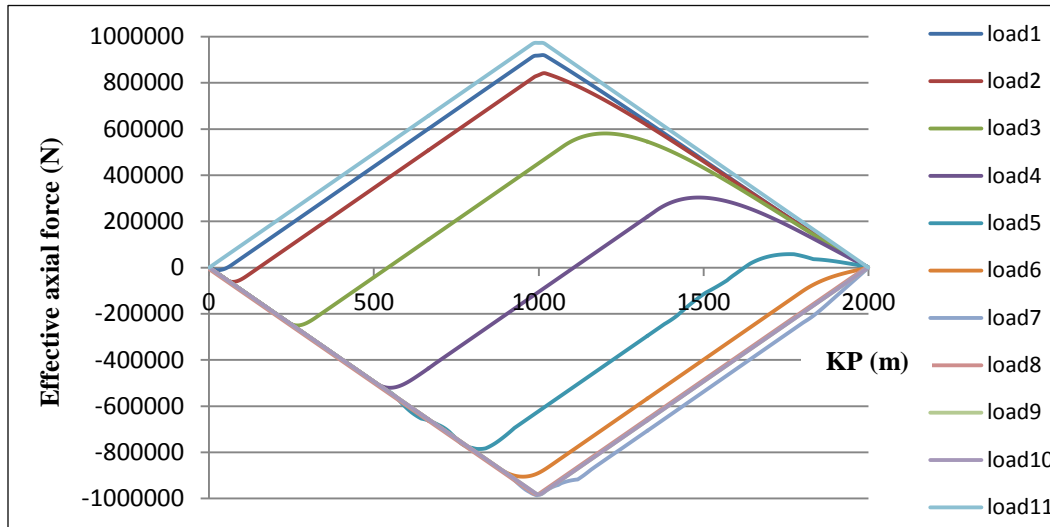


Figure 5.20: Effective Axial Force for 4th Cycle with Friction Factor 0.5

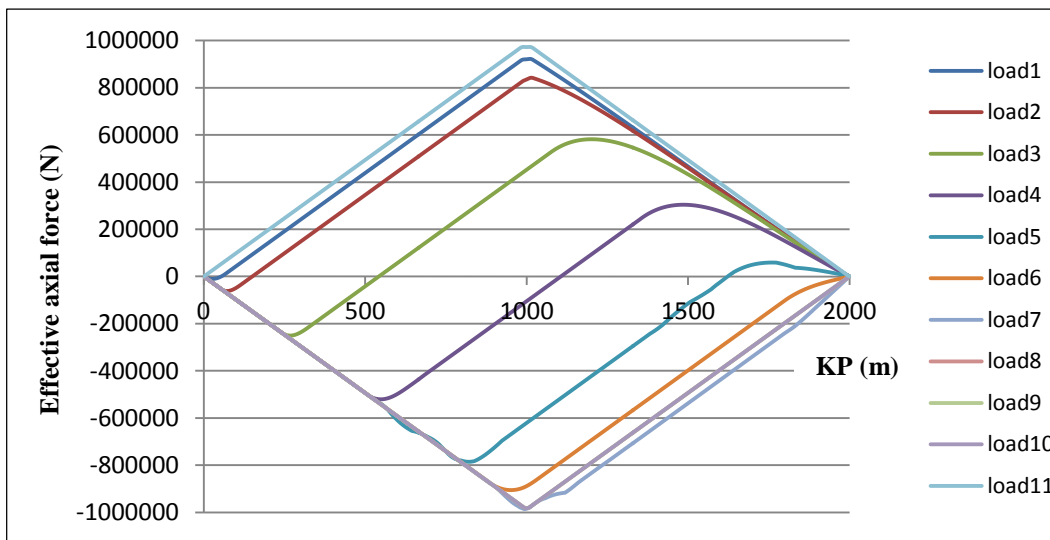


Figure 5.21: Effective Axial Force for 5th Cycle with Friction Factor 0.5

The calculated force data and its profile show that the EAF goes constant (less variation) after certain operating cycles. This case, it begins to happen after the 4th cycle. When the pipeline becomes fully mobilized, the maximum values of the EAF in each cycle (4th and 5th) are $-9.732 \times 10^5 \text{ N}$ and $-9.728 \times 10^5 \text{ N}$ respectively with the factor of 0.5. Similarly, it shows $-1.376 \times 10^6 \text{ N}$ and $-1.376 \times 10^6 \text{ N}$ with the factor of 0.7. Other cases: friction factor 0.3 and 2.0 also

indicate the similar results. The factor of 0.3 case is presented in Ch.5.2.1, and relevant EAF profiles of 2.0 case are presented separately in Appendix V.

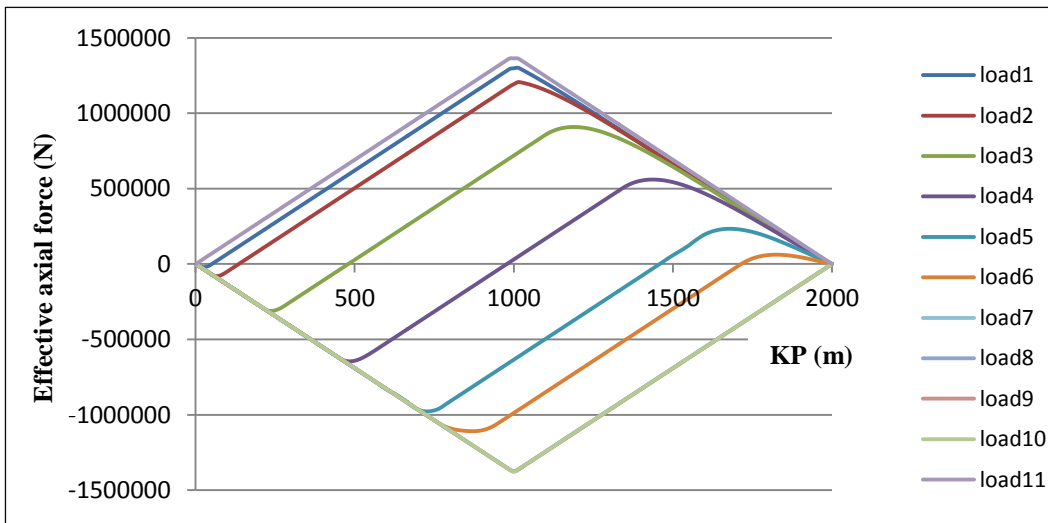


Figure 5.22: Effective Axial Force for 4th Cycle with Friction Factor 0.7

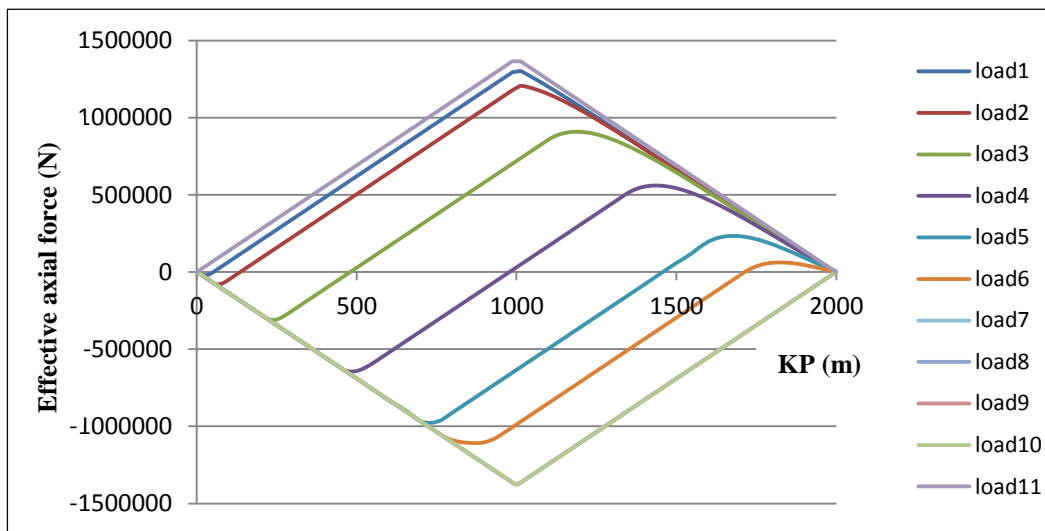


Figure 5.23: Effective Axial Force for 5th Cycle with Friction Factor 0.7

5.3.2 Axial Displacement

This section discusses the axial movements over a range of operating cycles (5-cycle) under different friction coefficient conditions. The results of the displacement in the section mainly deal with the axial displacements at Mid-point, Hot end and Cold end of the pipeline.

5.3.2.1 Mid-Point Axial Displacement

The table 5.4 and 5.5 show the axial displacement at the mid-point of the pipeline with friction factors: 0.5 and 0.7 respectively. Regarding the factor of 0.3 case is presented in Table 5.3 in Ch. 5.2.3.

Table 5.4: Mid-Point Axial Displacement with Friction Factor 0.5

| 1st Cycle | | 2nd Cycle | | 3rd Cycle | | 4th Cycle | | 5th Cycle | |
|-----------|----------|-----------|----------|-----------|----------|-----------|----------|-----------|----------|
| Load No. | DISP (m) | Load No. | DISP (m) | Load No. | DISP (m) | Load No. | DISP (m) | Load No. | DISP (m) |
| 1 | 0 | 1 | 0.0148 | 1 | 0.0964 | 1 | 0.1781 | 1 | 0.2598 |
| 2 | 0 | 2 | 0.0179 | 2 | 0.0995 | 2 | 0.1812 | 2 | 0.263 |
| 3 | 0.0001 | 3 | 0.0338 | 3 | 0.1154 | 3 | 0.1971 | 3 | 0.2788 |
| 4 | 0.0009 | 4 | 0.0756 | 4 | 0.1572 | 4 | 0.2388 | 4 | 0.3206 |
| 5 | 0.0129 | 5 | 0.1021 | 5 | 0.1838 | 5 | 0.2654 | 5 | 0.3472 |
| 6 | 0,0202 | 6 | 0.1001 | 6 | 0.1817 | 6 | 0.2636 | 6 | 0.3454 |
| 7 | 0.013 | 7 | 0.0952 | 7 | 0.1768 | 7 | 0.2584 | 7 | 0.3404 |
| 8 | 0.0137 | 8 | 0.0953 | 8 | 0.1769 | 8 | 0.2588 | 8 | 0.3406 |
| 9 | 0.0136 | 9 | 0.0953 | 9 | 0.177 | 9 | 0.2588 | 9 | 0.3406 |
| 10 | 0.0136 | 10 | 0.0953 | 10 | 0.1769 | 10 | 0.2588 | 10 | 0.3406 |
| 11 | 0.0136 | 11 | 0.0955 | 11 | 0.1772 | 11 | 0.259 | 11 | 0.3408 |
| 12 | 0.0139 | | | | | | | | |

Table 5.5: Mid-Point Axial Displacement with Friction Factor 0.7

| 1st Cycle | | 2nd Cycle | | 3rd Cycle | | 4th Cycle | | 5th Cycle | |
|-----------|----------|-----------|----------|-----------|----------|-----------|----------|-----------|----------|
| Load No. | DISP (m) | Load No. | DISP (m) | Load No. | DISP (m) | Load No. | DISP (m) | Load No. | DISP (m) |
| 1 | 0 | 1 | 0.0218 | 1 | 0.1256 | 1 | 0.2294 | 1 | 0.3332 |
| 2 | 0 | 2 | 0.0244 | 2 | 0.1283 | 2 | 0.232 | 2 | 0.3359 |
| 3 | 0 | 3 | 0.0407 | 3 | 0.1445 | 3 | 0.2483 | 3 | 0.3521 |
| 4 | 0.0004 | 4 | 0.0872 | 4 | 0.191 | 4 | 0.2948 | 4 | 0.3987 |
| 5 | 0.0115 | 5 | 0.125 | 5 | 0.2288 | 5 | 0.3325 | 5 | 0.4364 |
| 6 | 0.0255 | 6 | 0.129 | 6 | 0.2327 | 6 | 0.3366 | 6 | 0.4404 |
| 7 | 0.0237 | 7 | 0.1255 | 7 | 0.2293 | 7 | 0.3323 | 7 | 0.4362 |
| 8 | 0.0211 | 8 | 0.1247 | 8 | 0.2284 | 8 | 0.3323 | 8 | 0.4361 |
| 9 | 0.0211 | 9 | 0.1247 | 9 | 0.2284 | 9 | 0.3323 | 9 | 0.4361 |
| 10 | 0.0211 | 10 | 0.1246 | 10 | 0.2284 | 10 | 0.3323 | 10 | 0.4361 |
| 11 | 0.0211 | 11 | 0.1247 | 11 | 0.2285 | 11 | 0.3323 | 11 | 0.4362 |
| 12 | 0.0209 | | | | | | | | |

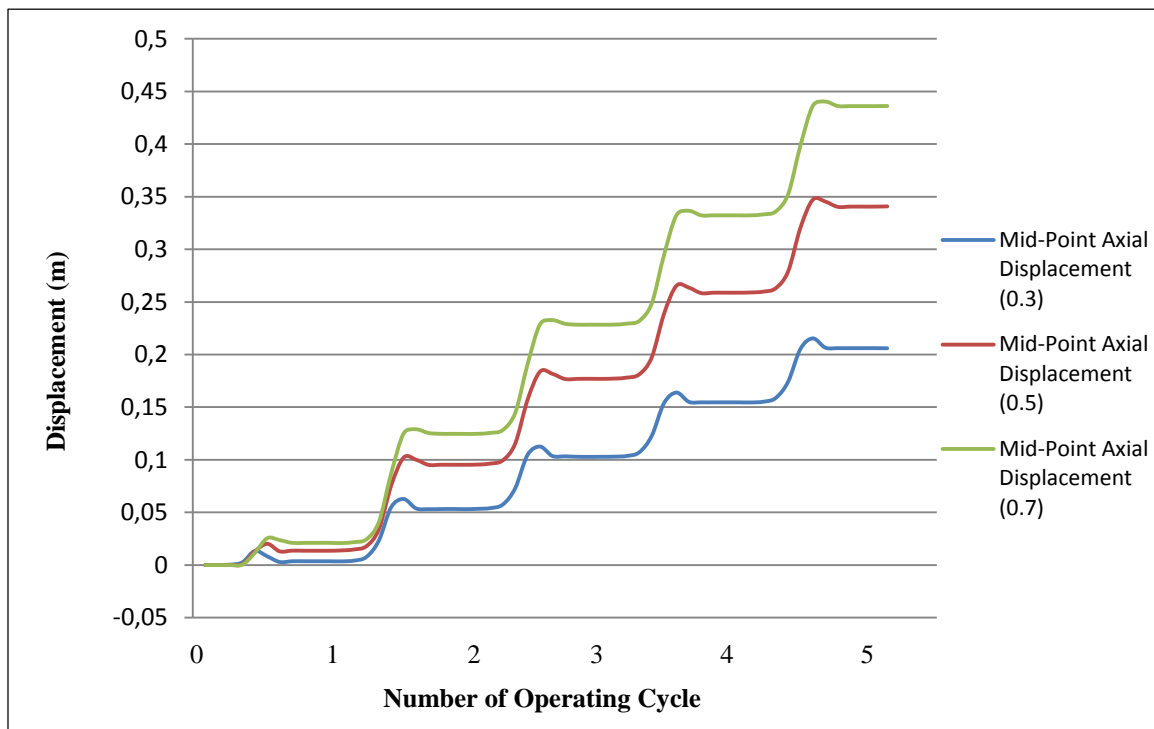


Figure 5.24: Axial Walking Displacement at Mid-Point with Friction Factor 0.3, 0.5 & 0.7

The axial displacements under the given conditions are plotted according to Tables 5.3 through 5.5, and it is shown as Figure 5.24. It indicates that the axial walking rises as the friction

increases in the range of friction factors. The walking rate per operational cycle with different values of the friction factor is given in Table 5.6:

Table 5.6: Results of Walking Rate

| Friction Factor | | Walking Rate |
|-----------------|-----|------------------|
| LB | 0.3 | Abt. 0.05m/cycle |
| BE | 0.5 | Abt. 0.08m/cycle |
| UB | 0.7 | Abt. 0.1m/cycle |

5.3.2.2 Axial Displacement with Friction Factor 2.0

It can be expected to get the different consequence concerning the walking in accordance with the results of the EAF with friction factor of 2.0, which is discussed in Ch.5.3.1. The Table 5.7 shows the axial displacement at the mid-point of the pipeline with the factor of 2.0:

Table 5.7: Mid-Point Axial Displacement with Friction Factor 2.0

| 1st Cycle | | 2nd Cycle | | 3rd Cycle | | 4th Cycle | | 5th Cycle | |
|-----------|----------|-----------|----------|-----------|----------|-----------|----------|-----------|----------|
| Load No. | DISP (m) | Load No. | DISP (m) | Load No. | DISP (m) | Load No. | DISP (m) | Load No. | DISP (m) |
| 1 | 0 | 1 | 0.0117 | 1 | 0.0553 | 1 | 0.1009 | 1 | 0.147 |
| 2 | 0 | 2 | 0.0117 | 2 | 0.0553 | 2 | 0.1009 | 2 | 0.147 |
| 3 | 0 | 3 | 0.0117 | 3 | 0.0553 | 3 | 0.101 | 3 | 0.147 |
| 4 | 0 | 4 | 0.0136 | 4 | 0.057 | 4 | 0.1034 | 4 | 0.1496 |
| 5 | 0.0012 | 5 | 0.0521 | 5 | 0.098 | 5 | 0.144 | 5 | 0.1902 |
| 6 | 0.0121 | 6 | 0.0565 | 6 | 0.1022 | 6 | 0.1482 | 6 | 0.1936 |
| 7 | 0.0131 | 7 | 0.0558 | 7 | 0.1015 | 7 | 0.1475 | 7 | 0.1936 |
| 8 | 0.0123 | 8 | 0.0555 | 8 | 0.1012 | 8 | 0.1472 | 8 | 0.1934 |
| 9 | 0.0119 | 9 | 0.0555 | 9 | 0.1012 | 9 | 0.1472 | 9 | 0.1934 |
| 10 | 0.0119 | 10 | 0.0553 | 10 | 0.101 | 10 | 0.147 | 10 | 0.1932 |
| 11 | 0.0119 | 11 | 0.0553 | 11 | 0.1009 | 11 | 0.147 | 11 | 0.1931 |
| 12 | 0.0117 | | | | | | | | |

It can be seen that the axial movement (walking) is reduced compared to the results with other factors (lower values) and gives approximate 0.046m/cycle under the condition. Therefore, the pipelines can partly response like a long pipeline, which is fully restrained over a fixed length under operation conditions, when the axial friction is high enough. As it becomes constrained, the walking phenomenon consequently is to decrease or to disappear.

5.4 Mitigation Measures for Pipeline Walking

This thesis work mainly focuses on pipeline walking which is resulted by cyclic heating and cooling operations of a pipeline especially when the pipeline asymmetrically loaded. This is because the fact that the heating operation is non-uniform, whereas the cooling operation is nearly uniform. [11] Consequently, the instability of pipeline on the seabed occurred by the pipeline walking phenomenon is to be taken into account, and mitigation methods can be discussed by considering the causes of pipeline walking.

This section outlines mitigation measures of pipeline walking based on an understanding of its mechanisms and the results from the case study. The selection of walking mitigation method is evidently depends on the consequential effects of accumulated axial displacement due to pipeline walking. Thus, each mitigation method and its impact on pipeline design are briefly discussed. However, installation, cost of method and planning are not to be presented since it is beyond the scope of this study.

5.4.1 Anchoring [11]

The pipeline anchors are the most common method to mitigate pipeline walking. It controls and limits the maximum axial displacement by inducing additional tension in the pipeline especially during a shutdown. A typical size of these anchors is in the range of 50 to 350 tons, and its general illustration is shown in Figure 5.25: [1]



Figure 5.25: A Typical Pipeline Restraining Anchor (Ryan Watson et al., 2010) [16]

The pipeline walking phenomenon is associated with the virtual anchor point shifts in the pipeline during heating and cooling operations under asymmetrical load conditions. This means the efficient mitigation can be set by correcting the separation between the virtual anchors. Thus, the end support anchoring can be introduced. It works by way of reducing the separation between the virtual anchors. Anchoring a pipeline especially in the cases of end tension or seabed slope gives equal amount of corrective tension at the opposite end. It functions that the asymmetric

loading is eliminated not to occur walking. Moreover, an anchor can be placed on the pipeline to force the virtual anchor points to share the same location on the pipe.

The tension induced by an anchor can be sufficient for a pipeline to be susceptible to lateral instability (buckling) while an anchor is eliminating walking. In addition, the walking phenomenon can still occur in that buckled region, so walking into a buckle may give over stress into the pipeline. [3] Consequently, it should ensure that the location of an anchor is to be well considered in terms of possible buckling in the pipeline.

5.4.2 Increase Axial Friction [1]

The walking phenomenon critically depends on the critical axial force. In some cases shows that the walking rate is to decrease due to the growth of an axial friction to a certain extent. [3] Even the sensitivity study in the thesis work also notes that aspect. Hence, increasing axial friction can be considered to mitigate pipeline walking, and there are several treatments for this achievement.

5.4.2.1 Pipe-Soil Interaction

By investigating a specific pipe-soil interaction on site, it can improve friction factors for design since lower values of friction factors can be expected. However, collecting soil data is quite time consuming activity and costly. Besides, a deep water soil survey is to be one of challenges to get the accurate analysis. It is not just because of the very low shear strength exhibited by most deep water seabed top layers, but also because of the very low effective stress level (a few kPa only). [3] Consequently, it may be impractical to produce such a high axial resistance especially in a deep water pipeline without additional mitigation to control pipeline walking.

5.4.2.2 Pipeline Weight Coating

A concrete weight coating can be a possible way to increase axial and lateral friction resistance which is advantageous to reduce expansion and walking. However, it is likely to experience lateral buckling due to the higher axial resistance, and the higher localized strains may also take place because of higher lateral frictions. [3]

5.4.2.3 Trench and Bury

Those can be used to increase the axial friction resistance in the pipeline. However, a high cost concern and limited equipment for deep water are challenges.

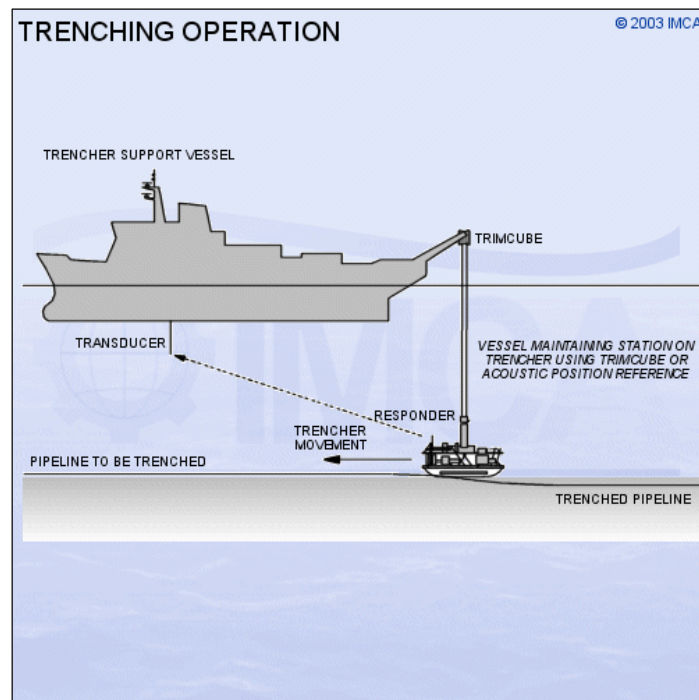


Figure 5.26: A Trenching Operation (from www.theareofdreging.com)

5.4.2.4 Rock Dumping and Mattress

It gives such a function of additional anchoring, so it can reduce the end expansion and walking in addition to buckling controls. However, a large amount of materials is to be required to limit the walking problem. In addition, installation time, cost and recruiting specific vessels for installation are other challenges.

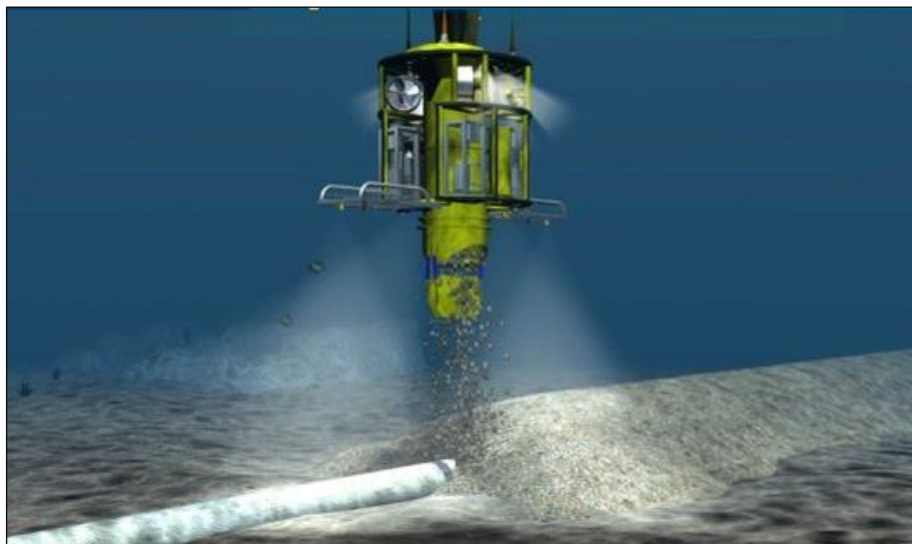


Figure 5.27: A Rock Dumping Operation (from www.nordnes.nl)

5.4.3 Increase Subsea Connection Line Capacity

When it comes to a limit state for the pipeline, the walking phenomenon is not a failure mode, [2] but it can lead to overstressing on subsea structure connections. Thus, by increasing the capacity of spools and/or jumpers it can accommodate the axial displacement of pipeline induced by walking. However, installation and handling limits may be restrictions for increasing their capacities. [3]

5.5 Summary

This chapter has discussed the results of the FEA on pipeline walking under the thermal cyclic loadings and dealt with different values of the axial friction factors for the sensitivity study. There are no variations in the EAF when the pipeline is fully mobilized (after the 7th load step in this case). From the second heat-up, two VAPs appear and move towards the mid-point and the cold-end respectively as the pipeline gradually heated-up. With regards to pipeline expansion, it becomes constant (less variations) when fully mobilized, especially at the mid-point of the pipeline in the case. Besides, the walking rate per cycle has increased as the value of the axial friction factor increase. However, the rate was reduced at the certain value of the factor (here, 2.0), and it showed that the axial movement decreases with further increase in friction factor.

In addition to that, the chapter has briefly presented the pipeline walking mitigation. Some measures are introduced and it is to be considered in terms of relevant mechanisms of pipeline walking: walking towards the tension end, bottom end of the slope, and the cold end when transient heating is applied. It implies that the direction of walking and the associated parameters are key factors for it. The increment of the axial friction can be selected as the mitigation method based on the results of the case study, and increase capacity of the subsea structures can be another option.

6. Conclusion and Further Study

6.1 General

This chapter deals with the conclusions of the thesis work based on the analysis results in Ch. 5. It describes the results briefly regarding the pipeline walking phenomenon under the thermal cyclic loadings in the FEA. The further study is also to present in connection with the works in the thesis.

6.2 Conclusions

The objective of the thesis is to study and understand pipeline walking when it is subjected to the succession of thermal cycles. For the case study, thus, the FE model is generated and the thermal gradients are modeled to simulate the propagation of temperatures along the pipeline during operational cycles (5cycles considered in the study). The API 5L X65 grade pipeline with the length of 2km laid on the flat seabed and the maximum operating temperature 88°C are selected for analysis. The followings are conclusions based on the FEA results:

1. The relatively short pipeline is prone to axial walking due to thermal transients. It is because the overall length of it is not insufficient to reach full restraint, and the VAP is located at the middle of the pipeline where the EAF gets its max value. Even the pipeline on the flat seabed with no end tension can experience the walking.
2. The axial movement under the thermal cyclic loadings is to translate from the hot-end towards the cold-end. The results in Ch.5.2.3 support the conclusion. Hence, considering the accurate assessment of walking for the reliability/capacity of the end connectors is important.
3. Once the pipeline is fully mobilized, no variations in the EAF occur. Besides, the EAF becomes constant after certain operations (after 4 cycles in the case study). Thus, the walking rate is to be predictable without simulating more cycles.
4. The pipe-soil interaction is one of the important parameters in the walking assessment. The walking rates grow as the axial friction factor increases according to Ch.5.3.2. However, It turns to decrease with the certain value of the friction factor (here, 2.0). Therefore, the increment of the axial friction can be one of possible methods to limit the walking rate.

6.3 Further Study

This section presents the further works, and the followings are to be performed:

1. It is quite difficult to predict the accurate axial friction especially in deep water due to the uncertainties of soil conditions. Hence, more specific parameter studies regarding soil conditions to be carried out in connection with pipeline walking.
2. Walking can be occurred by each of aforementioned mechanisms, but for many pipelines more than one mechanism may be active. Thus, effects of combinations are to be studied. Furthermore, the interaction between pipeline walking and lateral buckling can be studied especially for a long pipeline. The long pipeline is effectively split into several short pipelines due to buckling mitigation measures that acting as pipeline ends.

REFERENCE

- [1] Bruton, D. S., Sinclair, F. and Carr, M., “*Pipeline walking – Understanding the Field Layout Challenges, and Analytical Solutions Developed for the SAFEBUCK JIP*”, OTC 17945, Houston, TX, May 2006.
- [2] Bruton, D. A. S., Sinclair, F. and Carr, M., “*Lessons Learned From Observing Walking of Pipeline with Lateral Buckles, Including New Driving Mechanisms and Updated Analysis Models*”, OTC 20750, Huston, TX, May 2010.
- [3] Rong, H., Inglis R., Bell G., Huang Z. and Chan, R., “*Evaluation and Mitigation of Axial Walking with a Focus on Deep Water Flowlines*”, OTC 19862, Houston, TX, May 2009.
- [4] Palmer, Andrew C. and Ling, Michael T.S., “*Movement of Submarine Pipelines Close to Platforms*”, OTC 4067, Houston, TX, May 1981.
- [5] Kumar, Amitabh and M. Brian, “*Global Buckling and Axial Stability for HP/HT flowlines*”, OTC 20126, Houston, TX, May 2009.
- [6] Chen, Qiang (2012), “*Pipelines and Risers*”, Class notes, University of Stavanger (Unpublished).
- [7] Pipeline Encyclopedia, “*Pipeline Expansion*”, (Cited 11th Feb. 2013), Available from: <<http://pipelineencyclopedia.blogspot.no>>.
- [8] Karunakaran, D. (2012), “*Pipelines and Risers*”, Class notes, University of Stavanger (Unpublished).
- [9] Fyrileiv, Olav and Collberg, Leif, “*Influence of pressure in pipeline design-effective axial force*”, OMAE2005-67502, Proceedings of OMAE 2005, Halkidiki, Greece, 2005.
- [10] Bruton, David A.S., White, David J. and Carr. M., “*Pipe-Soil Interaction During Lateral Buckling and Pipeline walking – The SAFEBUCK JIP*”, OTC 19589, Houston, TX, May 2008.
- [11] Chaudhury, Gautam, “*Managing Unidirectional Movements (Walk) of HP/HT Submarine Flowlines During Heating and Shutdown Cooling*”, IOPF 2010-1003, Houston, TX, Oct. 2010.
- [12] Bruton, D., Carr, M., Crawford, M. and Poiate, E. “*The Safe Design of Hot On-Bottom Pipelines with Lateral Buckling using the Design Guideline Developed by the SAFEBUCK Joint Industry Project*”, Deep Offshore Technology Conference, Vitoria, Espirito, Brazil (2005), (Cited 2nd April 2013), Available from: <http://www.otmdevelopment4.co.uk/DOT2005-SAFEBUCK_JIP-Overview.pdf>.

- [13] Ommundsen, Marius Loen, “*UPHEAVAL BUCKLING OF BURIED PIPELINES*” MSc thesis, University of Stavanger, 2009, p.10.
- [14] Watson, R.D., Sinclair, F. and Bruton, D. A. S., “*SAFEBUCK JIP: Operational Integrity of Deepwater Flowlines*”, OTC 21724, Houston, TX, May 2011.
- [15] SAFEBUCK JIP, “Safe Design of Pipelines with Lateral Buckling Design Guideline”, Report Number BR02050/SAFEBUCK/B issued Aug. 2004, p. 18~20. (Confidential to JIP Participants).
- [16] Watson, R., Bruton D., Sinclair, F “*Influence of Multiphase Flow on Global Displacement of Deepwater Pipelines – In Design and Operation*”, IOPF 2010-6002, Houston, TX, Oct. 2010.
- [17] Brunner, M.S., Qi, X., Zheng, J. and Chao, J.C., “*Combined Effect of Flowline Walking and Riser Dynamic Loads on HP/HT Flowline Design*”, OTC 17806, Houston, TX, May 2006.
- [18] Subsea 7, “*Guideline for Pipeline Walking and Lateral Buckling*”, Doc. No. GR-DCE-RPL-018, Feb. 2010 (Confidential to Subsea 7).
- [19] AdvancePipeliner, “*Global Buckling and Walking in Subsea Pipelines: Consequences and Mitigation Measures*”, (Cited 2nd Feb. 2013), Available from: <<http://www.advancepipeliner.com/site/index.php/component/content/article/131-allcategories/61-global-buclking-and-walking-in-subsea-pipelines-consequences-and-mitigation-measures.html>>.
- [20] Subsea 7, “*Design Guidelines Pipeline walking analysis*”, Doc. No. CEO1PD-P-GU-129, Nov. 2007 (Confidential to Subsea 7).
- [21] ANSYS, Inc., “*Theory Reference for the Mechanical APDL and Mechanical Applications*”, Release 12.1, Nov. 2009, p.793~814⁴/ p. 880~885⁵.
- [22] ANSYS Inc., “*ANSYS User Manuals released 13.0*”, 2010, (Cited 22nd April 2013), Available from: <https://www.sharcnet.ca/Software/Fluent13/help/ans_elem/Hlp_E_PIPE288.html>.
- [23] ANSYS, Inc., “*Contact Technology Guide*”, Release 12.1, Nov. 2009, p. 69~71.
- [24] Bai, Yong “Pipelines and risers”, Elsevier Ocean Engineering book series vol.3, p. 101~114.
- [25] DNV-OS-F101, DNV Offshore Standard “Submarine Pipeline Systems”, Det Norske Veritas, August 2012, Sec.4 G400.

⁴ Ch. 3.2.3/ 3.3.2

⁵ Ch.3.3.1

[26] Casola, F., Chayeb, A. E., Greco S., Carlucci, A., “*Characteristic of Pipe Soil Interaction and Influence on HPHT Pipeline Design*”, ISBN 978-1-880653-96-8 (Set); ISSN 1098-6189 (Set), Proceedings of ISOPE, Maui, Hawaii, USA 2011.

[27] Subsea 7, “*Pipelines Design Centre of Excellence Documentation*”, Doc. No. GD-GL-PD-018, Feb. 2007 (Confidential to Subsea 7).

[28] Duncan, J. M., Wright, Stephen G., “*Soil Strength and Slope Stability*”, JOHN WILEY & SONS Inc., Jan. 2005, p. 19.

[29] Oliphant J., Maconochie, A., “*Axial Pipeline-Soil Interaction*”, ISBN 1-880653-66-4 (Set); ISSN 1098-6189 (Set), Proceedings of ISOPE, San Francisco, USA 2006.

[30] Mebarkia, S., “*Effect of High-Pressure/High Temperature Flowlines and Soil Interaction on Deepwater Subsea Development*”, OTC 18107, Houston, TX, May 2006.

[31] DNV-RP-F110, DNV Recommended Practice “*Global Buckling of Submarine Pipelines-Structural Design due to High Temperature/High Pressure*”, Det Norske Veritas, Oct. 2007, Ch.5.2.2/3.

Appendix I

Pipeline Model Parameter Calculation

1. General

This appendix consists of calculations related to the rigid pipeline model which is introduced in chapter 4. The objective of the separate sheets is to validate the results of the FE analysis by ANSYS with respect to pipeline walking. The calculations are carried out according to ref [15] and [20].

2. Input data

2.1 Pipeline

| | |
|---|---------|
| Length (L) | 2000m |
| Pipeline outer diameter (D_o) | 323.9mm |
| Wall Thickness (t) | 25.4mm |
| External (insulation) coating thickness (t_e) | 5mm |
| Concrete coating thickness (t_c) | 30mm |

2.2 Material Properties

2.2.1 Pipeline

| | |
|--|------------------------------|
| Density of pipe steel (ρ_{pipe}) | 7850kg/m ³ |
| SMYS of pipe steel (σ_{SMYS}) | 450MPa |
| Young's modulus of pipe steel (E) | 207 x 10 ³ MPa |
| Thermal expansion coefficient (a_T) | 1.17 x 10 ⁻⁵ / °C |
| Poisson's ratio of pipe steel (ν) | 0.3 |

2.2.2 Insulation / Concrete Coating

| | |
|---|-----------------------|
| Density of insulation coating (ρ_{ext}) | 910kg/m ³ |
| Density of concrete coating (ρ_{conc}) | 2400kg/m ³ |

2.3 Operating Data

| | |
|--|----------------------|
| Operating temperature (T_{OP}) | 88°C |
| Shutdown (ambient) temperature (T_{AB}) | 3.5°C |
| Operating pressure (P_{OP}) | 15Mpa |
| Density of fluid content in pipe (ρ_{oil}) | 900kg/m ³ |

2.3 Environmental and Soil Data

2.3.1 Environmental Data

| | |
|-------------------------------------|-----------------------|
| Density of seawater (ρ_{sw}) | 1027kg/m ³ |
| Water depth (WD) | 100m |

2.3.2 Soil Data

| | |
|-----------------------------------|---------------------|
| Axial friction factor (μ_a) | 0.3 (Initial value) |
|-----------------------------------|---------------------|

3. Calculations

Unit: 1MPa = 1N/mm²; g = 9.81m/s²;

3.1 Parameter Calculations

- Effective Pipe Diameter (t_{eff}) : $D_o + 2(t_e + t_c) = 323.9 + 2(5 + 30) = 393.9\text{mm}$
- Internal diameter (D_i) : $D_o - 2t = 323.9 - 2 \cdot 25.4 = 273.1\text{mm}$
- Cross sectional area of pipe (A_s) :
 $\rightarrow \frac{\pi}{4}(D_o^2 - D_i^2) = \frac{\pi}{4}(323.9^2 - 273.1^2) = 23819\text{mm}^2 = 0.023819\text{m}^2$
- Cross sectional area of insulation coating (A_{ext}) :
 $\rightarrow \frac{\pi}{4}\{(D_o + 2 \cdot t_e)^2 - D_o^2\} = \frac{\pi}{4}\{(323.9 + 2 \cdot 5)^2 - 323.9^2\} = 5166\text{mm}^2$
 $= 0.005166\text{m}^2$
- Cross sectional area of concrete coating (A_{conc}) :
 $\rightarrow \frac{\pi}{4}\{(D_o + 2 \cdot t_e + 2 \cdot t_c)^2 - (D_o + 2 \cdot t_e)^2\} =$
 $\frac{\pi}{4}\{(323.9 + 2 \cdot 5 + 2 \cdot 30)^2 - (323.9 + 2 \cdot 5)^2\} = 34296.77\text{mm}^2$
 $\approx 0.034297\text{m}^2$
- Mass of pipe steel per unit length (m_{pipe}) :
 $\rightarrow A_s \cdot \rho_{pipe} = 23819\text{mm}^2 \cdot 7850\text{kg/m}^3 = 0.023819 \cdot 7850 = 186.979\text{kg/m}$
- Mass of insulation coating per unit length (m_{ext}) :
 $\rightarrow A_{ext} \cdot \rho_{ext} = 5166\text{mm}^2 \cdot 910\text{kg/m}^3 = 0.005166 \cdot 910 = 4.7\text{kg/m}$

- Mass of concrete coating per unit length (m_{conc}) :
$$\rightarrow A_{\text{conc}} \cdot \rho_{\text{conc}} = 0.034297\text{m}^2 \cdot \frac{2400\text{kg}}{\text{m}^3} = 82.31\text{kg/m}$$
- Mass of content (m_{oil}) :
$$\rightarrow \frac{\pi}{4}(D_i^2)\rho_{\text{oil}} = \frac{\pi}{4}(273.1^2\text{mm}^2) \cdot 900\text{kg/m}^3 = \frac{\pi}{4}(273.1^2 \cdot 0.001^2)900$$
$$= 52.72\text{kg/m}$$
- Pipeline total mass per unit length (in air) (m_{total}) :
$$\rightarrow m_{\text{pipe}} + m_{\text{oil}} + m_{\text{ext}} + m_{\text{conc}} = 186.979 + 52.72 + 4.7 + 82.31$$
$$= 326.71\text{kg/m}$$
- Mass of pipe buoyancy per unit length (B_{pipe}) :
$$\rightarrow \frac{\pi}{4}(t_{\text{eff}}^2) \cdot \rho_w = \frac{\pi}{4}(413.9^2\text{mm}^2) \cdot 1027\text{kg/m}^3 = 134549.1(0.001)^2 \cdot 1027$$
$$= 138.2\text{kg/m}$$
- Mass of submerged pipeline per unit length (in water) (m_{sub}) :
$$\rightarrow m_{\text{total}} - B_{\text{pipe}} = 326.71 - 138.2 = 188.51\text{kg/m}$$
- Weight of pipeline per unit length (dry weight) (W_{air}) :
$$\rightarrow m_{\text{total}} \cdot g = 326.71 \cdot 9.81 = 3205.03\text{N/m}$$
- Weight of submerged pipeline per unit length (W_{sub}) :
$$\rightarrow (m_{\text{sub}}) \cdot g = (188.51) \cdot 9.81 = 1849.3\text{N/m} \approx 1.85\text{kN/m}$$

3.2 Walking Rate

- Friction force ($F_{\text{friction}} = f$) :
$$\rightarrow \mu_a \cdot W_{\text{sub}} = 0.3 \cdot 1849.3 = 554.79\text{N/m} \approx 0.56\text{kN/m}$$
- Thermal gradients force (f_{θ}) :
$$\rightarrow A_s \cdot E \cdot a_T \cdot q_{\theta} = 0.023819\text{m}^2 \cdot 207 \times 10^3\text{Mpa} \cdot 1.17 \times 10^{-5}\text{°C} \cdot \left(\frac{88\text{°C} - 3.5\text{°C}}{2000\text{m}}\right)$$
$$= 2437.3\text{N/m} \approx 2.44\text{kN/m}$$
- Walk per cycle due to Thermal Transients (Δ_{θ}) :
$$\rightarrow \Delta_{\theta} = \frac{L^2}{16 \cdot A_s \cdot E} \cdot (\sqrt{24 \cdot f_{\theta} \cdot f} - f_{\theta} - 4f)$$

$$= \frac{(2000\text{m})^2}{16 \cdot 0.023819\text{m}^2 \cdot 207 \times 10^6\text{kpa}} \cdot (\sqrt{24 \cdot 2.44 \cdot 0.56} - 2.44 - 4 \cdot 0.56)$$
$$= 0.053\text{m} \quad (\text{Since } f > \frac{f_{\theta}}{6})$$

Appendix II

Temperature Profile Preparation

1. General

This appendix presents interpolated temperatures along the pipeline to create the temperature load profiles. The Mathcad v15 is used and it is created based on the maximum operating temperature: 88°C in the thesis work. The profile is made based on Figure A-II.1 that is taken from Figure 3.1 in Ch.3.

The body force, which is the thermal load in the thesis work, is applied to the pipeline model in the FEA. Thus, each element of the model has been taken temperatures based on these temperature profiles.

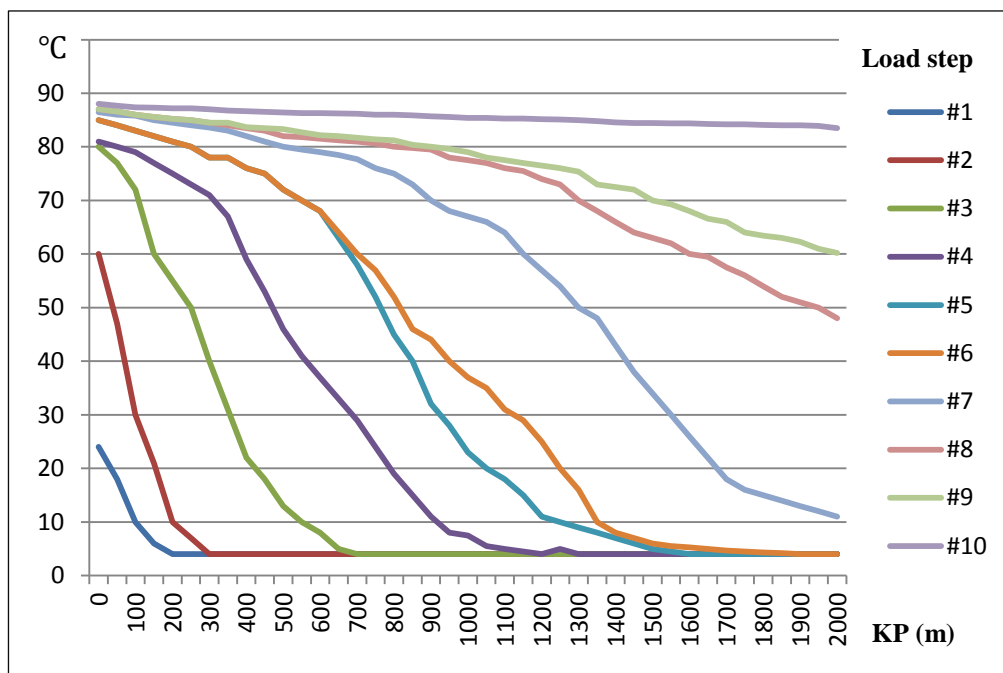


Figure A-II.1: Temperature Transients used in Pipeline Walking Analysis

1. Temperature Load #1 Interpolation

Temp. Load #1 Table (Tin):

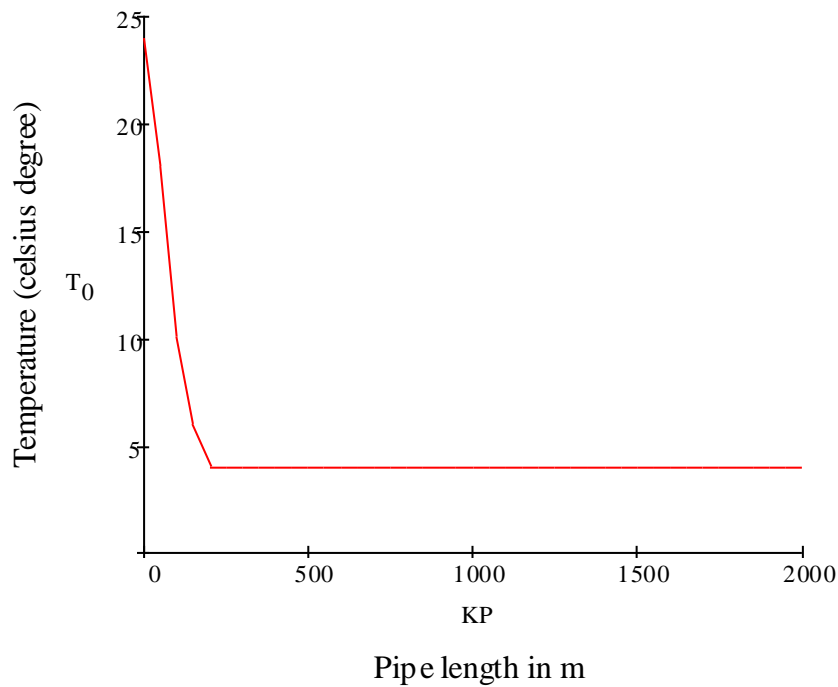
Tin :=

| | 0 | 1 |
|---|-----|-----|
| 0 | 0 | 24 |
| 1 | 50 | 18 |
| 2 | 100 | 10 |
| 3 | 150 | 6 |
| 4 | 200 | 4 |
| 5 | 250 | 4 |
| 6 | 300 | 4 |
| 7 | 350 | 4 |
| 8 | 400 | 4 |
| 9 | 450 | ... |

$$KP := Tin^{(0)}$$

$$T_0 := Tin^{(1)}$$

Temperature profile of temp load step #1



Tout :=

| | 0 | 1 |
|---|----|-----|
| 0 | 1 | 1 |
| 1 | 2 | 2 |
| 2 | 3 | 3 |
| 3 | 4 | 4 |
| 4 | 5 | 5 |
| 5 | 6 | 6 |
| 6 | 7 | 7 |
| 7 | 8 | 8 |
| 8 | 9 | 9 |
| 9 | 10 | ... |

Element_N := Tout^{<0>}

KPout := Tout^{<1>}

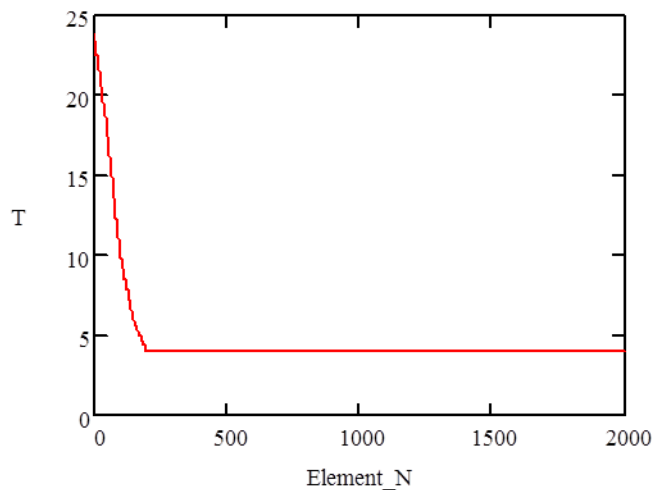
Number of data points:

n := rows(KPout)

Interpolate data:

i := 0..n - 1

T_i := linterp(KP, T₀, KPout_i)



----->
out := WRITEPRN("Interpolated Temperature Load_#1", T)

2. Temperature Load #2 Interpolation

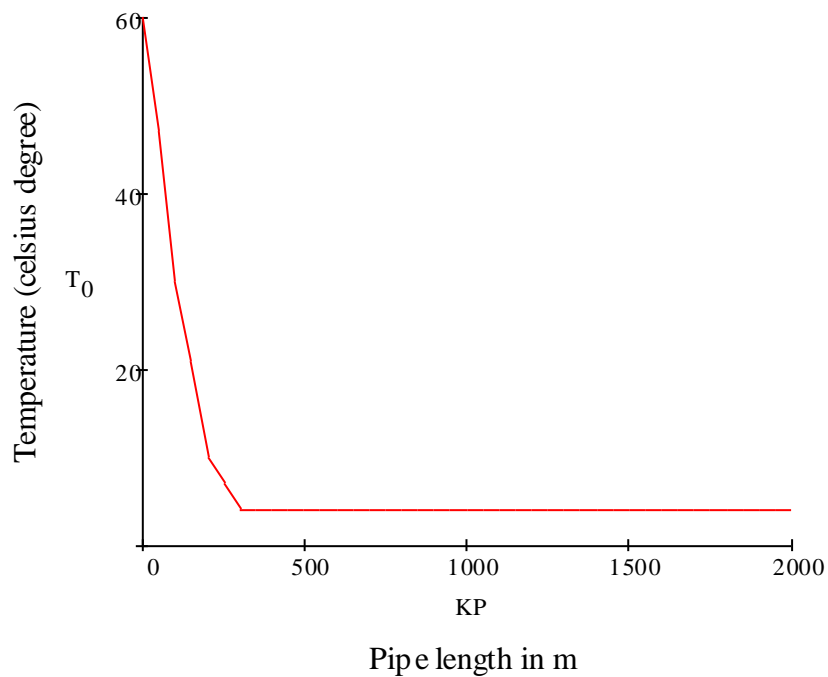
Temp. Load #2 Table (Tin):

Tin :=

| | 0 | 1 |
|---|-----|-----|
| 0 | 0 | 60 |
| 1 | 50 | 47 |
| 2 | 100 | 30 |
| 3 | 150 | 21 |
| 4 | 200 | 10 |
| 5 | 250 | 7 |
| 6 | 300 | 4 |
| 7 | 350 | 4 |
| 8 | 400 | 4 |
| 9 | 450 | ... |

KP := Tin^{<0>}
T₀ := Tin^{<1>}

Temperature profile of temp load step #2



Tout :=

| | 0 | 1 |
|---|----|-----|
| 0 | 1 | 1 |
| 1 | 2 | 2 |
| 2 | 3 | 3 |
| 3 | 4 | 4 |
| 4 | 5 | 5 |
| 5 | 6 | 6 |
| 6 | 7 | 7 |
| 7 | 8 | 8 |
| 8 | 9 | 9 |
| 9 | 10 | ... |

Element_N := Tout^{<0>}

KPout := Tout^{<1>}

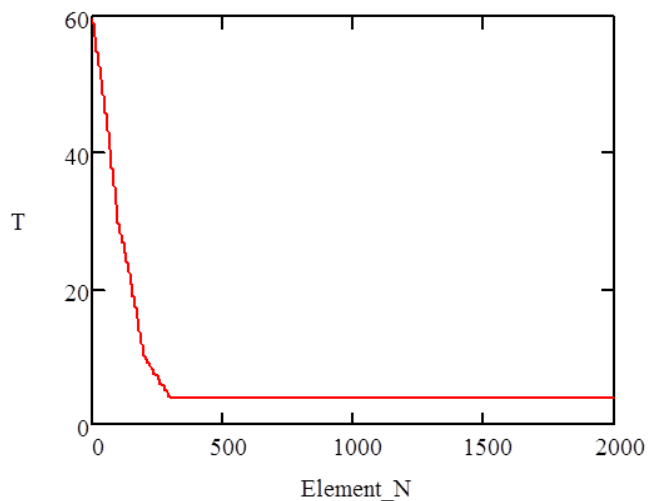
Number of data points:

n := rows (KPout)

Interpolate data:

i := 0..n - 1

T_i := linterp(KP, T₀, KPout_i)



out :=WRITEPRN("Interpolated Temperature Load_#2", T)

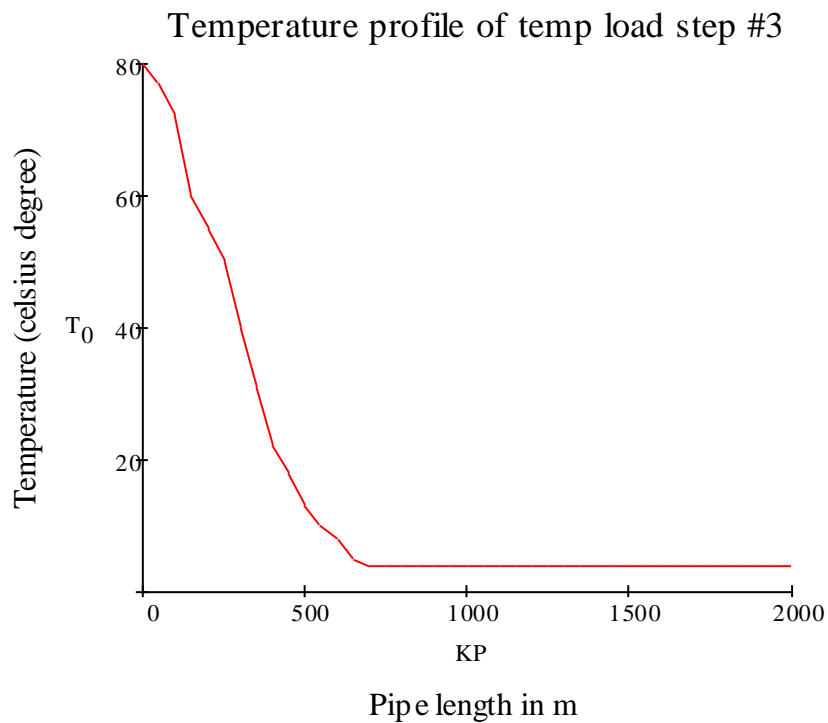
3. Temperature Load #3 Interpolation

Temp. Load #3 Table (Tin):

Tin :=

| | 0 | 1 |
|---|-----|-----|
| 0 | 0 | 80 |
| 1 | 50 | 77 |
| 2 | 100 | 72 |
| 3 | 150 | 60 |
| 4 | 200 | 55 |
| 5 | 250 | 50 |
| 6 | 300 | 40 |
| 7 | 350 | 31 |
| 8 | 400 | 22 |
| 9 | 450 | ... |

KP := Tin^{<0>}
T₀ := Tin^{<1>}



Tout :=

| | 0 | 1 |
|---|----|-----|
| 0 | 1 | 1 |
| 1 | 2 | 2 |
| 2 | 3 | 3 |
| 3 | 4 | 4 |
| 4 | 5 | 5 |
| 5 | 6 | 6 |
| 6 | 7 | 7 |
| 7 | 8 | 8 |
| 8 | 9 | 9 |
| 9 | 10 | ... |

Element_N := Tout^{<0>}

KPout := Tout^{<1>}

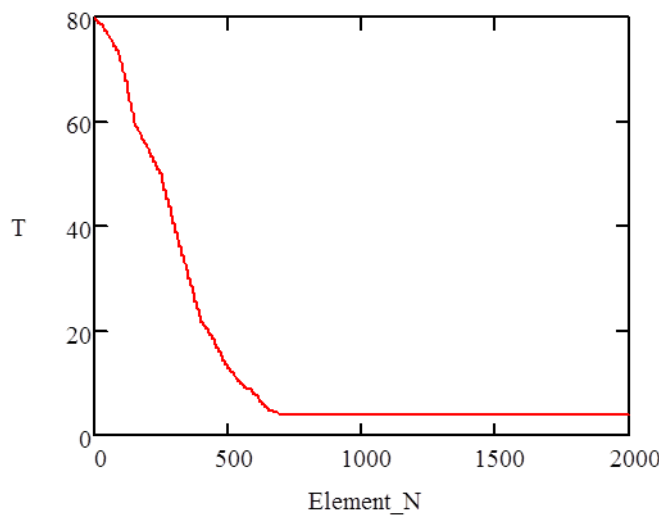
Number of data points:

n := rows (KPout)

Interpolate data:

i := 0..n - 1

T_i := linterp(KP, T₀, KPout_i)



out :=WRITEPRN("Interpolated Temperature Load_#3", T)

4. Temperature Load #4 Interpolation

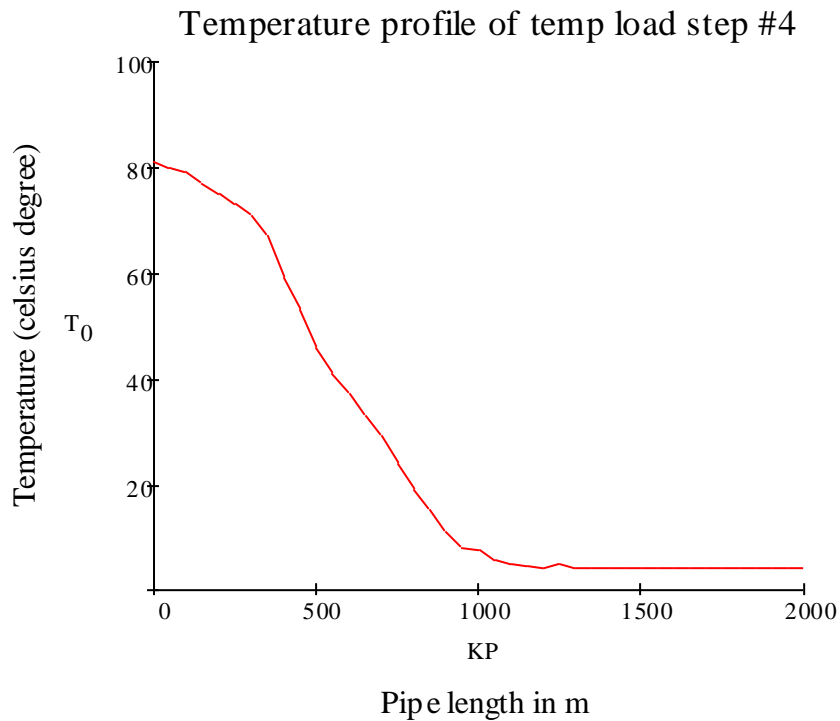
Temp. Load #4 Table (Tin):

Tin :=

| | 0 | 1 |
|---|-----|-----|
| 0 | 0 | 81 |
| 1 | 50 | 80 |
| 2 | 100 | 79 |
| 3 | 150 | 77 |
| 4 | 200 | 75 |
| 5 | 250 | 73 |
| 6 | 300 | 71 |
| 7 | 350 | 67 |
| 8 | 400 | 59 |
| 9 | 450 | ... |

KP := Tin^{<0>}

T₀ := Tin^{<1>}



Tout :=

| | 0 | 1 |
|---|----|-----|
| 0 | 1 | 1 |
| 1 | 2 | 2 |
| 2 | 3 | 3 |
| 3 | 4 | 4 |
| 4 | 5 | 5 |
| 5 | 6 | 6 |
| 6 | 7 | 7 |
| 7 | 8 | 8 |
| 8 | 9 | 9 |
| 9 | 10 | ... |

Element_N := Tout^{<0>}

KPout := Tout^{<1>}

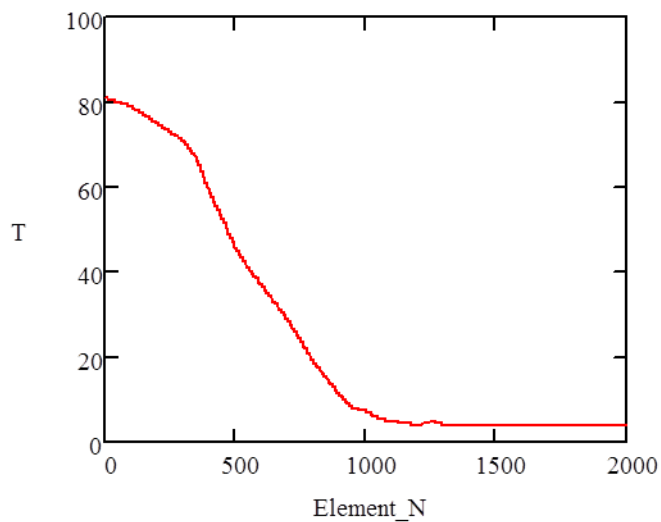
Number of data points:

n := rows(KPout)

Interpolate data:

i := 0..n - 1

T_i := linterp(KP, T₀, KPout_i)



out := WRITEPRN("Interpolated Temperature Load_#4", T)

5. Temperature Load #5 Interpolation

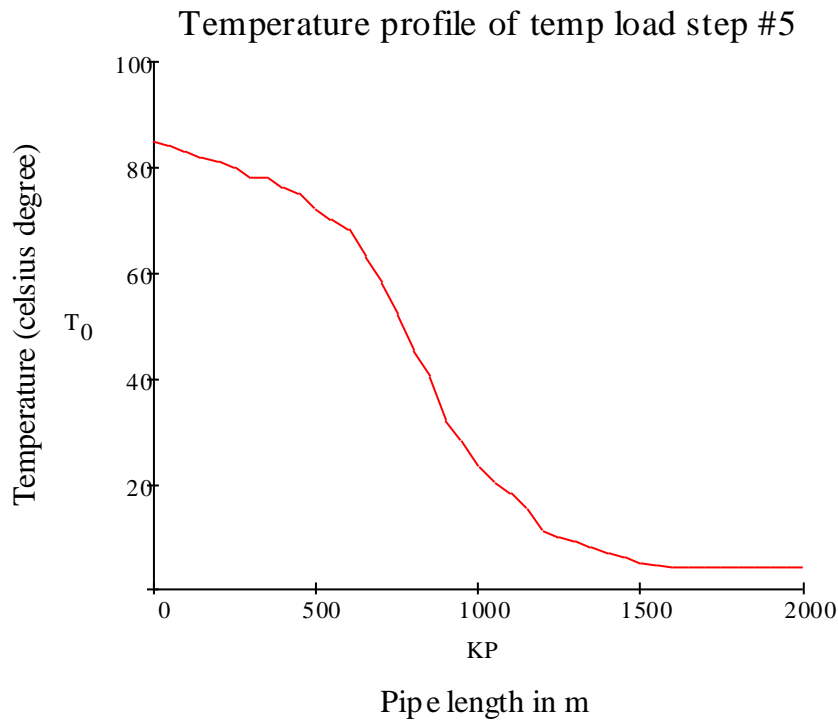
Temp. Load #5 Table (Tin):

Tin :=

| | 0 | 1 |
|---|-----|-----|
| 0 | 0 | 85 |
| 1 | 50 | 84 |
| 2 | 100 | 83 |
| 3 | 150 | 82 |
| 4 | 200 | 81 |
| 5 | 250 | 80 |
| 6 | 300 | 78 |
| 7 | 350 | 78 |
| 8 | 400 | 76 |
| 9 | 450 | ... |

KP := Tin^{<0>}

T₀ := Tin^{<1>}



Tout :=

| | 0 | 1 |
|---|----|-----|
| 0 | 1 | 1 |
| 1 | 2 | 2 |
| 2 | 3 | 3 |
| 3 | 4 | 4 |
| 4 | 5 | 5 |
| 5 | 6 | 6 |
| 6 | 7 | 7 |
| 7 | 8 | 8 |
| 8 | 9 | 9 |
| 9 | 10 | ... |

Element_N := Tout^{<0>}

KPout := Tout^{<1>}

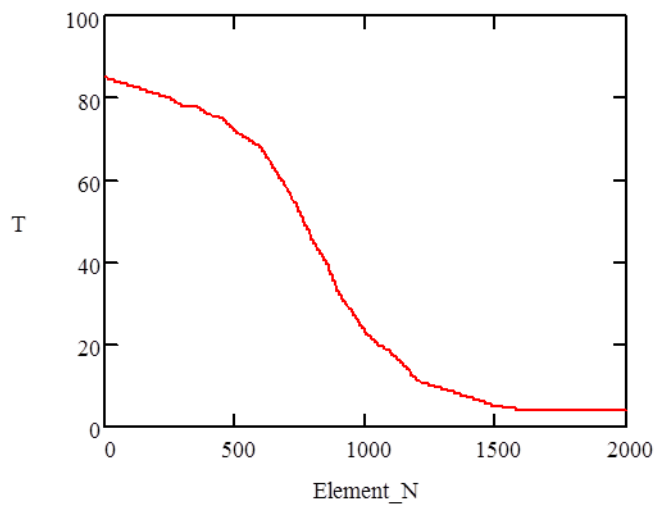
Number of data points:

n := rows(KPout)

Interpolate data:

i := 0..n - 1

T_i := linterp(KP, T₀, KPout_i)



out := WRITEPRN("Interpolated Temperature Load_#5", T)

6. Temperature Load #6 Interpolation

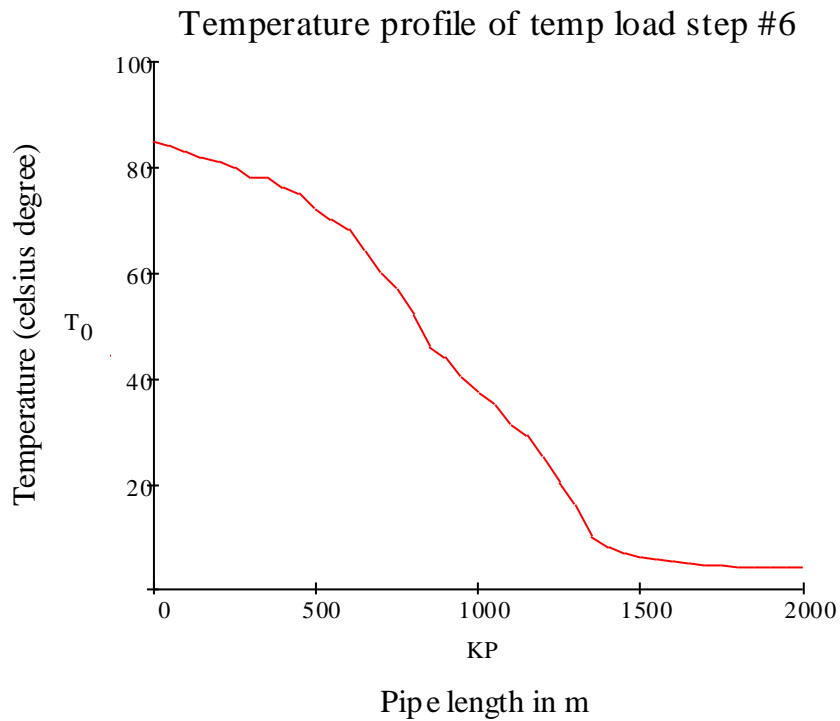
Temp. Load #6 Table (Tin):

Tin :=

| | 0 | 1 |
|---|-----|-----|
| 0 | 0 | 85 |
| 1 | 50 | 84 |
| 2 | 100 | 83 |
| 3 | 150 | 82 |
| 4 | 200 | 81 |
| 5 | 250 | 80 |
| 6 | 300 | 78 |
| 7 | 350 | 78 |
| 8 | 400 | 76 |
| 9 | 450 | ... |

KP := Tin^{<0>}

T₀ := Tin^{<1>}



Tout :=

| | 0 | 1 |
|---|----|-----|
| 0 | 1 | 1 |
| 1 | 2 | 2 |
| 2 | 3 | 3 |
| 3 | 4 | 4 |
| 4 | 5 | 5 |
| 5 | 6 | 6 |
| 6 | 7 | 7 |
| 7 | 8 | 8 |
| 8 | 9 | 9 |
| 9 | 10 | ... |

Element_N := Tout^{<0>}

KPout := Tout^{<1>}

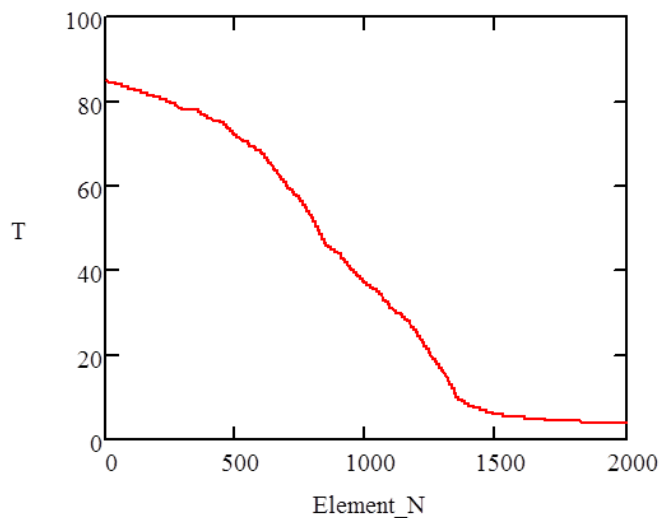
Number of data points:

n := rows(KPout)

Interpolate data:

i := 0..n - 1

T_i := linterp(KP, T₀, KPout_i)



out := WRITEPRN("Interpolated Temperature Load_#6", T)

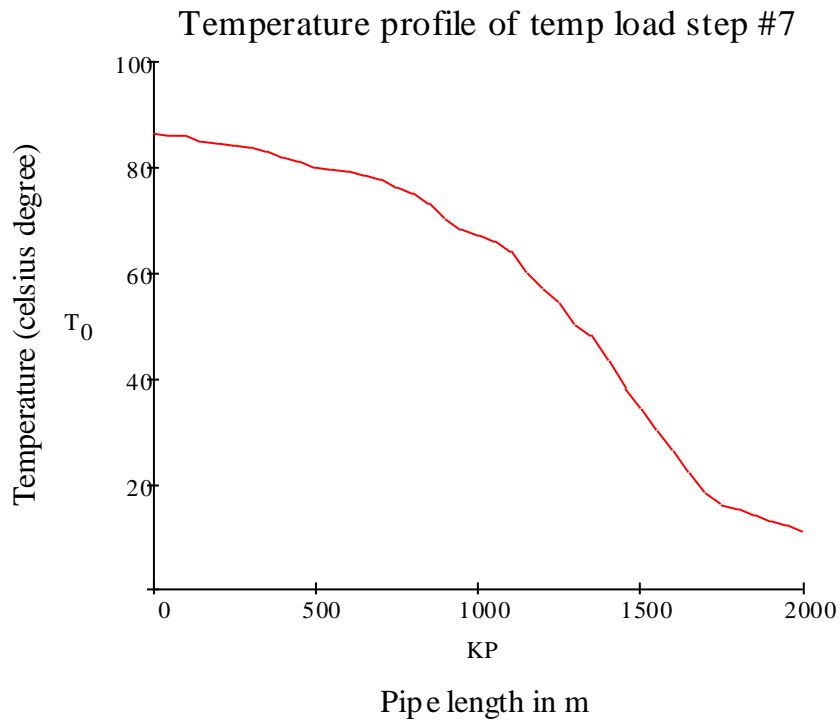
7. Temperature Load #7 Interpolation

Temp. Load #7 Table (Tin):

Tin :=

| | 0 | 1 |
|---|-----|------|
| 0 | 0 | 86.5 |
| 1 | 50 | 86 |
| 2 | 100 | 85.8 |
| 3 | 150 | 85 |
| 4 | 200 | 84.5 |
| 5 | 250 | 84 |
| 6 | 300 | 83.6 |
| 7 | 350 | 83 |
| 8 | 400 | 82 |
| 9 | 450 | ... |

KP := Tin^{<0>}
T₀ := Tin^{<1>}



Tout :=

| | 0 | 1 |
|---|----|-----|
| 0 | 1 | 1 |
| 1 | 2 | 2 |
| 2 | 3 | 3 |
| 3 | 4 | 4 |
| 4 | 5 | 5 |
| 5 | 6 | 6 |
| 6 | 7 | 7 |
| 7 | 8 | 8 |
| 8 | 9 | 9 |
| 9 | 10 | ... |

Element_N := Tout^{<0>}

KPout := Tout^{<1>}

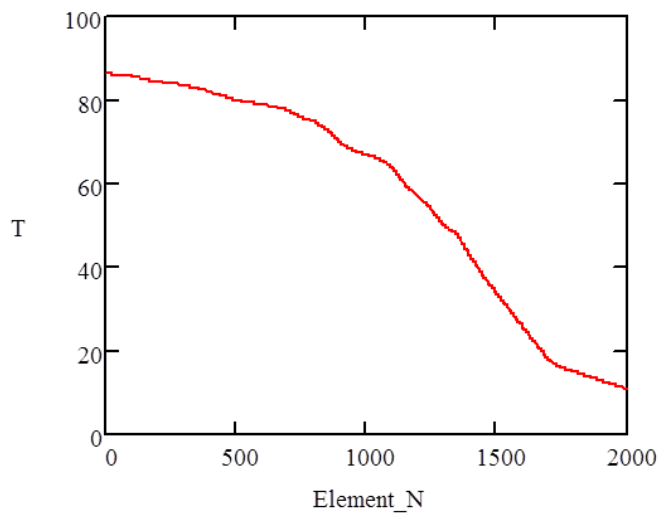
Number of data points:

n := rows(KPout)

Interpolate data:

i := 0..n - 1

T_i := linterp(KP, T₀, KPout_i)



out := WRITEPRN("Interpolated Temperature Load_#7", T)

8. Temperature Load #8 Interpolation

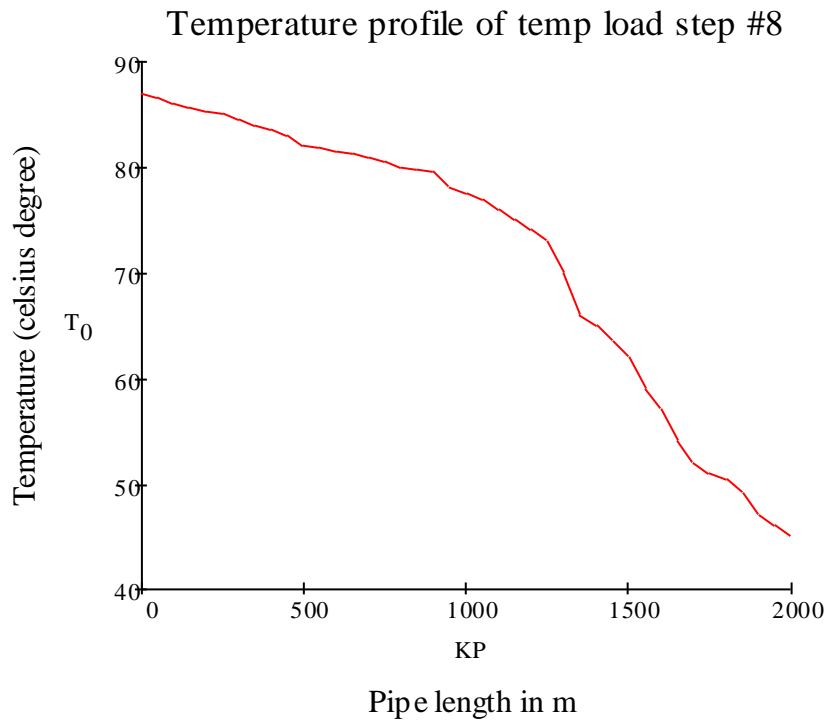
Temp. Load #8 Table (Tin):

Tin :=

| | 0 | 1 |
|---|-----|------|
| 0 | 0 | 87 |
| 1 | 50 | 86.6 |
| 2 | 100 | 86 |
| 3 | 150 | 85.6 |
| 4 | 200 | 85.2 |
| 5 | 250 | 85 |
| 6 | 300 | 84.5 |
| 7 | 350 | 84 |
| 8 | 400 | 83.5 |
| 9 | 450 | ... |

KP := Tin^{<0>}

T₀ := Tin^{<1>}



Tout :=

| | 0 | 1 |
|---|----|-----|
| 0 | 1 | 1 |
| 1 | 2 | 2 |
| 2 | 3 | 3 |
| 3 | 4 | 4 |
| 4 | 5 | 5 |
| 5 | 6 | 6 |
| 6 | 7 | 7 |
| 7 | 8 | 8 |
| 8 | 9 | 9 |
| 9 | 10 | ... |

Element_N := Tout^{<0>}

KPout := Tout^{<1>}

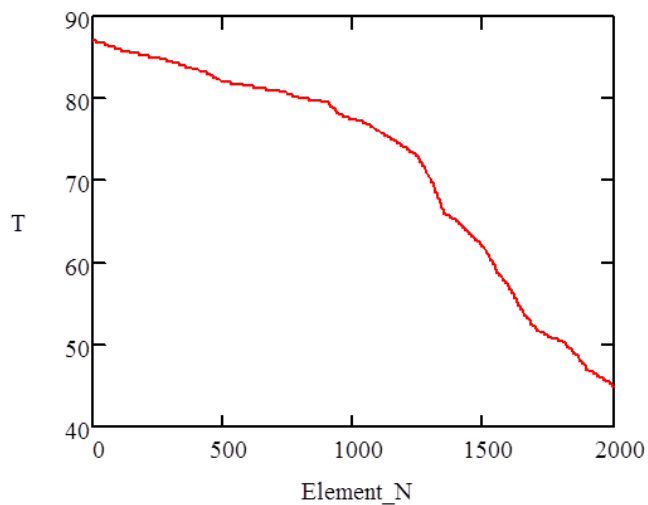
Number of data points:

n := rows(KPout)

Interpolate data:

i := 0..n - 1

T_i := linterp(KP, T₀, KPout_i)



out := WRITEPRN("Interpolated Temperature Load_#8", T)

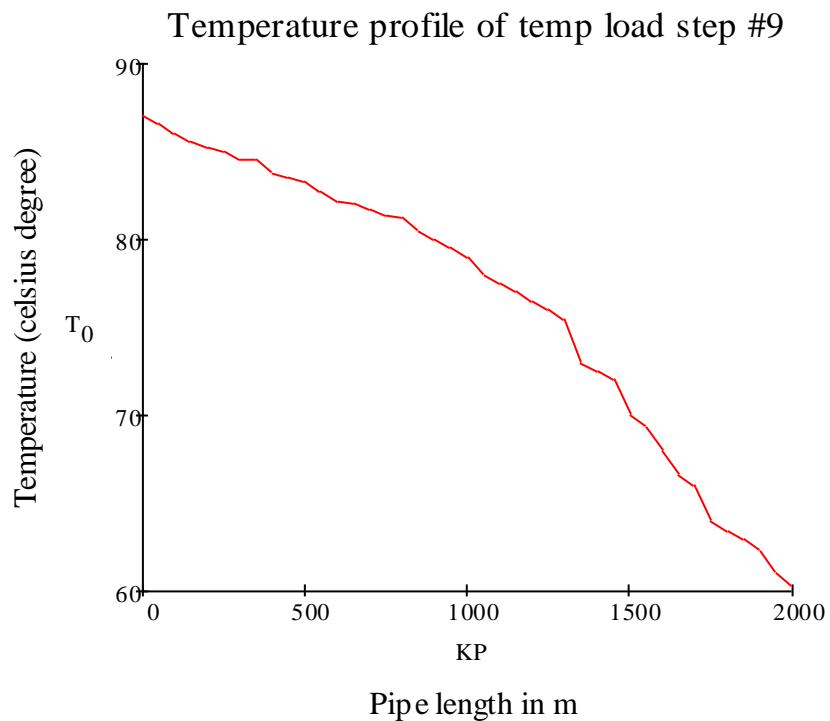
9. Temperature Load #9 Interpolation

Temp. Load #9 Table (Tin):

Tin :=

| | 0 | 1 |
|---|-----|------|
| 0 | 0 | 87 |
| 1 | 50 | 86.6 |
| 2 | 100 | 86 |
| 3 | 150 | 85.6 |
| 4 | 200 | 85.2 |
| 5 | 250 | 85 |
| 6 | 300 | 84.5 |
| 7 | 350 | 84.5 |
| 8 | 400 | 83.7 |
| 9 | 450 | ... |

KP := Tin^{<0>}
T₀ := Tin^{<1>}



Tout :=

| | 0 | 1 |
|---|----|-----|
| 0 | 1 | 1 |
| 1 | 2 | 2 |
| 2 | 3 | 3 |
| 3 | 4 | 4 |
| 4 | 5 | 5 |
| 5 | 6 | 6 |
| 6 | 7 | 7 |
| 7 | 8 | 8 |
| 8 | 9 | 9 |
| 9 | 10 | ... |

Element_N := Tout^{<0>}

KPout := Tout^{<1>}

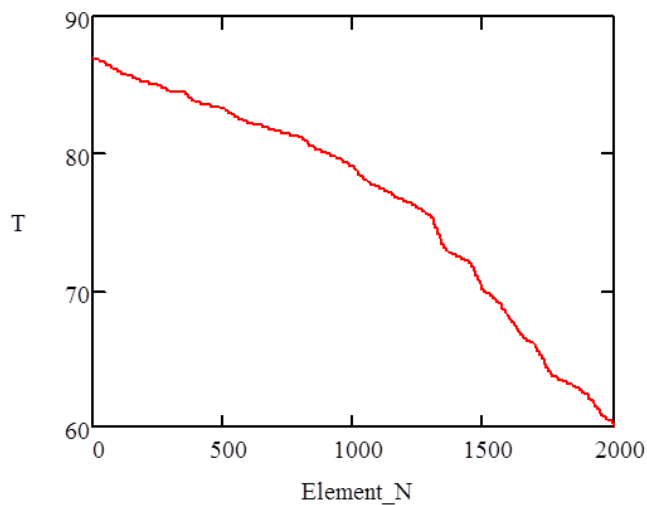
Number of data points:

n := rows(KPout)

Interpolate data:

i := 0..n - 1

T_i := linterp(KP, T₀, KPout_i)



out := WRITEPRN("Interpolated Temperature Load_#9", T)

10. Temperature Load #10 Interpolation

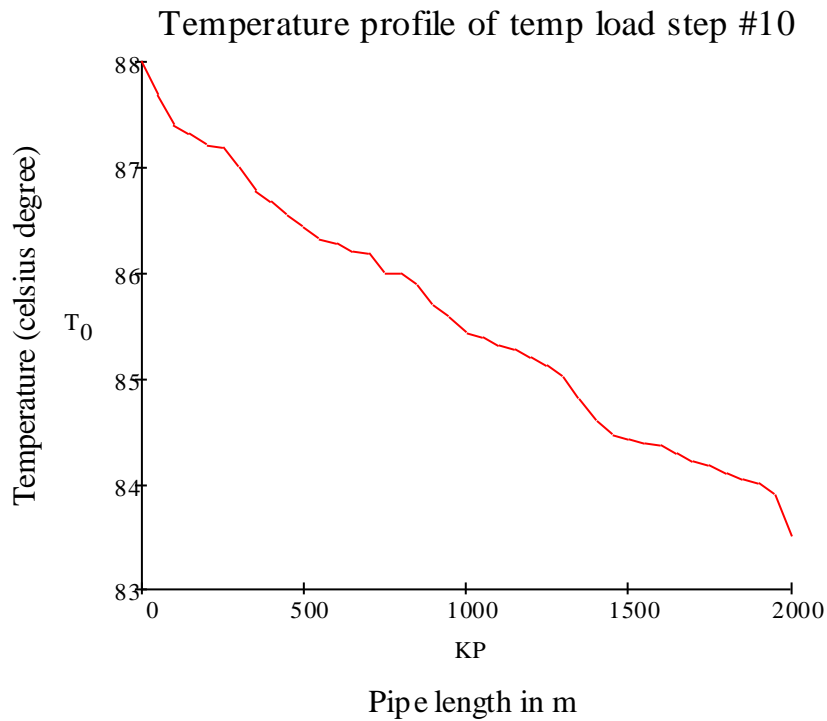
Temp. Load #10 Table (Tin):

Tin :=

| | 0 | 1 |
|---|-----|-------|
| 0 | 0 | 88 |
| 1 | 50 | 87.67 |
| 2 | 100 | 87.4 |
| 3 | 150 | 87.32 |
| 4 | 200 | 87.2 |
| 5 | 250 | 87.18 |
| 6 | 300 | 87 |
| 7 | 350 | 86.76 |
| 8 | 400 | 86.67 |
| 9 | 450 | ... |

KP := Tin^{<0>}

T₀ := Tin^{<1>}



Tout :=

| | 0 | 1 |
|---|----|-----|
| 0 | 1 | 1 |
| 1 | 2 | 2 |
| 2 | 3 | 3 |
| 3 | 4 | 4 |
| 4 | 5 | 5 |
| 5 | 6 | 6 |
| 6 | 7 | 7 |
| 7 | 8 | 8 |
| 8 | 9 | 9 |
| 9 | 10 | ... |

Element_N := Tout^{<0>}

KPout := Tout^{<1>}

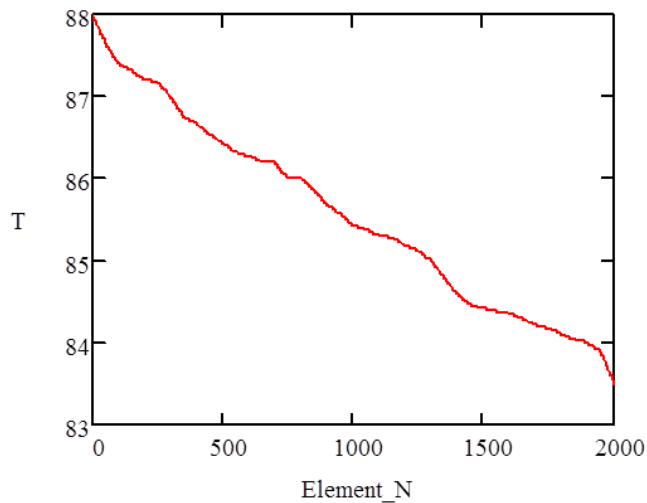
Number of data points:

n := rows(KPout)

Interpolate data:

i := 0..n - 1

T_i := linterp(KP, T₀, KPout_i)



out := WRITEPRN("Interpolated Temperature Load_#10", T)

Appendix III

Pipeline Model Material Property

Ramberg-Osgood Stress-Strain Curve

Given parameters:

| | |
|----------------------|-----------------------------------|
| Youngs Modulus: | $E := 207\text{GPa}$ |
| Yield Stress: | $\text{SMYS} := 450\text{Mpa}$ |
| Tensile Stress: | $\text{SMTS} := 535\text{MPa}$ |
| Elongation at break: | $\Delta l_{\text{break}} := 20\%$ |

Known points on the stress-strain curve:

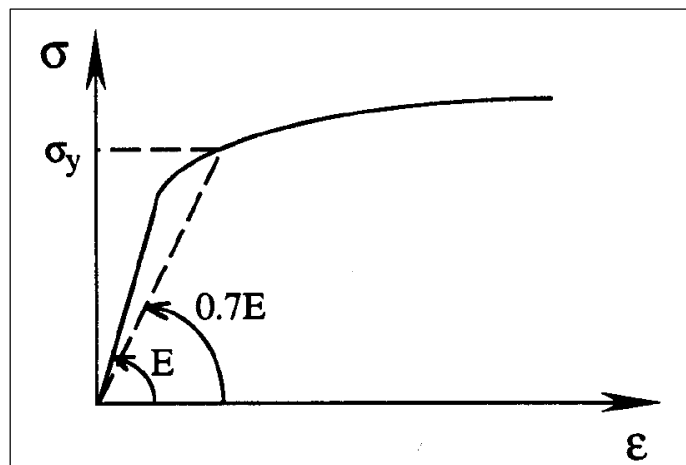
| | |
|---------------|---|
| Yield point: | $\sigma_y := \text{SMYS} = 450\text{MPa}$ |
| Second point: | $\sigma_2 := \text{SMTS} = 535\text{MPa}$ |

Ramberg-Osgood material model:

$$\varepsilon(\sigma) = \frac{\sigma}{E} \left[1 + \frac{3}{7} \cdot \left(\frac{\sigma}{\sigma_{0.7}} \right)^{n-1} \right]$$

Calculating the Ramberg-Osgood curve parameters:

The 0.7 is also called the Ramberg-Osgood yield parameter, and is sometimes denoted R or y . It is found by drawing a line in the stress-strain graph with a slope of $0.7E$ from origin. The Ramberg-Osgood yield parameter is the corresponding stress where this line intersects the stress-strain curve.



Re-arranging equation:

$$\varepsilon = \frac{\sigma}{E} \left[1 + \frac{3}{7} \cdot \left(\frac{\sigma}{\sigma_{0.7}} \right)^{n-1} \right]$$

$$\varepsilon \cdot E = \sigma + \frac{3}{7} \cdot \sigma \cdot \left(\frac{\sigma}{\sigma_{0.7}} \right)^{n-1}$$

$$\varepsilon \cdot E = \sigma + \frac{3}{7} \cdot \frac{\sigma^n}{\sigma_{0.7}^{n-1}}$$

$$\varepsilon \cdot E - \sigma = \frac{3}{7} \cdot \frac{\sigma^n}{\sigma_{0.7}^{n-1}}$$

$$\sigma_{0.7}^{n-1} = \frac{3}{7} \cdot \frac{\sigma^n}{\varepsilon \cdot E - \sigma}$$

Since 0.7 and n are constants, the following can be used:

$$\sigma_{0.7_1}^{n_1-1} = \sigma_{0.7_2}^{n_2-1} \quad \text{Since} \quad \sigma_{0.7_1} = \sigma_{0.7_2} \quad \text{and} \quad n_1 = n_2$$

Hence:

$$\frac{3}{7} \cdot \frac{\sigma_1^n}{\varepsilon_1 \cdot E - \sigma_1} = \frac{3}{7} \cdot \frac{\sigma_2^n}{\varepsilon_2 \cdot E - \sigma_2} \quad \frac{3}{7} \text{ is cancelled, thus:}$$

$$\frac{\sigma_1^n}{\sigma_2^n} = \frac{\varepsilon_1 \cdot E - \sigma_1}{\varepsilon_2 \cdot E - \sigma_2} \quad \text{Or} \quad \left(\frac{\sigma_1}{\sigma_2} \right)^n = \frac{\varepsilon_1 \cdot E - \sigma_1}{\varepsilon_2 \cdot E - \sigma_2}$$

Further:

$$\ln \left[\left(\frac{\sigma_1}{\sigma_2} \right)^n \right] = n \cdot \ln \left(\frac{\sigma_1}{\sigma_2} \right) = \ln \left(\frac{\varepsilon_1 \cdot E - \sigma_1}{\varepsilon_2 \cdot E - \sigma_2} \right)$$

Hence:

$$n(\sigma_1, \varepsilon_1, \sigma_2, \varepsilon_2) := \frac{\ln \left(\frac{\varepsilon_1 \cdot E - \sigma_1}{\varepsilon_2 \cdot E - \sigma_2} \right)}{\ln \left(\frac{\sigma_1}{\sigma_2} \right)}$$

And:

$$E1 := \frac{E}{1\text{MPa}}$$

$$E1 = 2.07 \times 10^5$$

Remove unit for the calculation

$$\sigma_{0.7}(\sigma_x, \varepsilon_x, n) := \left(\frac{3}{7} \cdot \frac{\sigma_x^n}{\varepsilon_x \cdot E1 - \sigma_x} \right)^{\frac{1}{n-1}}$$

This is true for any and corresponding.

For the current case:

$$n := n(\sigma_y, \varepsilon_y, \sigma_2, \varepsilon_2)$$

$$n = 19.965$$

$$\sigma_{0.7} := \sigma_{0.7}\left(\frac{\sigma_y}{1\text{MPa}}, \varepsilon_y, n\right) \cdot 1\text{MPa} \quad \sigma_{0.7} = 424.426\text{MPa}$$

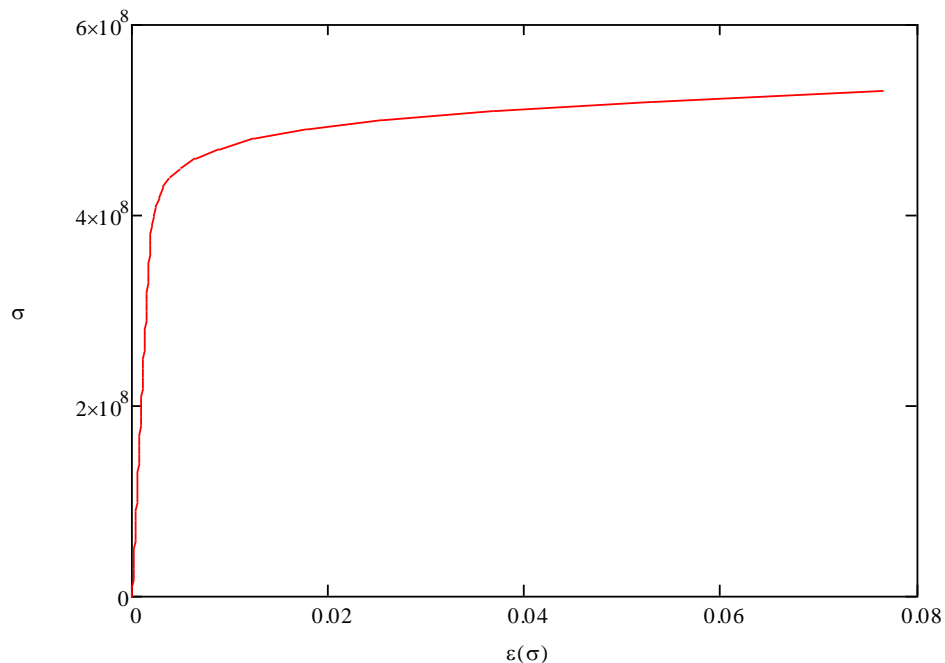
Repeating expression, required for graphing

$$\varepsilon(\sigma) := \frac{\sigma}{E} \left[1 + \frac{3}{7} \cdot \left(\frac{\sigma}{\sigma_{0.7}} \right)^{n-1} \right]$$

Setting plot range:

$$\sigma := 0\text{MPa}, 10\text{MPa} .. \sigma_2$$

Ramberg-Osgood curve:



Appendix IV-1

Finite Element Analysis

ANSYS Scripts for Modeling

Master thesis
Phenomenon of Pipeline Walking in High Temperature Pipeline

```
!*****
!* Title: *
!* *
!* Pipeline walking for high temperature subsea pipeline by thermal transient *
!* *
!* Presented by Se-Hoon Yoon *
!* (Graduate student of Offshore technology in University of Stavanger, Norway) *
!* *****
!* Description: *
!* It presents APDL (ANSYS Parametric Design Language) to analyze pipeline walking. *
!* *
!* Status/Comments: *
!* The each temperature load step profile is given as 'inp' filename extension *
!* *****
```

! File Desc.: Model 22in pipeline

FINI

/CLEAR

*SET,LOADCASE,"Test2"

/TITLE,%LOADCASE%

!File Desc.: Pipeline walking by thermal transient

/FILENAME,%LOADCASE%

/UNITS,MKS ! MKS system (m,kg,s,deg C)

```
!#####
!# Various parameters ## Unit are [m] [N] [Kg] [s] [deg C] #
!#####
```

```
pi=4*ATAN(1.0) ! Pi
g=9.81 ! Gravitational Acceleration (m/s^2)
WD=-100 ! Water Depth (m)
```

```
/PREP7 ! Enter model creation preprocessor
!ANTYPE,0,NEW ! 0=STATIC
ACEL,,g ! Define gravity
```

```
ET,1,PIPE288 ! Pipe elements
SECTYPE,1,PIPE ! Define pipe section type
```


SECDATA,323.9E-3,25.4E-3 ! Define pipe section:OD,Tkwall [m]

ET,2,TARGE170 ! Seabed element
ET,3,CONTA175 ! Contact elements

!-----
! PIPELINE DATA
!-----

!#DIMENSION FOR WEIGHT CALCULATION

OD=323.9E-3 ! Pipe Outer Diameter (m)
tkwall=25.4E-3 ! Pipe Wall Thickness (m)
DI=OD-2*tkwall ! Pipe Inner Diameter (m)

L=2000 ! Pipeline Length (m)

t_ext=5E-3 ! External Coating Thickness (m)
t_conc=30E-3 ! Concrete Coating Thickness (m)

!#OPERATIONAL DATA

DEN_SW=1027 ! Water Density (Kg/m³)
DENSFL=900 ! Content Density OIL (Kg/m³)

Pres_d=15E6 ! Design Pressure (N/m²)
Pres_op=15E6 ! Operating Pressure (N/m²)

T_amb=3.5 ! Ambient Temperature (deg C)
T_op=88 ! Operating Temperature (deg C)

!R_lay=0 ! Residual Lay Tension

!#MATERIAL PROPERTIES

!MP,DENS,1,7850 ! Pipe Material density (Kg/m³)
! defined as equivalent density

MPTEMP,1,0,100 ! Define temperatures for Young's modulus
MP,EX,1,207E9 ! Young's modulus (N/m²)

```
MP,ALPX,1,1.17E-5          ! Thermal expansion coefficient (/deg C)

MP,PRXY,1,0.3             ! Poisson ratio

!#COATING DENSITY
P_EXT=910                 ! Insulation or Coating Density (Kg/m^3)
P_CONC=2400               ! Concrete Coating Density (Kg/m^3)

!-----
! **DEFINE STRESS-PLASTIC STRAIN CURVE**
!-----
TB,MISO,1,2,4             !PLASTIC      ! Activate a data table
                          ! Hardening using von Misses or Hill plasticity
TBTEMP,20.0              ! Temperature = 20.0deg C
TBPT,,0.0,0.0
TBPT,,0.0019,393.3E6
TBPT,,0.005,450E6
TBPT,,0.092,535E6
TBTEMP,100.0             ! Temperature = 100.0deg C
TBPT,,0.0,0.0
TBPT,,0.0018,372.6E6
TBPT,,0.005,420E6
TBPT,,0.092,505E6

!-----
! SEABED DATA
!-----
!DEFINE SEABED SOIL FRICTION
FRICLAX=0.3              ! Soil friction coefficient in axial direction
FRICLLAT=0.8            ! Soil friction coefficient in lateral direction

TB,FRIC,2,,ORTHO        ! Define orthotropic soil friction
TBDATA,1,FRICLAX,FRICLLAT

igap=0                  ! Initial gap between pipeline and seabed

!-----
! PIPE SYSTEM PARAMETER CALCULATION
!-----
```

Master thesis
Phenomenon of Pipeline Walking in High Temperature Pipeline

D_EFF=OD+2*(t_ext+t_conc) ! Effective Pipe Diameter (m)
AS=pi*(OD**2-DI**2)/4 ! Cross-sectional Area of Pipe Steel (m^2)
AS_EXT=pi*((OD+2*t_ext)**2-OD**2)/4 ! Cross-sectional Area of External Coating (m^2)
AS_CONC=pi*((OD+2*t_ext+2*t_conc)**2-(OD+2*t_ext)**2)/4 ! Cross-sectional Area of Concrete Coating (m^2)

M_STEEL=AS*7850 ! Pipe Steel Mass (Kg/m)
M_EXT=AS_EXT*P_EXT ! External Coating Mass (Kg/m)
M_CONC=AS_CONC*P_CONC ! Concrete Coating Mass (Kg/m)
M_CONT=pi*(DI**2)*DENSFL/4 ! Content Mass (Kg/m)
M_WATE=pi*(DI**2)*DEN_SW/4 ! Water Mass (Kg/m)

M_BUOY=pi*(D_EFF**2)*DEN_SW/4 ! Buoyancy Mass (Kg/m)
MWALL=M_STEEL+M_EXT+M_CONC ! Pipeline Total Mass (Kg/m) (weight on air)
M_SUB=MWALL-M_BUOY ! Submerged Mass (Kg/m) (weight in water)

W_CONT=M_CONT*g ! Content Weight (N/m)
W_WATE=M_WATE*g ! Flooded Weight (N/m)
W_SUB=M_SUB*g ! Empty Pipe Submerged Weight (N/m)
EQ_DEN=M_SUB/AS ! Submerged pipe Equivalent Density (kg/m^3)

DENSIN=((t_ext*P_EXT)+(t_conc*P_CONC))/(t_ext+t_conc) ! Insulation Eqv. Density (Corr. & Concr. Coat.) (N/m)
TKIN=t_ext+t_conc ! Insulation thickness (Corr. & Concr. Coat.) (m)
AREAIN=AS_EXT+AS_CONC ! Insulation Area (Corrosion coat.& Concrete Coat.) (m^2)

!-----
! **APPLY WEIGHT ON PIPELINE**
!-----

MP,DENS,1,EQ_DEN ! Pipe Material density (Kg/m^3)
! Using Equivalent Density for submerged weight
SECCONROLS,M_CONT ! Added mass: content(kg/m)

!-----
! ELEMENT REAL CONSTANT
!-----

!# FOR PIPELINE !

KEYOPT,1,1,0 ! Temperature Through wall gradient
KEYOPT,1,4,1 ! Thin Pipe Theory

```
KEYOPT,1,6,0      ! Internal and External pressure cause loads on end caps
KEYOPT,1,7,0      ! Output control for section forces/moments and strains/curvatures
KEYOPT,1,8,0      ! Output control at integration points (1=Maximum and minimum stresses/strains)
KEYOPT,1,9,2
KEYOPT,1,15,0     ! One result for each section integration point

!-----!
!# SEABED !
!-----!
R,22,,0.01,0.5   ! Define Contact Stiffness Factor and Penetration Tolerance Factor

KEYOPT,3,10,2     ! Set option 10 (Contact Stiffness Update) for element type 3 to 2 (Each substep based on mean
                  ! Stress of underlying elements from the previous substep (pair based))
                  ! Update stiffness automatically based on maximum penetration
KEYOPT,3,2,1      ! Penalty method, static stiffness of seabed
KEYOPT,3,4,2      !
KEYOPT,3,10,2     !
KEYOPT,3,12,0     ! Behavior of Contact Surface (0=standard)
```

```
!-----!
!                               PIPELINE MODELING
!-----!
```

```
#####
!#      Generate Keypoints (m)                                     #
#####
K,      1      ,      0.0      ,      WD      ,      0.0
K,      11     ,      2000.0   ,      WD      ,      0.0
```

```
!*****
!* Create nodes to describe local coordinate systems for ends      *
!*****
K,      12     ,      -25.0    ,      WD      ,      0.0
K,      13     ,      0.0      ,      WD+25.0 ,      0.0
K,      14     ,      2025.0   ,      WD      ,      0.0
K,      15     ,      2000.0   ,      WD+25.0 ,      0.0
```

```
!*****
!* Create new coordinate systems for ends (11,12)                  *
!*****
```

Master thesis
Phenomenon of Pipeline Walking in High Temperature Pipeline

CSKP, 11 ,0 ,1 ,12 ,13
CSKP, 12 ,0 ,11 ,14 ,15

CSYS,0 ! Activate the default coordinate system (0)

!#####
!# Pipe Nodes #
!#####
EndNode=2000

*DO, I, 1, EndNode
N, I, L/EndNode*I, WD, 0
*ENDDO

!*****
!* Meshing of straight pipe elements *
!*****

TYPE,1 ! Element type, material, constants
MAT,1
SECNUM,1
*DO,I,1,endnode-1
E,I,I+1
*ENDDO

!-----
! SEABED MODELING
!-----
!*****
!* Meshing of seabed elements
!*****

! Define nodes for seabed area
N, 3001 , -15.0 , WD-igap , 15.0
N, 3002 , 2015 , WD-igap , 15.0
N, 3003 , 2015 , WD-igap , -15.0
N, 3004 , -15.0 , WD-igap , -15.0

!#DEFINE TARGET ELEMENT##

!-----

TYPE,2 ! Select material and properties for seabed
MAT,2
REAL,22
TSHAPE,QUAD ! SET TARGET SHAPE
NUMSTR,ELEM,30001
E,3001,3002,3003,3004 ! Define Element

NSEL,S,NODE,,1,endnode ! Select pipe nodes
TYPE,3 ! Select element type 3
REAL,22
NUMSTR,ELEM,40001
ESURF
ALLSEL ! - Seabed done

!-----

! MISC: END LOCAL COORDINATE

!-----

 ! Rotate end nodes to local coordinate system
e1=1 ! Identify end node and
CSYS,11 ! Change nodal coordinate system
NROTAT,e1

e2=EndNode ! Identify end node and
CSYS,12 ! Change nodal coordinate system
NROTAT,e2

CSYS,0

GPLOT

!-----

! DISPLAY MODEL

!-----

/ESHAPE,1 ! Display elements as solids
/TRIAD,rbot ! Display XYZ triad in right bottom corner
/PSYMB,NDIR,1 ! Display nodal coordinate system if other than global

FINISH ! Exit the preprocessor
!/EOF

!#####
!# SOLUTION PROCESSOR #
!#####

/CONFIG,NRES,20000
/SOLU ! Enter solution processor
ANTYPE,STATIC ! 0=STATIC
!OUTRES,ALL,ALL
NLGEOM,ON ! Includes large deflection effects in a static or full transient analysis

NEQIT,1000 ! Specifies the maximum number of equilibrium iterations for nonlinear analyses

AUTOTS,ON ! Automatic time stepping

NROPT,UNSYM ! Specifies the Newton-Raphson options in a static or full transient analysis
! (FULL or UNSYM= the stiffness matrix is updated at every equilibrium iteration)

NSUBST,5,20,2 ! Specifies the number of substeps to be taken every load step (nbr this step, maximum number of
! Substeps to be taken (i.e. min. time step), minimum number of step (i.e. max time step)

TREF,T_amb ! Reference Temperature (deg C) for Thermal Strain Calculation

CNCHECK,AUTO ! Adjust the initial status of contact pairs

STABILIZE,CONSTANT,DAMPING,0.1,AnyTime
MONITOR,1,1000,UX
MONITOR,2,1000,UY

!*****
!* LOAD STEPS
!*****

TIME,1 ! Set the time for the end of the load step
/STITLE,1,PIPELINE LAID ON SEABED-INITIAL CONDITION

! Set Boundary Condition

```
NSEL,S,NODE,,1,EndNode
D,ALL,ROTZ
ALLSEL
SOLVE
SAVE
```

```
!*****
!*                               LOAD STEP cycle #1
!*****
```

```
!-----
TIME,2
/STITLE,1,APPLY OPERATING PRESSURE AND TEMPERATURE
NSUBST,10,2000,10
```

```
/Input,T1,inp                               ! Surface Loads PIPE288: Pressures -- 1-PINT, 2-PX, 3-PY, 4-PZ, 5-POUT
                                              ! 1st temperature load step
```

```
ALLSEL
SOLVE
SAVE
```

```
!-----
TIME,3
NSUBST,10,2000,10
```

```
                                              ! Surface Loads PIPE288: Pressures -- 1-PINT, 2-PX, 3-PY, 4-PZ, 5-POUT

/Input,T2,inp                               ! 2nd temperature load step
```

```
ALLSEL
SOLVE
SAV
```

```
!-----
TIME,4
NSUBST,10,2000,10
```

```
                                              ! Surface Loads PIPE288: Pressures -- 1-PINT, 2-PX, 3-PY, 4-PZ, 5-POUT

/Input,T3,inp                               ! 3rd temperature load step
```

```
ALLSEL
```


SOLVE
SAVE

!-----

TIME,5
NSUBST,10,2000,10

! Surface Loads PIPE288: Pressures -- 1-PINT, 2-PX, 3-PY, 4-PZ, 5-POUT

/Input,T4,inp
ALLSEL
SOLVE
SAVE

! 4th temperature load step

!-----

TIME,6
NSUBST,10,2000,10

! Surface Loads PIPE288: Pressures -- 1-PINT, 2-PX, 3-PY, 4-PZ, 5-POUT

/Input,T5,inp
ALLSEL
SOLVE
SAVE

! 5th temperature load step

!-----

TIME,7
NSUBST,10,2000,10

! Surface Loads PIPE288: Pressures -- 1-PINT, 2-PX, 3-PY, 4-PZ, 5-POUT

/Input,T6,inp
ALLSEL
SOLVE
SAVE

! 6th temperature load step

!-----

TIME,8
NSUBST,10,2000,10

! Surface Loads PIPE288: Pressures -- 1-PINT, 2-PX, 3-PY, 4-PZ, 5-POUT

/Input,T7,inp
ALLSEL

! 7th temperature load step

SOLVE
SAVE

!-----

TIME,9
NSUBST,10,2000,10

! Surface Loads PIPE288: Pressures -- 1-PINT, 2-PX, 3-PY, 4-PZ, 5-POUT

/Input,T8,inp
ALLSEL
SOLVE
SAVE

! 8th temperature load step

!-----

TIME,10
NSUBST,10,2000,10

! Surface Loads PIPE288: Pressures -- 1-PINT, 2-PX, 3-PY, 4-PZ, 5-POUT

/Input,T9,inp
ALLSEL
SOLVE
SAVE

! 9th temperature load step

!-----

TIME,11
NSUBST,10,2000,10

! Surface Loads PIPE288: Pressures -- 1-PINT, 2-PX, 3-PY, 4-PZ, 5-POUT

/Input,T10,inp
ALLSEL
SOLVE
SAVE

! 10th temperature load step

!-----

TIME,12
NSUBST,10,2000,10

! Surface Loads PIPE288: Pressures -- 1-PINT, 2-PX, 3-PY, 4-PZ, 5-POU

ESEL,S,ENAME,,PIPE288
BFE,ALL,Temp,1,T_amb

! Select All lines

! Shutdown

ALLSEL
SOLVE
SAVE

```
!*****  
!*                               LOAD STEP cycle #2  
!*****
```

```
!-----
```

TIME,13
NSUBST,200,2000,10

! Surface Loads PIPE288: Pressures -- 1-PINT, 2-PX, 3-PY, 4-PZ, 5-POUT
! 1st temperature load step

/Input,T1,inp

ALLSEL
SOLVE
SAVE

```
!-----
```

TIME,14
NSUBST,10,2000,10

! Surface Loads PIPE288: Pressures -- 1-PINT, 2-PX, 3-PY, 4-PZ, 5-POUT

/Input,T2,inp

! 2nd temperature load step

ALLSEL
SOLVE
SAVE

```
!-----
```

TIME,15
NSUBST,10,2000,10

! Surface Loads PIPE288: Pressures -- 1-PINT, 2-PX, 3-PY, 4-PZ, 5-POUT

/Input,T3,inp

! 3rd temperature load step

ALLSEL
SOLVE
SAVE

```
!-----  
TIME,16  
/STITLE,1,APPLY OPERATING PRESSURE AND TEMPERATURE  
NSUBST,10,2000,10  
! Surface Loads PIPE288: Pressures -- 1-PINT, 2-PX, 3-PY, 4-PZ, 5-POUT  
  
/Input,T4,inp ! 4th temperature load step  
ALLSEL  
SOLVE  
SAVE  
  
!-----  
TIME,17  
/STITLE,1,APPLY OPERATING PRESSURE AND TEMPERATURE  
NSUBST,10,2000,10  
! Surface Loads PIPE288: Pressures -- 1-PINT, 2-PX, 3-PY, 4-PZ, 5-POUT  
  
/Input,T5,inp ! 5th temperature load step  
ALLSEL  
SOLVE  
SAVE  
  
!-----  
TIME,18  
/STITLE,1,APPLY OPERATING PRESSURE AND TEMPERATURE  
NSUBST,10,2000,10  
! Surface Loads PIPE288: Pressures -- 1-PINT, 2-PX, 3-PY, 4-PZ, 5-POUT  
  
/Input,T6,inp ! 6th temperature load step  
ALLSEL  
SOLVE  
SAVE  
  
!-----  
TIME,19  
/STITLE,1,APPLY OPERATING PRESSURE AND TEMPERATURE  
NSUBST,10,2000,10  
! Surface Loads PIPE288: Pressures -- 1-PINT, 2-PX, 3-PY, 4-PZ, 5-POUT  
  
/Input,T7,inp ! 7th temperature load step
```

ALLSEL
SOLVE
SAVE

!-----

TIME,20
/STITLE,1,APPLY OPERATING PRESSURE AND TEMPERATURE
NSUBST,10,2000,10

! Surface Loads PIPE288: Pressures -- 1-PINT, 2-PX, 3-PY, 4-PZ, 5-POUT

/Input,T8,inp ! 8th temperature load step
ALLSEL
SOLVE
SAVE

!-----

TIME,21
/STITLE,1,APPLY OPERATING PRESSURE AND TEMPERATURE
NSUBST,10,2000,10

! Surface Loads PIPE288: Pressures -- 1-PINT, 2-PX, 3-PY, 4-PZ, 5-POUT

/Input,T9,inp ! 9th temperature load step
ALLSEL
SOLVE
SAVE

!-----

TIME,22
/STITLE,1,APPLY OPERATING PRESSURE AND TEMPERATURE
NSUBST,10,2000,10

! Surface Loads PIPE288: Pressures -- 1-PINT, 2-PX, 3-PY, 4-PZ, 5-POUT

/Input,T10,inp ! 10th temperature load step
ALLSEL
SOLVE
SAVE

!-----

TIME,23
/STITLE,1,APPLY OPERATING PRESSURE AND TEMPERATURE

NSUBST,10,2000,10
! Surface Loads PIPE288: Pressures -- 1-PINT, 2-PX, 3-PY, 4-PZ, 5-POUT

ESEL,S,ENAME,,PIPE288
BFE,ALL,Temp,1,T_amb
! Shutdown

ALLSEL
SOLVE
SAVE

!*****
!* LOAD STEP cycle #3
!*****

!-----
TIME,24
/STITLE,1,APPLY OPERATING PRESSURE AND TEMPERATURE
NSUBST,10,2000,10
! Surface Loads PIPE288: Pressures -- 1-PINT, 2-PX, 3-PY, 4-PZ, 5-POUT

/Input,T1,inp
! 1st temperature load step

ALLSEL
SOLVE
SAVE

!-----
TIME,25
/STITLE,1,APPLY OPERATING PRESSURE AND TEMPERATURE
NSUBST,10,2000,10
! Surface Loads PIPE288: Pressures -- 1-PINT, 2-PX, 3-PY, 4-PZ, 5-POUT

/Input,T2,inp
! 2nd temperature load step

ALLSEL
SOLVE
SAVE

!-----
TIME,26
/STITLE,1,APPLY OPERATING PRESSURE AND TEMPERATURE

NSUBST,10,2000,10

! Surface Loads PIPE288: Pressures -- 1-PINT, 2-PX, 3-PY, 4-PZ, 5-POUT

/Input,T3,inp
ALLSEL
SOLVE
SAVE

! 3rd temperature load step

!-----

TIME,27

/STITLE,1,APPLY OPERATING PRESSURE AND TEMPERATURE

NSUBST,10,2000,10

! Surface Loads PIPE288: Pressures -- 1-PINT, 2-PX, 3-PY, 4-PZ, 5-POUT

/Input,T4,inp
ALLSEL
SOLVE
SAVE

! 4th temperature load step

!-----

TIME,28

/STITLE,1,APPLY OPERATING PRESSURE AND TEMPERATURE

NSUBST,10,2000,10

! Surface Loads PIPE288: Pressures -- 1-PINT, 2-PX, 3-PY, 4-PZ, 5-POUT

/Input,T5,inp
ALLSEL
SOLVE
SAVE

! 5th temperature load step

!-----

TIME,29

/STITLE,1,APPLY OPERATING PRESSURE AND TEMPERATURE

NSUBST,10,2000,10

! Surface Loads PIPE288: Pressures -- 1-PINT, 2-PX, 3-PY, 4-PZ, 5-POUT

/Input,T6,inp
ALLSEL
SOLVE
SAVE

! 6th temperature load step

```
!-----  
TIME,30  
/STITLE,1,APPLY OPERATING PRESSURE AND TEMPERATURE  
NSUBST,10,2000,10  
! Surface Loads PIPE288: Pressures -- 1-PINT, 2-PX, 3-PY, 4-PZ, 5-POUT  
  
/Input,T7,inp ! 7th temperature load step  
ALLSEL  
SOLVE  
SAVE  
  
!-----  
TIME,31  
/STITLE,1,APPLY OPERATING PRESSURE AND TEMPERATURE  
NSUBST,10,2000,10  
! Surface Loads PIPE288: Pressures -- 1-PINT, 2-PX, 3-PY, 4-PZ, 5-POUT  
  
/Input,T8,inp ! 8th temperature load step  
ALLSEL  
SOLVE  
SAVE  
  
!-----  
TIME,32  
/STITLE,1,APPLY OPERATING PRESSURE AND TEMPERATURE  
NSUBST,10,2000,10  
! Surface Loads PIPE288: Pressures -- 1-PINT, 2-PX, 3-PY, 4-PZ, 5-POUT  
  
/Input,T9,inp ! 9th temperature load step  
ALLSEL  
SOLVE  
SAVE  
  
!-----  
TIME,33  
/STITLE,1,APPLY OPERATING PRESSURE AND TEMPERATURE  
NSUBST,10,2000,10  
! Surface Loads PIPE288: Pressures -- 1-PINT, 2-PX, 3-PY, 4-PZ, 5-POUT  
  
/Input,T10,inp ! 10th temperature load step
```


ALLSEL
SOLVE
SAVE

!-----
TIME,34
/STITLE,1,APPLY OPERATING PRESSURE AND TEMPERATURE
NSUBST,10,2000,10
! Surface Loads PIPE288: Pressures -- 1-PINT, 2-PX, 3-PY, 4-PZ, 5-POUT

ESEL,S,ENAME,,PIPE288 ! Select All lines
BFE,ALL,Temp,1,T_amb ! Shutdown

ALLSEL
SOLVE
SAVE

!*****
!* LOAD STEP cycle #4
!*****

!-----
TIME,35
/STITLE,1,APPLY OPERATING PRESSURE AND TEMPERATURE
NSUBST,200,2000,10
! Surface Loads PIPE288: Pressures -- 1-PINT, 2-PX, 3-PY, 4-PZ, 5-POUT

/Input,T1,inp ! 1st temperature load step

ALLSEL
SOLVE
SAVE

!-----
TIME,36
/STITLE,1,APPLY OPERATING PRESSURE AND TEMPERATURE
NSUBST,200,2000,10
! Surface Loads PIPE288: Pressures -- 1-PINT, 2-PX, 3-PY, 4-PZ, 5-POUT

/Input,T2,inp ! 2nd temperature load step

ALLSEL
SOLVE
SAVE

!-----

TIME,37
/STITLE,1,APPLY OPERATING PRESSURE AND TEMPERATURE
NSUBST,200,2000,10

! Surface Loads PIPE288: Pressures -- 1-PINT, 2-PX, 3-PY, 4-PZ, 5-POUT

/Input,T3,inp
ALLSEL
SOLVE
SAVE

! 3rd temperature load step

!-----

TIME,38
/STITLE,1,APPLY OPERATING PRESSURE AND TEMPERATURE
NSUBST,200,2000,10

! Surface Loads PIPE288: Pressures -- 1-PINT, 2-PX, 3-PY, 4-PZ, 5-POUT

/Input,T4,inp
ALLSEL
SOLVE
SAVE

! 4th temperature load step

!-----

TIME,39
/STITLE,1,APPLY OPERATING PRESSURE AND TEMPERATURE
NSUBST,200,2000,10

! Surface Loads PIPE288: Pressures -- 1-PINT, 2-PX, 3-PY, 4-PZ, 5-POUT

/Input,T5,inp
ALLSEL
SOLVE
SAVE

! 5th temperature load step

!-----

TIME,40
/STITLE,1,APPLY OPERATING PRESSURE AND TEMPERATURE

NSUBST,200,2000,10

! Surface Loads PIPE288: Pressures -- 1-PINT, 2-PX, 3-PY, 4-PZ, 5-POUT

/Input,T6,inp
ALLSEL
SOLVE
SAVE

! 6th temperature load step

!-----

TIME,41

/STITLE,1,APPLY OPERATING PRESSURE AND TEMPERATURE

NSUBST,200,2000,10

! Surface Loads PIPE288: Pressures -- 1-PINT, 2-PX, 3-PY, 4-PZ, 5-POUT

/Input,T7,inp
ALLSEL
SOLVE
SAVE

! 7th temperature load step

!-----

TIME,42

/STITLE,1,APPLY OPERATING PRESSURE AND TEMPERATURE

NSUBST,200,2000,10

! Surface Loads PIPE288: Pressures -- 1-PINT, 2-PX, 3-PY, 4-PZ, 5-POUT

/Input,T8,inp
ALLSEL
SOLVE
SAVE

! 8th temperature load step

!-----

TIME,43

/STITLE,1,APPLY OPERATING PRESSURE AND TEMPERATURE

NSUBST,200,2000,10

! Surface Loads PIPE288: Pressures -- 1-PINT, 2-PX, 3-PY, 4-PZ, 5-POUT

/Input,T9,inp
ALLSEL
SOLVE
SAVE

! 9th temperature load step

```
!-----  
TIME,44  
/STITLE,1,APPLY OPERATING PRESSURE AND TEMPERATURE  
NSUBST,200,2000,10  
! Surface Loads PIPE288: Pressures -- 1-PINT, 2-PX, 3-PY, 4-PZ, 5-POUT  
  
/Input,T10,inp ! 10th temperature load step  
ALLSEL  
SOLVE  
SAVE
```

```
!-----  
TIME,45  
/STITLE,1,APPLY OPERATING PRESSURE AND TEMPERATURE  
NSUBST,200,2000,10  
! Surface Loads PIPE288: Pressures -- 1-PINT, 2-PX, 3-PY, 4-PZ, 5-POUT  
  
ESEL,S,ENAME,,PIPE288 ! Select All lines  
BFE,ALL,Temp,1,T_amb ! Shutdown
```

```
ALLSEL  
SOLVE  
SAVE
```

```
!*****  
!* LOAD STEP cycle #5  
!*****
```

```
!-----  
TIME,46  
/STITLE,1,APPLY OPERATING PRESSURE AND TEMPERATURE  
NSUBST,200,2000,10  
! Surface Loads PIPE288: Pressures -- 1-PINT, 2-PX, 3-PY, 4-PZ, 5-POUT  
  
/Input,T1,inp ! 1st temperature load step  
  
ALLSEL  
SOLVE  
SAVE
```

```
!-----  
TIME,47  
/STITLE,1,APPLY OPERATING PRESSURE AND TEMPERATURE  
NSUBST,200,2000,10  
! Surface Loads PIPE288: Pressures -- 1-PINT, 2-PX, 3-PY, 4-PZ, 5-POUT  
  
/Input,T2,inp ! 2nd temperature load step  
ALLSEL  
SOLVE  
SAVE  
  
!-----  
TIME,48  
/STITLE,1,APPLY OPERATING PRESSURE AND TEMPERATURE  
NSUBST,200,2000,10  
! Surface Loads PIPE288: Pressures -- 1-PINT, 2-PX, 3-PY, 4-PZ, 5-POUT  
  
/Input,T3,inp ! 3rd temperature load step  
ALLSEL  
SOLVE  
SAVE  
  
!-----  
TIME,49  
/STITLE,1,APPLY OPERATING PRESSURE AND TEMPERATURE  
NSUBST,200,2000,10  
! Surface Loads PIPE288: Pressures -- 1-PINT, 2-PX, 3-PY, 4-PZ, 5-POUT  
  
/Input,T4,inp ! 4th temperature load step  
ALLSEL  
SOLVE  
SAVE  
  
!-----  
TIME,50  
/STITLE,1,APPLY OPERATING PRESSURE AND TEMPERATURE  
NSUBST,200,2000,10  
! Surface Loads PIPE288: Pressures -- 1-PINT, 2-PX, 3-PY, 4-PZ, 5-POUT  
  
/Input,T5,inp ! 5th temperature load step
```

ALLSEL
SOLVE
SAVE

!-----

TIME,51
/STITLE,1,APPLY OPERATING PRESSURE AND TEMPERATURE
NSUBST,200,2000,10

! Surface Loads PIPE288: Pressures -- 1-PINT, 2-PX, 3-PY, 4-PZ, 5-POUT

/Input,T6,inp
ALLSEL
SOLVE
SAVE

! 6th temperature load step

!-----

TIME,52
/STITLE,1,APPLY OPERATING PRESSURE AND TEMPERATURE
NSUBST,200,2000,10

! Surface Loads PIPE288: Pressures -- 1-PINT, 2-PX, 3-PY, 4-PZ, 5-POUT

/Input,T7,inp
ALLSEL
SOLVE
SAVE

! 7th temperature load step

!-----

TIME,53
/STITLE,1,APPLY OPERATING PRESSURE AND TEMPERATURE
NSUBST,200,2000,10

! Surface Loads PIPE288: Pressures -- 1-PINT, 2-PX, 3-PY, 4-PZ, 5-POUT

/Input,T8,inp
ALLSEL
SOLVE
SAVE

! 8th temperature load step

!-----

TIME,54
/STITLE,1,APPLY OPERATING PRESSURE AND TEMPERATURE

NSUBST,200,2000,10

! Surface Loads PIPE288: Pressures -- 1-PINT, 2-PX, 3-PY, 4-PZ, 5-POUT

/Input,T9,inp
ALLSEL
SOLVE
SAVE

! 9th temperature load step

!-----

TIME,55
/STITLE,1,APPLY OPERATING PRESSURE AND TEMPERATURE
NSUBST,200,2000,10

! Surface Loads PIPE288: Pressures -- 1-PINT, 2-PX, 3-PY, 4-PZ, 5-POUT

/Input,T10,inp
ALLSEL
SOLVE
SAVE

! 10th temperature load step

!-----

TIME,56
/STITLE,1,APPLY OPERATING PRESSURE AND TEMPERATURE
NSUBST,200,2000,10

! Surface Loads PIPE288: Pressures -- 1-PINT, 2-PX, 3-PY, 4-PZ, 5-POUT

ESEL,S,ENAME,,PIPE288
BFE,ALL,Temp,1,T_amb

! Select All lines

ALLSEL
SOLVE
SAVE

/DSCALE,all,10

FINI
/EOF

Appendix IV-2

Finite Element Analysis ANSYS Scripts for Results Extraction

1. Effective Axial Force:

```
Finish
/FILNAM,Test2           ! File name used for analysis
resume,Test2,db        ! Upload the analysis database
/post1
endElem=1999           ! Number of nodes
StartStep=1            ! Start Step for 1st Cycle
EndStep=2              ! End Step for 1st Cycle
nlcases=EndStep-StartStep+1 ! Maximum 10
*dim,final,array,endElem,nlcases
*do,I,1,nlcases
  set,StartStep+I-1
  *do,J,1,endElem
    *GET,FX_I,ELEM,J,SMISC,63
    final(J,I)=FX_I
  *enddo
*enddo
*cfcopen, Tension1_1, txt ! Write to file tnesion.txt
/INPUT,tstepif,mac      ! Read input from file "tstepif.mac"
*cfclose
/EOF
```

2. Axial Displacement:

```
Finish
/FILNAM,Test2           ! File name used for analysis
resume,Test2,db        ! Upload the analysis database
```

```
/post1
endnode=2000           ! Number of nodes
StartStep=11          ! Start Step for 1st Cycle
EndStep=12            ! End Step for 1st Cycle
nlcases=EndStep-StartStep+1 ! Maximum 10
*dim,final,array,endnode,nlcases

*do,I,1,nlcases
  set,StartStep+I-1
  *do,J,1,endnode
    *GET,DisX,NODE,J,U,X
    final(J,I)=DisX
  *enddo
*enddo

*cfcopen, DX_1st_cyc-1, txt      !write to file DX_1st_cyc.txt

/INPUT,tstepif,mac
*cfclose
/EOF
```

3. “tstepif.mac”:

```
*IF,nlcases,EQ,1,THEN

*vwrite, final(1,1)
(f16.4)                !format

*ELSEIF,nlcases,EQ,2,THEN

*vwrite, final(1,1),',', final(1,2)
(f16.4, a1,f16.4)      !format
```

```
*ELSEIF,nlcases,EQ,3,THEN
```

```
*vwrite, final(1,1),',', final(1,2),',', final(1,3)  
(f16.4, a1,f16.4, a1,f16.4) !format
```

```
*ELSEIF,nlcases,EQ,4,THEN
```

```
*vwrite, final(1,1),',', final(1,2),',', final(1,3),',', final(1,4)  
(f16.4, a1,f16.4, a1,f16.4, a1,f16.4) !format
```

```
*ELSEIF,nlcases,EQ,5,THEN
```

```
*vwrite, final(1,1),',', final(1,2),',', final(1,3),',', final(1,4),',', final(1,5)  
(f16.4, a1,f16.4, a1,f16.4, a1,f16.4, a1,f16.4) !format
```

```
*ELSEIF,nlcases,EQ,6,THEN
```

```
*vwrite, final(1,1),',', final(1,2),',', final(1,3),',', final(1,4),',', final(1,5),',', final(1,6)  
(f16.4, a1,f16.4, a1,f16.4, a1,f16.4, a1,f16.4, a1,f16.4)
```

```
*ELSEIF,nlcases,EQ,7,THEN
```

```
*vwrite, final(1,1),',', final(1,2),',', final(1,3),',', final(1,4),',', final(1,5),',', final(1,6),',', final(1,7)  
(f16.4, a1,f16.4, a1,f16.4, a1,f16.4, a1,f16.4, a1,f16.4, a1,f16.4)
```

```
*ELSEIF,nlcases,EQ,8,THEN
```

```
*vwrite, final(1,1),',', final(1,2),',', final(1,3),',', final(1,4),',', final(1,5),',', final(1,6),',', final(1,7),',', final(1,8)  
(f16.4, a1,f16.4, a1,f16.4, a1,f16.4, a1,f16.4, a1,f16.4, a1,f16.4, a1,f16.4)
```

```
*ELSEIF,nlcases,EQ,9,THEN
```

*vwrite, final(1,1),',', final(1,2),',', final(1,3),',', final(1,4),',', final(1,5),',', final(1,6),',', final(1,7),',', final(1,8),',', final(1,9)
(f16.4, a1,f16.4, a1,f16.4, a1,f16.4, a1,f16.4, a1,f16.4, a1,f16.4, a1,f16.4, a1,f16.4, a1,f16.4)

*ELSEIF,nlcases,EQ,10,THEN

*vwrite, final(1,1),',', final(1,2),',', final(1,3),',', final(1,4),',', final(1,5),',', final(1,6),',', final(1,7),',', final(1,8),',', final(1,9),',', final(1,10)
(f16.4, a1,f16.4, a1,f16.4, a1,f16.4, a1,f16.4, a1,f16.4, a1,f16.4, a1,f16.4, a1,f16.4, a1,f16.4, a1,f16.4)

*ELSEIF,nlcases,EQ,11,THEN

*vwrite, final(1,1),',', final(1,2),',', final(1,3),',', final(1,4),',', final(1,5),',', final(1,6),',', final(1,7),',', final(1,8),',', final(1,9),',', final(1,10),',', final(1,11)
(f16.4, a1,f16.4, a1,f16.4, a1,f16.4, a1,f16.4, a1,f16.4, a1,f16.4, a1,f16.4, a1,f16.4, a1,f16.4, a1,f16.4)

*ELSEIF,nlcases,EQ,12,THEN

*vwrite, final(1,1),',', final(1,2),',', final(1,3),',', final(1,4),',', final(1,5),',', final(1,6),',', final(1,7),',', final(1,8),',', final(1,9),',', final(1,10),',', final(1,11),',',
final(1,12)
(f16.4, a1,f16.4, a1,f16.4, a1,f16.4, a1,f16.4, a1,f16.4, a1,f16.4, a1,f16.4, a1,f16.4, a1,f16.4, a1,f16.4, a1,f16.4)

*ELSEIF,nlcases,EQ,13,THEN

*vwrite, final(1,1),',', final(1,2),',', final(1,3),',', final(1,4),',', final(1,5),',', final(1,6),',', final(1,7),',', final(1,8),',', final(1,9),',', final(1,10),',', final(1,11),',',
final(1,12),',', final(1,13)
(f16.4, a1,f16.4, a1,f16.4, a1,f16.4, a1,f16.4, a1,f16.4, a1,f16.4, a1,f16.4, a1,f16.4, a1,f16.4, a1,f16.4, a1,f16.4)

*ELSEIF,nlcases,EQ,14,THEN

*vwrite, final(1,1),',', final(1,2),',', final(1,3),',', final(1,4),',', final(1,5),',', final(1,6),',', final(1,7),',', final(1,8),',', final(1,9),',', final(1,10),',', final(1,11),',',
final(1,12),',', final(1,13),',', final(1,14)
(f16.4, a1,f16.4, a1,f16.4, a1,f16.4, a1,f16.4, a1,f16.4, a1,f16.4, a1,f16.4, a1,f16.4, a1,f16.4, a1,f16.4, a1,f16.4)

*ELSEIF,nlcases,EQ,15,THEN

```
*vwrite, final(1,1),',', final(1,2),',', final(1,3),',', final(1,4),',', final(1,5),',', final(1,6),',', final(1,7),',', final(1,8),',', final(1,9),',', final(1,10),',', final(1,11),',',  
final(1,12),',', final(1,13),',', final(1,14),',', final(1,15)  
(f16.4, a1,f16.4, a1,f16.4, a1,f16.4, a1,f16.4, a1,f16.4, a1,f16.4, a1,f16.4, a1,f16.4, a1,f16.4, a1,f16.4, a1,f16.4, a1,f16.4, a1,f16.4, a1,f16.4)
```

```
*ELSEIF,nlcases,EQ,16,THEN
```

```
*vwrite, final(1,1),',', final(1,2),',', final(1,3),',', final(1,4),',', final(1,5),',', final(1,6),',', final(1,7),',', final(1,8),',', final(1,9),',', final(1,10),',', final(1,11),',',  
final(1,12),',', final(1,13),',', final(1,14),',', final(1,15),',', final(1,16)  
(f16.4, a1,f16.4, a1,f16.4, a1,f16.4, a1,f16.4, a1,f16.4, a1,f16.4, a1,f16.4, a1,f16.4, a1,f16.4, a1,f16.4, a1,f16.4, a1,f16.4, a1,f16.4, a1,f16.4)
```

```
*ELSEIF,nlcases,EQ,17,THEN
```

```
*vwrite, final(1,1),',', final(1,2),',', final(1,3),',', final(1,4),',', final(1,5),',', final(1,6),',', final(1,7),',', final(1,8),',', final(1,9),',', final(1,10),',', final(1,11),',',  
final(1,12),',', final(1,13),',', final(1,14),',', final(1,15),',', final(1,16),',', final(1,17)  
(f16.4, a1,f16.4, a1,f16.4, a1,f16.4, a1,f16.4, a1,f16.4, a1,f16.4, a1,f16.4, a1,f16.4, a1,f16.4, a1,f16.4, a1,f16.4, a1,f16.4, a1,f16.4, a1,f16.4)
```

```
*ELSEIF,nlcases,EQ,18,THEN
```

```
*vwrite, final(1,1),',', final(1,2),',', final(1,3),',', final(1,4),',', final(1,5),',', final(1,6),',', final(1,7),',', final(1,8),',', final(1,9),',', final(1,10),',', final(1,11),',',  
final(1,12),',', final(1,13),',', final(1,14),',', final(1,15),',', final(1,16),',', final(1,17),',', final(1,18)  
(f16.4, a1,f16.4, a1,f16.4, a1,f16.4, a1,f16.4, a1,f16.4, a1,f16.4, a1,f16.4, a1,f16.4, a1,f16.4, a1,f16.4, a1,f16.4, a1,f16.4, a1,f16.4, a1,f16.4, a1,f16.4,  
a1,f16.4)
```

```
*ELSEIF,nlcases,EQ,19,THEN
```

```
*vwrite, final(1,1),',', final(1,2),',', final(1,3),',', final(1,4),',', final(1,5),',', final(1,6),',', final(1,7),',', final(1,8),',', final(1,9),',', final(1,10),',', final(1,11),',',  
final(1,12),',', final(1,13),',', final(1,14),',', final(1,15),',', final(1,16),',', final(1,17),',', final(1,18),',', final(1,19)  
(f16.4, a1,f16.4, a1,f16.4, a1,f16.4, a1,f16.4, a1,f16.4, a1,f16.4, a1,f16.4, a1,f16.4, a1,f16.4, a1,f16.4, a1,f16.4, a1,f16.4, a1,f16.4, a1,f16.4, a1,f16.4,  
a1,f16.4, a1,f16.4)
```

```
*ENDIF
```

Appendix V

EAF with Friction Factor (0.5, 0.7 & 0.2) including Axial Walking Displacement at Mid-Point

1. Friction Factor 0.5:

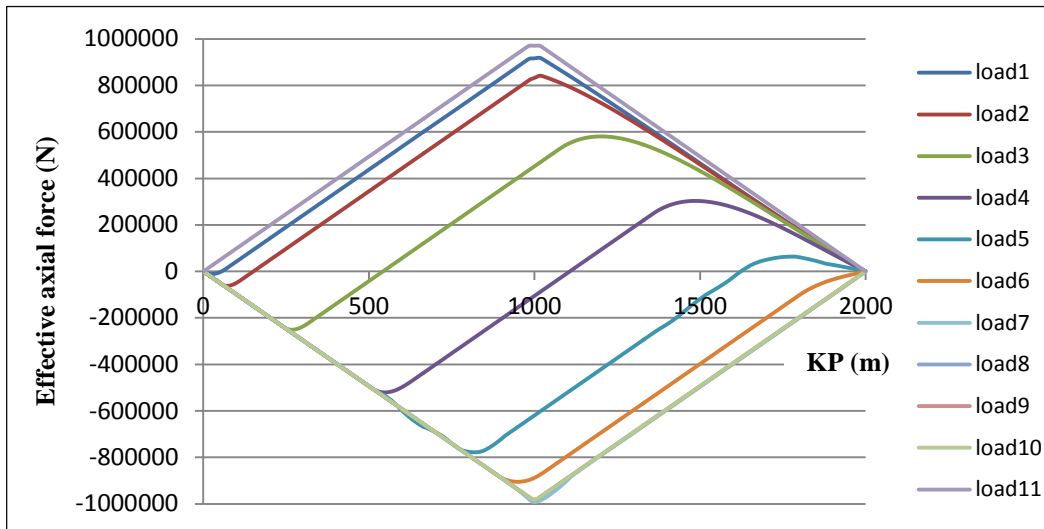


Figure A-V.1: Effective Axial Force for 2nd Cycle with Friction factor 0.5

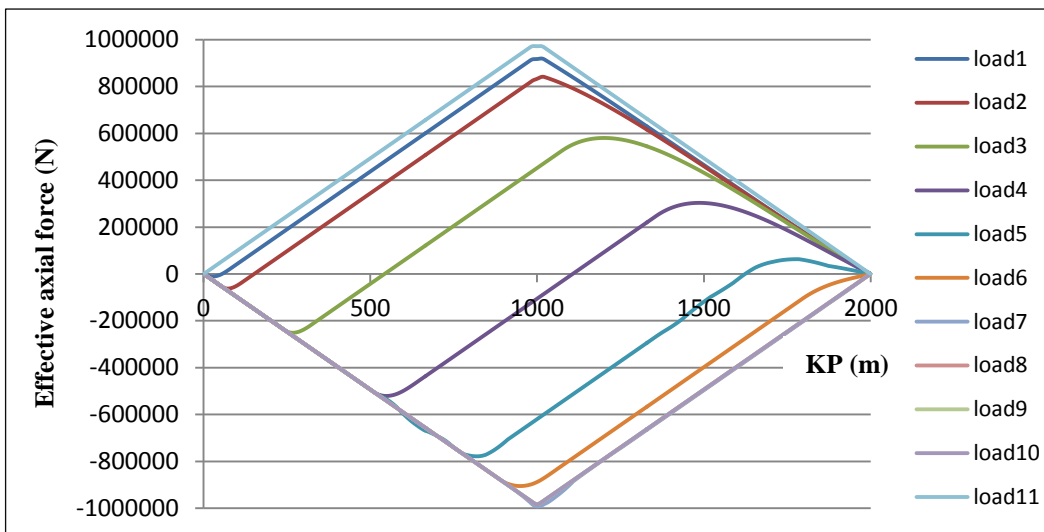


Figure A-V.2: Effective Axial Force for 3rd Cycle with Friction factor 0.5

2. Friction Factor 0.7:

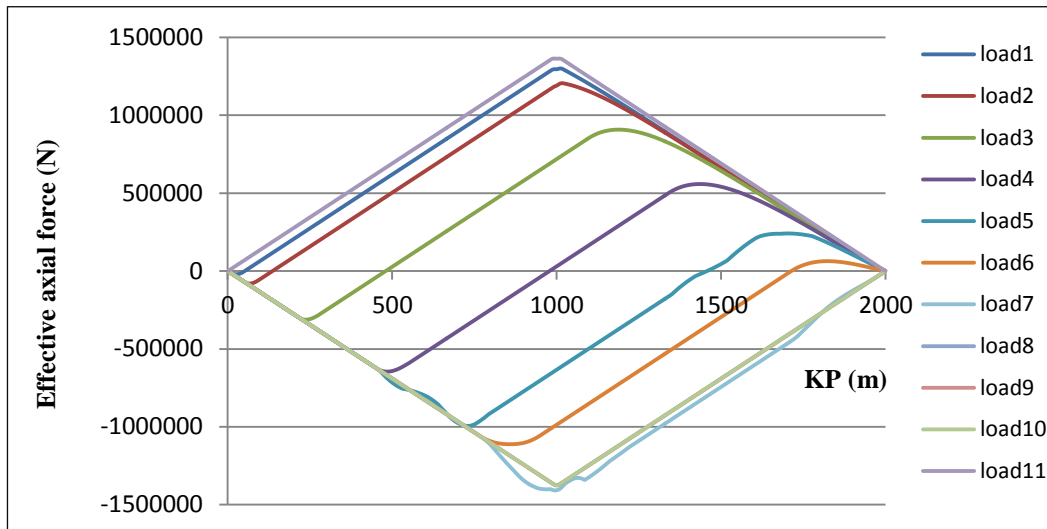


Figure A-V.3: Effective Axial Force for 2nd Cycle with Friction factor 0.7

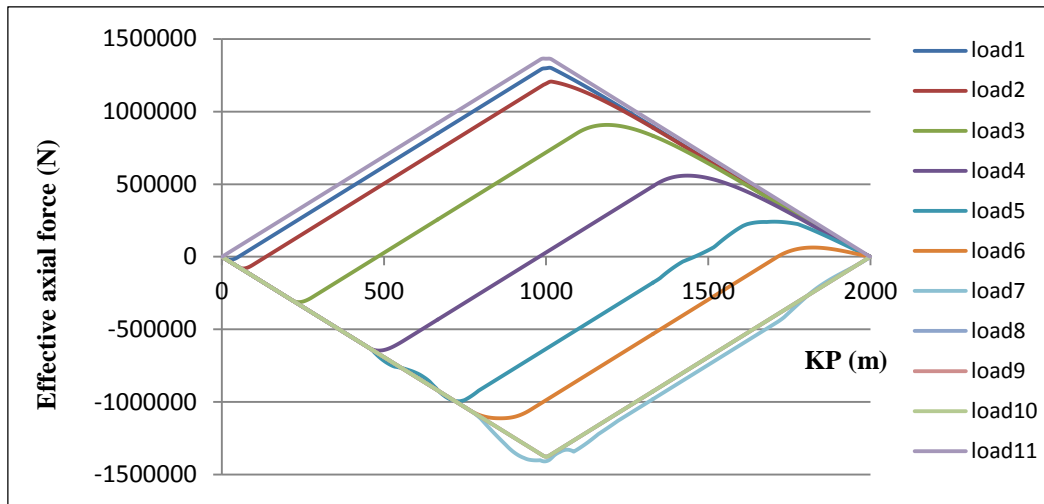


Figure A-V.4: Effective Axial Force for 3rd Cycle with Friction factor 0.7

3. Friction Factor 2.0:

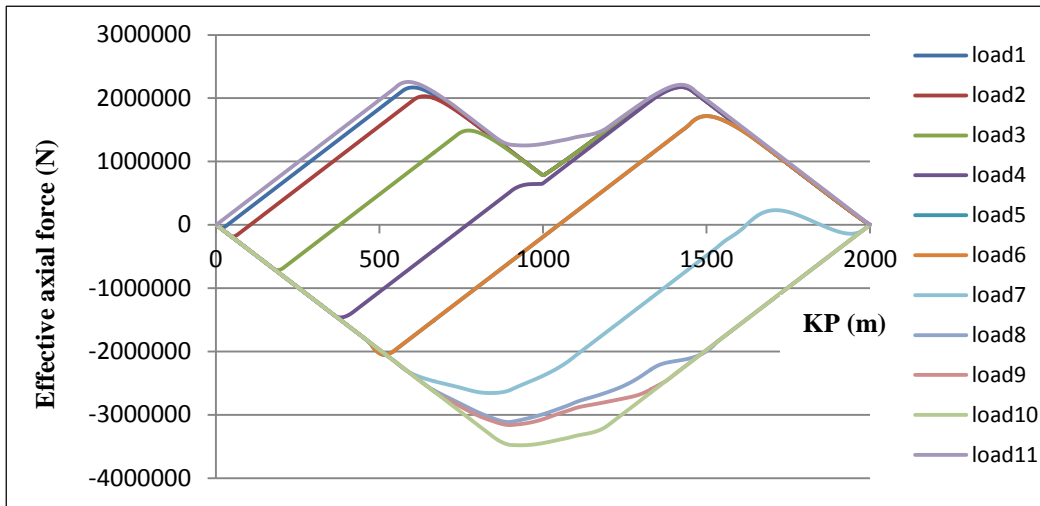


Figure A-V.5: Effective Axial Force for 2nd Cycle with Friction factor 2.0

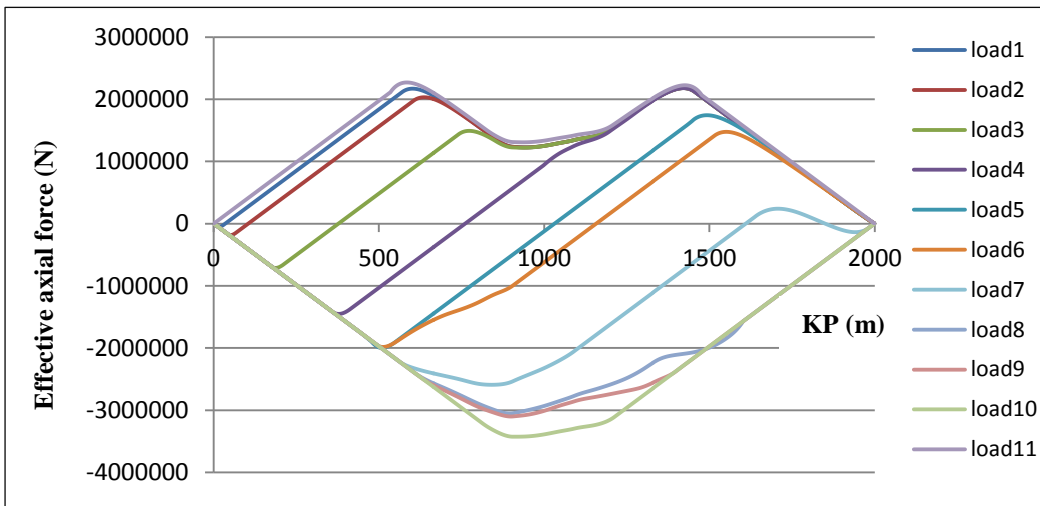


Figure A-V.6: Effective Axial Force for 3rd Cycle with Friction factor 2.0

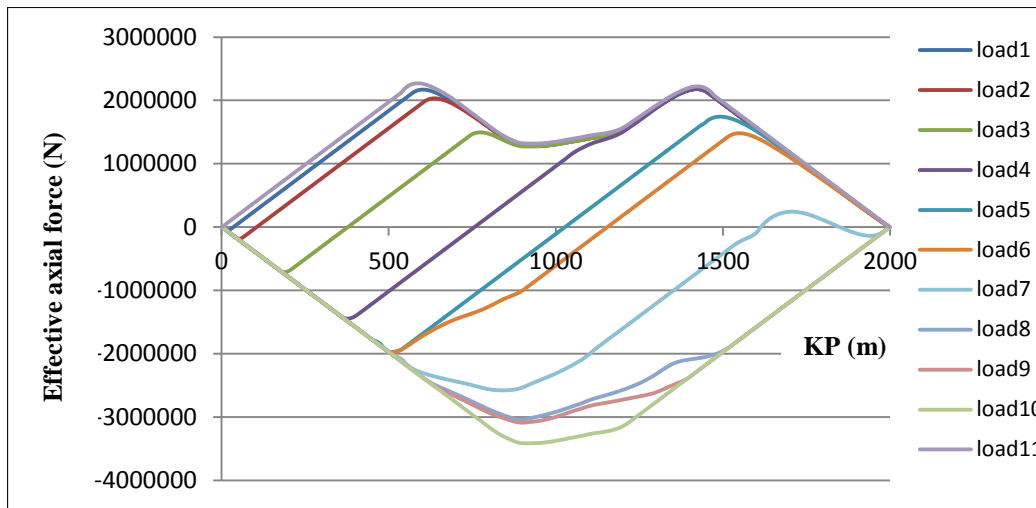


Figure A-V.7: Effective Axial Force for 4th Cycle with Friction factor 2.0

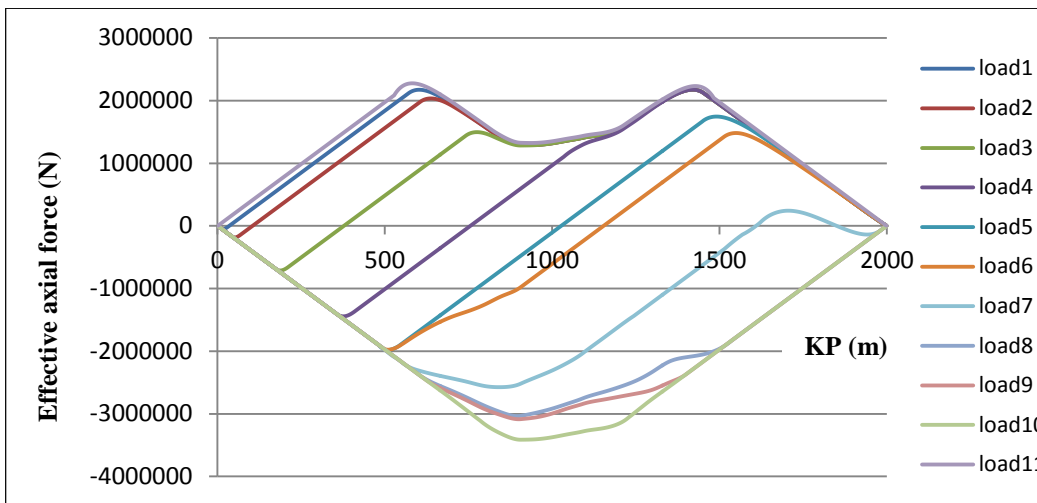


Figure A-V.8: Effective Axial Force for 5th Cycle with Friction factor 2.0

4. Walking at Mid-Point:

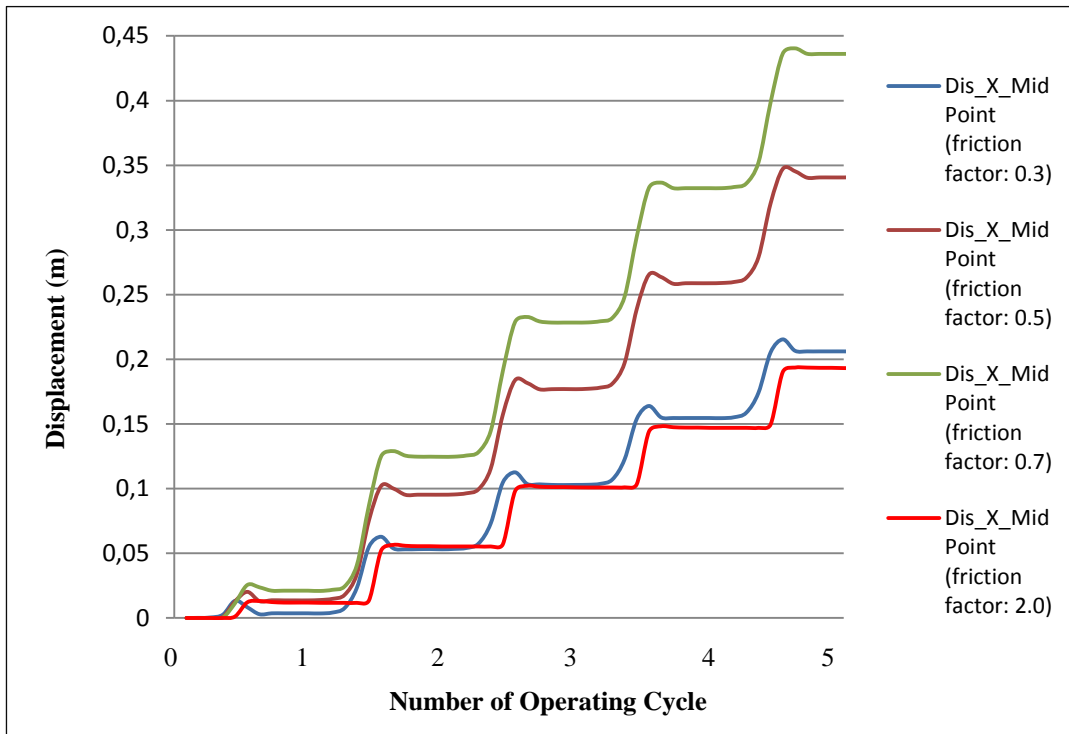


Figure A-V.9: Axial Walking Displacement at Mid-Point